UNIVERSIDAD CARLOS III DE MADRID

DOCTORAL THESIS

"OPTIMIZATION OF CONSTRUCTION COST AND MAGNETIC FIELDS OF UNDERGROUND POWER LINES"

Author:

Víctor J. Hernández Jiménez

Advisors:

Dr. Edgardo Daniel Castronuovo

Department of Electrical Engineering

Leganés, September 2016

TESIS DOCTORAL

OPTIMIZATION OF CONSTRUCTION COST AND MAGNETIC FIELDS OF UNDERGROUND POWER LINES

Autor: Víctor Julián Hernández Jiménez

Director: Edgardo Daniel Castronuovo

Firma del Tribunal Calificador:

Firma

Presidente: Renato Rizzo

Vocal: Pablo Martin Muñoz

Secretaria: Hortensia Amarís Duarte

Calificación:

Leganés, 29 de septiembre de 2016.

"No importa que tan lento vayas, lo importante es nunca detenerse"

Confucio (551-479 a.C.)

“El que lee mucho y anda mucho, ve mucho y sabe mucho”

Miguel de Cervantes (1547-1616)

Agradecimientos

Quiero agradecer a mi esposa Verónica y a mis niños, Carlos, Hugo y al bebé que gozosamente esperamos, por ser la alegría de mi vida, fuente de ilusión y motivación para realizar este trabajo y de todo lo que hago. También, quiero agradecer a mis padres y hermanos por haber sido desde siempre mis guías y mis compañeros de viaje.

Por supuesto, dar las gracias a mi director de tesis Edgardo por su apoyo, sus ideas y su conocimiento. Ha sido determinante para la realización de este trabajo. No quiero olvidarme de Ismael Sanchez por su ayuda y colaboración con la parte estadística del trabajo.

Además, agradecer a mis compañeros de Red Eléctrica de España, por su apoyo y por lo mucho que aprendo de ellos cada día.

Muchas gracias a todos.

Summary

For several reasons, including environmental, security and land occupation restrictions, underground power cables are intensively used, especially for transmission of electric energy in urban areas. The current flowing through these cables generates magnetic fields. Nevertheless, exposure to magnetic fields is restricted for providing protection of population against possible health effects. This thesis focuses on two important aspects for society: the limitations of magnetic fields generated by underground electrical grids and the reduction in the construction cost, when allocating underground cables.

This work proposes several methods for the minimization of construction costs, constraining the magnetic fields generated by multi-circuit underground power lines to the limits settled by legislation. As the limits for magnetic fields are not the same in all countries and regions, different stringent constraints are considered in the study. Magnetic fields depend on electrical currents flowing through circuits and, as demand, production and even the grid configuration change, they vary along time. This thesis proposes new statistic optimization methods, considering temporal variations in the electrical currents for the calculation of the cable bundles optimal disposition. Cables can be buried or installed in galleries. Thus, in this work, a new method for the optimization of gallery dimensions and cables disposition within the gallery is also developed.

Proposed optimization methods have been tested using real data and installations. The results show that very low, almost negligible, values of magnetic field can be achieved, when adopting the adequate disposition of cables. In addition, that statistic approach is essential for obtaining optimal solutions when dealing with time-varying currents.

Resumen

Por múltiples razones, entre las que se incluyen razones medioambientales, de seguridad y restricciones en el uso del suelo, los cables subterráneos son ampliamente usados, especialmente para el transporte de energía eléctrica en zonas urbanas. La circulación de corrientes a través de los cables produce campos magnéticos. No obstante, la exposición a campos magnéticos se restringe, para la protección de la población contra sus posibles efectos sobre la salud. Esta tesis se centra en dos aspectos importantes para la sociedad: la limitación del campo magnético generado por redes eléctricas subterráneas y la reducción de sus costes de instalación.

En este trabajo se proponen varios métodos para la minimización de los costes de construcción de líneas eléctricas subterráneas de múltiples circuitos, limitando los campos magnéticos generados a los valores establecidos por la legislación. Como estos límites son diferentes en los diversos países y regiones, se consideran diferentes límites en el estudio. Los campos magnéticos generados dependen del valor de las corrientes que fluyen a través de los circuitos y como la demanda, la producción e incluso la topología de la red cambia, las corrientes varían a lo largo de tiempo. Esta tesis propone nuevos métodos estadísticos de optimización para el cálculo de la disposición óptima de los cables considerando variaciones temporales en las corrientes. Los cables pueden estar enterrados o bien, instalados en galerías. Por ello, en este trabajo, también se ha desarrollado un nuevo método para la optimización de las dimensiones de galerías y la colocación de los cables dentro de ella.

Los métodos propuestos han sido probados usando instalaciones y datos reales. Los resultados muestran que se pueden conseguir valores muy bajos, casi imperceptibles, de campo magnético con una adecuada disposición de los cables. También, que métodos estadísticos son esenciales para obtención de las soluciones óptimas con corrientes variando a lo largo del tiempo.

Contents

List of Tables

List of Figures

Chapter 1. Introduction

1.1 Motivation

Nowadays, electricity is an essential service for the progress and welfare of our society. Electricity modifies essentially our everyday life and activities. Production of goods, transportation, telecommunications, lighting, operation of electronic equipment,... are just a few examples of basic activities where electricity plays an important role.

Electricity allows power when and where it is required, frequently at points far away from the centers of production, thanks to the easiness of its transmission through transmission and distribution grids. On this purpose, power lines are fundamental, being responsible for transportation of power flows through the electric grid.

Underground power transmission lines are especially used in urban areas. Because of their lower visual impact, underground lines have greater social acceptance than overhead power lines. Therefore, a rising social pressure for increasing the use of underground power lines, not only in urban surroundings but also in regions where visual impact could be significant, is observed. Moreover, in some underground activities (as mining, underground transportation, etc.) only underground power cables can be used. Therefore, underground power transmission lines, which can manage up to hundreds of kilovolts and megawatts, are widely spread.

Underground power transmission lines are constituted by isolated cables, composed by a core of conducting material coated with an insulating material, usually buried at short distance from the surface of the ground or allocated in galleries. The electric current flowing through underground cables produces magnetic fields, frequently higher than those generated by overhead power lines, because of the reduced distances to the population.

Today, society wants enjoy technological advances respecting the environment and the health of the people. In this context, the population exposure to magnetic fields and the possible effects on the health of persons cause a deep concern. The possible effects of magnetic fields in our organism are the subject of many ongoing researches and studies. Legislation for limiting the people exposure to varying electric, magnetic and electromagnetic fields has been developed in recent years in many regions and countries, for legally set restrictions to the population exposure. A revision of the most significant limits for industrial frequency is included in following chapters.

The construction costs of underground lines are also important, being one of the most significant factors when analyzing future installation projects. This thesis combines these two aspects that interest and concern to the society: the limitation of the magnetic field generated by electrical grids and, at the same time, the minimization of the installation cost.

1.2 Purpose and Objectives

The objective of this work is the development of new methods for the optimization of construction costs and the limitation of magnetic field generated in multi-circuit underground power lines. Real data are used to obtain results and to analyze the behavior of proposed methods.

Some partial objectives have been accomplished, to fulfill the previously defined general goal:

- Analysis of the state-of-the-art, on matters related to underground grids and magnetic field generated by underground cables. This analysis is focused on:

- Design of underground power lines, components, materials of cables and underground construction techniques.
- Study of national and international legislation related to exposure limitation to low-frequency magnetic field.
- Review of methods in the literature for the calculation of magnetic field generated by underground cables.
- Execution of an actualized review of the state-of-the-art related to methods for mitigation of magnetic fields generated by power lines.

- Development of an algorithm for calculating the most economical positions for cables directly buried in multi-circuit underground power lines, considering the construction costs for installation and the restrictions for the magnetic fields generated. In this development, it is required:

  - Proposition of a nonlinear optimization problem (using all continuous variables) for calculating the solution.
  - Obtaining results, in cases of 4 and 6 3-phase cable bundles with the same current flowing in all circuits and calculation of less costly configurations with reduced magnetic fields.
  - Analysis of the influence of different currents in the circuits. A sensitive analysis, depending on different values of modules and phases for defined currents, is developed.

- Utilization of a statistical approach for obtaining the optimal arrangement of cable bundles in multi-circuit underground power lines with electrical currents varying along time. The proposed optimization considers also construction costs and geometry of the terrain. For this objective, it is required:

  - Homogenization and utilization of real data, recorded during three years, for testing the methods and obtaining real results.
  - Proposition and implementation of two new optimization methods, based in statistical approaches.

- Analysis of the results, studying advantages and disadvantages of each one of the proposed methods, when compared with a more conventional approach.

- Finally, to deal with underground cables installed in galleries, optimization methods in order to minimize construction costs and magnetic fields for general and occupational exposure are proposed. Statistical approach is also used to obtain optimal solutions with time varying currents. On this assignment, the following tasks are performed:

  - Development of two new algorithms for obtaining the optimal arrangement of cables and dimensions of galleries.
  - Application of real data for getting optimal solutions for the design of galleries and the allocation of cables.
  - Evaluation of the efficiency of statistical approach, to provide cheaper and less magnetic field solutions.

1.3 Thesis Structure

In Chapter 2, a brief introduction is performed, including: revision of cables types, methods of calculation of magnetic fields produced by cables, legislation limiting magnetic field exposure and methods in the literature for the mitigation of magnetic fields.

The main chapters of this thesis are structured in function of papers submitted to relevant electrical journals and conferences. Chapters 3, 4 and 5 are presented as independent papers, with abstract, introduction and bibliography. They can be independently read. Some results of Chapter 3 are published in a research paper. Results from Chapters 4 and 5 are still in revision processes, for publication in international journals.

In Chapter 3, a method for obtaining the optimal disposition of cables for the minimization of construction costs when maintaining relatively low the magnetic field

generated by multi-circuit underground power lines is proposed. A nonlinear optimization approach is followed. Some results are shown, applying the proposed method to 4 and 6 3-phase cable bundles.

In Chapter 4, the statistical calculation of optimal dispositions of cables for time changing currents is addressed. The same previous objective is searched: the minimization of construction cost when limiting magnetic fields. Two original statistical algorithms for calculating the optimal geometry and phase disposition of underground cables are proposed. Results obtained from the application of real data show that statistical approaches provide cheaper configurations with smaller magnetic fields.

In Chapter 5, underground power lines with cables allocated in galleries are focused. Two new statistical algorithms for obtaining optimal dimensions of galleries and positions of cables are proposed, in order to optimize construction costs when limiting magnetic fields for general and professional public. A four circuit power line in an underground gallery is used to test the proposed methods. As in the previous chapter, the statistical approaches for time varying currents in the circuits provide more realistic and accurate results.

Finally, in Chapter 6 the main conclusions, contributions and future works are shown.

Chapter 2. Dealing with Magnetic Fields Generated for Underground Power Lines

Underground power line is a technology widely used for transmission of electric energy in urban areas. This chapter contains an introduction to this technology, describing the principal types of underground power lines, the main parts of cables and the earthing system.

Greeks, more than 2000 years ago, knew that certain mineral (now called magnetite) has the property of attracting iron pieces. The relationship between electricity and magnetism was not known until the 19th century, when Hans Oersted discovered that an electrical current influences on the direction of a compass needle. Subsequently, Ampère proposed a theoretical model of magnetism, which postulates that the fundamental source of the electromagnetism is not a magnetic pole, but an electric current. The basic magnetic interaction is the magnetic force between two electric charges in relative movement, which is transmitted through the magnetic field. The moving charges produce a magnetic field, and this field in turn applies a force on another moving charge [2-1].

In this chapter, the phenomenon by which a moving electric charge and, therefore, a set of moving charges flowing through an electrical conductor (the electric current) creates a magnetic field, is described. Power lines are a habitual application, with electric current flowing through conductors. A characterization of the magnetic field generated by cables is shown, too.

The effects of magnetic fields in population create concern and numerous studies about how limiting human exposure to magnetic field have been published. Therefore, in this chapter, a review of the legislation and standards for the limitation to magnetic fields is performed.

Many studies and methods have been proposed with the aim of limiting the magnetic field generated by electrical facilities. In this chapter, a review about the action lines researched for reduction of the magnetic field creates by power lines can be found, too.

2.1 Underground Power Lines: Basic Concepts and Electric Cables Constitution

The society demands electrical infrastructures with reduced visual and environmental impact. Therefore, there is an increasing social pressure for installation of underground cables, instead of overhead power lines. Currently, even existing and operational overhead power lines are being substituted by underground cables.

The main application of underground power lines is the transmission and distribution of electric power in urban and industrial areas, although they are also used in the connection of overhead lines to substations allocated in the interior of buildings, in the connection of generators, in many industrial facilities, in mining and in other multiple applications.

In underground power lines, usually, cables are buried under the terrain. To build them, usually a trench is previously made, and then, the laying of cables is performed [2-2]. But, in other many other applications, the installation of cables in galleries is preferable [2-3], [2-4], [2-5]. In the next figure, both installations are shown.

a) Trench for a underground power line with buried cables (photo of the author).

b) Underground cables in gallery [2-3].

Figure 2-1: Underground power cables, directly buried and in gallery.

Cables conforming underground power lines can be classified in function of:

- *Voltage level:* low voltage (up to rated voltages of 1 kV) and high voltage (rated voltages higher than 1 kV). Within last group, there are cables for third category lines (from 1kV up to 30kV), second category lines (from 30kV to 66kV), first class lines (between 66kV and 220kV) and special category lines (rated voltage higher or equal to 220kV) [2-6].
- *Number of phases:* single-pole cables, where each phase or pole is a single cable, and three-pole cables, which have a common insulation for the three phases [2-7].

a) Three-pole cable. *b) Single-pole cables.*

Figure 2-2: Single-pole and three-pole cables [2-2].

- *Insulation:* there are two large families of isolated wires: oil and extruded insulated cables. In the first group, oil filled or mass impregnated insulation techniques are distinguished. The extruded group includes insulations with PVC (polyvinyl chloride), PE (polyethylene), EPR (ethylene propylene) and XLPE (cross-linked Polyethylene) [2-7], [2-8].

2.1.1 Cable Components

2.1.1.1 Conductor

The conductor is the central core of insulated cables. It fulfills electrical and mechanical functions. The electrical function of the conductor is the transmission of the current, in permanent regimen, in overload and in short circuit circumstances. Mechanically, the conductor must withstand longitudinal loads while cable laying operations. The basic features that a conductor must meet are having a good conductivity and a regular outer surface. Thus, the most frequent materials for the conductor are copper and aluminum. Copper has less electrical resistance than aluminum (40% less), with less losses in the operation. However, cooper is heavier than

aluminum; the density of copper is 3.3 higher than for aluminum. Therefore, taking into account both effects, an equivalent aluminum conductor is 50% lighter than a cupper one. Despite the previous aspect, copper is widely used in high and extra-high voltage cables, where usually a high transmission capability is needed, and where the election of the material of conductor is conditioned by the maximum section that can be manufactured. The final selection of the type of conductor to be used in a particular application must consider numerous factors, including availability, economic and technical aspects [2-8].

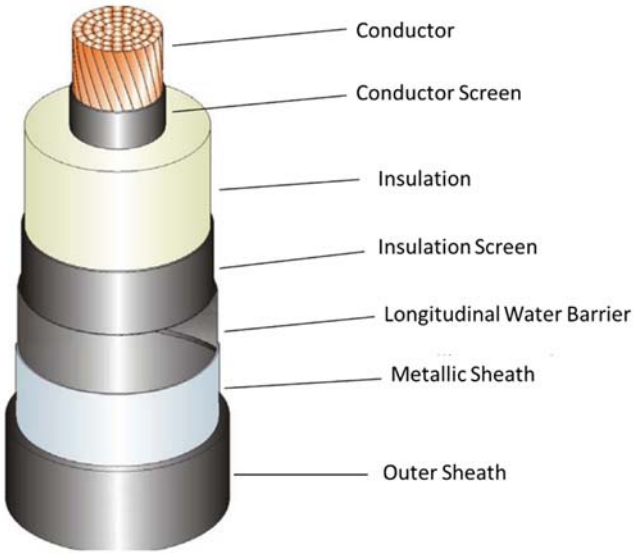

Figure 2-3: Single-pole power cable.

The ampacity of a cable is limited by the maximum temperature that can be maintained by the insulating material, conforming the working temperature of the conductor. The maximum admissible current flowing through a cable depends on the maximum working temperature and in the way how heat is dissipated at steady-state. [2-9]. In several application, reaching the best ampacity possible can be important to achieve the power transmission required. In [2-10] a method for calculating the locations of underground cables, for the best total ampacity, is presented. In the method, a combinatorial optimization based on a genetic algorithm explores the different

possible configurations of cables. In [2-11], the best ampacity for underground cables buried in non-homogeneous soils is studied. A semi-empirical correlating equation for the design of buried electrical power cables is proposed in the work, obtained from numerical simulations.

2.1.1.2 Electrical Insulation

High and extra-high voltage electrical cables have different types of insulation, always inside the two aforementioned families (oil insulated and extruded).

The oil insulated cables are formed by layers of paper (made of cellulose fibers), impregnated by a synthetic oil. Two types of design are used: oil filled or mass impregnated. In the first type, oil circulates through the inner part of the conductor soaking paper that, in conjunction with the oil, constitutes the insulation. In the second type of cables, the oil is confined in layers of insulating paper [2-7].

In the last fifteen years, extruded insulation has displaced impregnated paper techniques for high voltage cables, except for certain very extra-high-voltages and HVDC subsea applications. Types of plastic used in extruded insulation are PE, EPR, PVC and, most currently, XLPE. This plastic is basically PE, subjected to a chemical process called “crosslinking” to form transverse bonds between neighboring linear PE chains. The crosslinking process improves the PE resistance to the deformation at higher temperatures [2-8].

The electrical insulation must insulate the conductor from the metallic sheath, which it is earthed. The insulation also must withstand the electric field, at rated voltage and at transient overvoltages.

The main characteristic of the insulation of a cable is the value of its dielectric strength, usually measured in kV/cm. The maximum electric field to which the insulation is subjected must be lower than its dielectric strength, to support the voltage in the operation of the cable [2-8].

2.1.1.3 Conductor and Insulation Screen

The conductor screen is the interface between conductor and insulation, usually a thin layer consisting of semiconductor materials, which sit on the surface of the conductor results in a smooth surface. With the conductor screen, the electric field is homogeneous and the conductor screen also reduces the concentration of electric field on some specific points. In addition, the conductor screen allows moving progressively from the insulation, which contains electric field, to the conductor, where the electric field is null. A total contact between conductor and insulation is obtained, avoiding the existence of air between the two layers and the subsequent ionization, which would be dangerous to the integrity of the insulation [2-8].

The insulation screen, located between the insulation and the metallic sheath of the cable, has the same functions and composition as the previously mentioned conductor screen [2-8].

2.1.1.4 Longitudinal Water Barrier

It is a swelling tape placed between the metallic sheath and the insulation screen to reduce large values of humidity in the insulation [2-8].

2.1.1.5 Metallic Sheath

The metallic sheath is a conductive element allocated between the insulation screen and the outer sheath, present in underground cables.

The functions of the metallic sheath in insulated cables are [2-8]:

- To cancel the electric field on the outside of the cable, therefore, the electric field on insulation is radial;
- To be an active conductor for capacitive currents that cross insulation due to dielectric losses, for the induced currents by magnetic fields produced by the cable conductors or by nearby cables and zero sequence current (in case of shortcircuit), draining these currents to earth.
- To contribute to the mechanical protection against external aggression.

2.1.1.6 Outer Sheath

The outer sheath is the external layer that surrounds the cables and it is used for isolating the cable from the external environment, protecting the interior metal elements both mechanically (from external aggressions, as moisture and corrosion, in laying and operation) and electrically (isolating to the earthing metallic sheath). Usually, the material used for outer sheath in underground cables is PE [2-8].

2.1.2 Methods of Metallic Sheath Earthing

When an alternative current flows through the conductor, in the metallic sheath is induced a voltage, proportional to the circulating current, the distance between the phases and the length of the line.

If the two ends of the metallic sheath are earthed (called both ends connection), a circuit through the metallic sheath is established, with circulation of current due to this induced voltage. The circulation of currents is null in facilities with metallic sheaths earthing at only a single point (called single point connection) and in those cables with metallic sheaths permuted, in order to compensate the voltage induced (cross bonding connection) [2-2], [2-8].

Usually, power lines with insulated cables are designed to reduce the induced voltages in the metallic sheaths, not allowing a permanent circulation of induced currents and limiting the overvoltage at the ends of the sheaths. This is achieved by using the following types of conductor sheaths grounding systems.

The single point connection is mainly used in short cables. The maximum length for this type of connection is restricted by the maximum allowed value of induced voltage. The maximum voltage of the metallic sheath, respect to the earth voltage, is observed at the end with dischargers [2-2], [2-8].

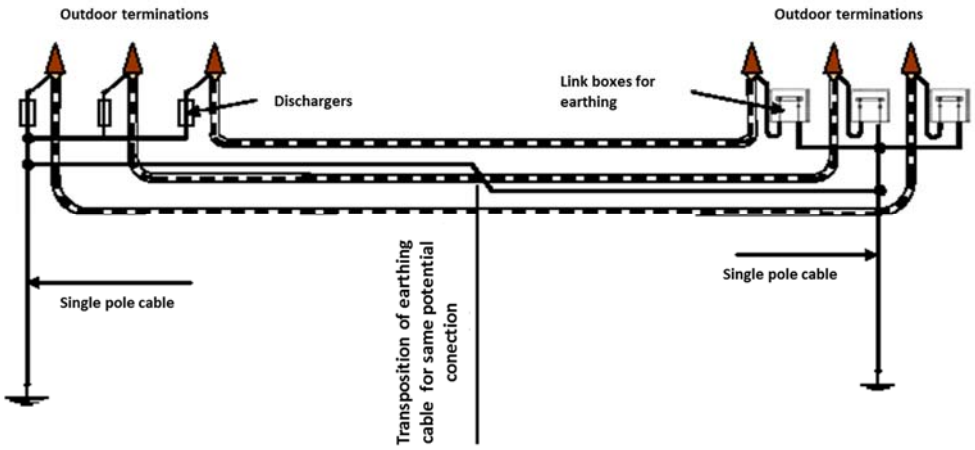

Figure 2-4: Single-point or connection of conductor sheath at one end only (own material).

The cross bonding connection of metallic sheaths consists in the interruption of the conductor sheaths, transposing orderly these connections to neutralize the voltage induced in the total of three consecutive stages. The sheaths are connected to earth at both ends of the line. To attain a more precise cancellation of the induced voltages, phase conductors are also transposed [2-2], [2-8].

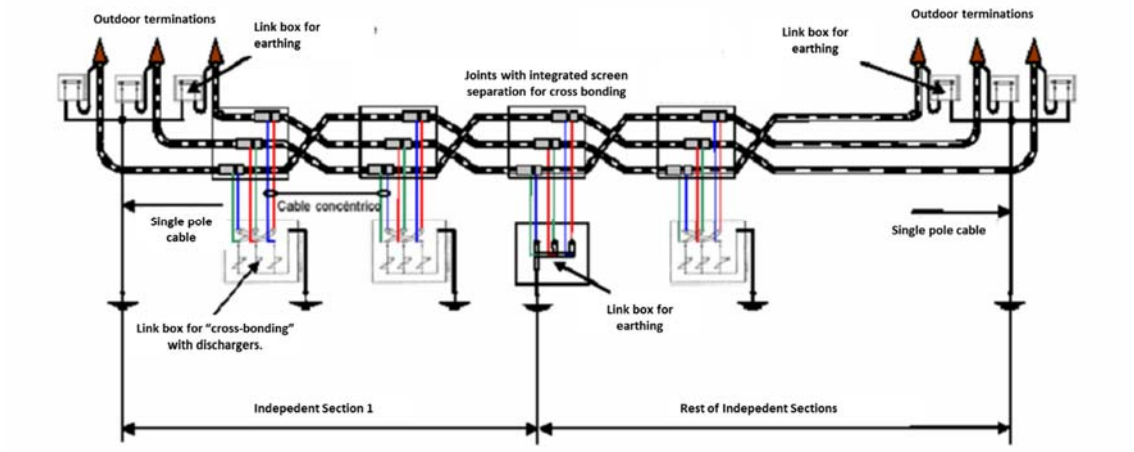

Figure 2-5: Cross-bonding connection(own material).

This type of connection is used in long lines, where it is necessary to perform two or more intermediate joints.

2.2 Sources of Magnetic Field

2.2.1 Magnetic Field Generated by Electric Charges in Movement

A electric charge moving with a velocity ***v*** creates a magnetic field. The magnetic field produced by an electric charge *q* flowing in a vacuum at a speed *v* in a point *P* a distance of *R* far from *q* is determined by expression [2-1].

$$\vec{B} = \frac{\mu_0}{4\pi} \frac{q \cdot \vec{v} \times \vec{r}}{R^2} \qquad (2\text{-}1)$$

Where,

$\mu_0 = 4\pi \cdot 10^{-7} \left(\frac{T \cdot m}{A} \right)$, is a constant of proportionality, the permeability of free space.

q, is the value of the electric charge expressed in Coulombs (C).

$\vec{v}$, is the vector of speed of the electric charge, its module is expressed in meters divided by seconds (m/s).

R, is the module of the distance vector that links from the electric charge to the point P, expressed in meters (m).

$\vec{r}$, is the unit vector, pointing from the electric charge to the point P.

$\vec{B}$, is the vector of magnetic field, its module is expressed in Tesla (T), its direction results as the cross product of the vectors $\vec{v}$ and $\vec{r}$ and it is perpendicular to the plane defined by them.

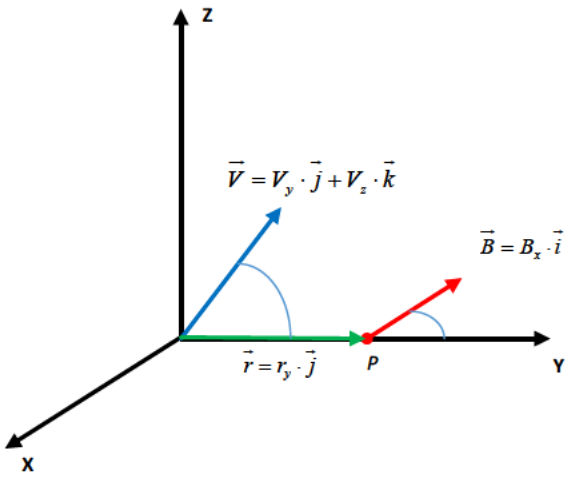

Figure 2-6: Magnetic field produced by a moving electric charge.

2.2.2 Magnetic Field Generated by Electric Currents. Biot and Savart Law

The differential of magnetic field $d\vec{B}$ produced by an infinitesimal element of current $I \cdot d\vec{l}$ in a point P can be calculated substituting $q \cdot \vec{v}$ in equation (2-1) by $I \cdot d\vec{l}$, obtaining [2-1]:

$$\vec{B} = \frac{\mu_0}{4\pi} \frac{I \cdot d\vec{l} \times \vec{r}}{R^2} \qquad (2\text{-}2)$$

Expression (2-2) is known as the Biot-Savart law.

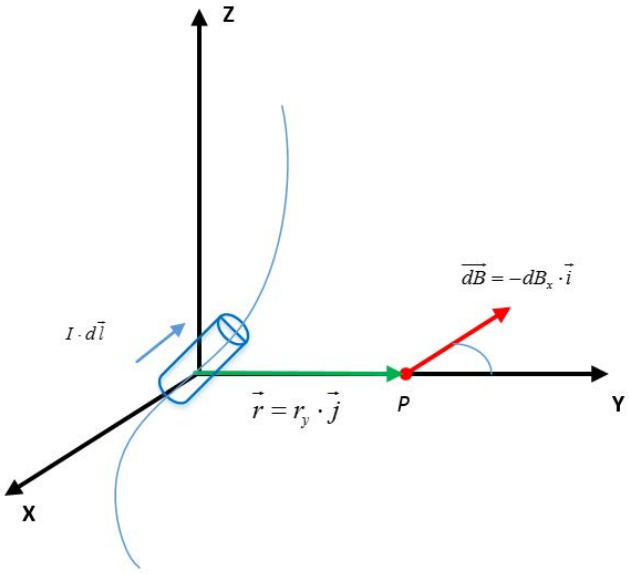

Figure 2-7: Differential of magnetic field generated by a differential element of current at a point P.

Where,

I, is the electric current, (A).

$d\vec{l}$, is the unit vector tangential to the path of electric current, (m).

Magnetic Field Generated by an Electrical Current in a Straight Wire of Infinite Length

A particular case of Biot-Savart law is the calculation of the magnetic field generated by an electrical current in a linear conductor. This case is of special interest for the calculation of the magnetic field generated for power cables. Considering some simplifying hypothesis, the magnetic field produced by circulating currents through electrical power cables in a point *P* can be written as in (2-3), [2-1].

$$dB = \frac{\mu_0}{4\pi}\frac{I \cdot dx}{R^2}\sin\varphi = \frac{\mu_0}{4\pi}\frac{I \cdot dx}{R^2}\cos\theta \qquad (2\text{-}3)$$

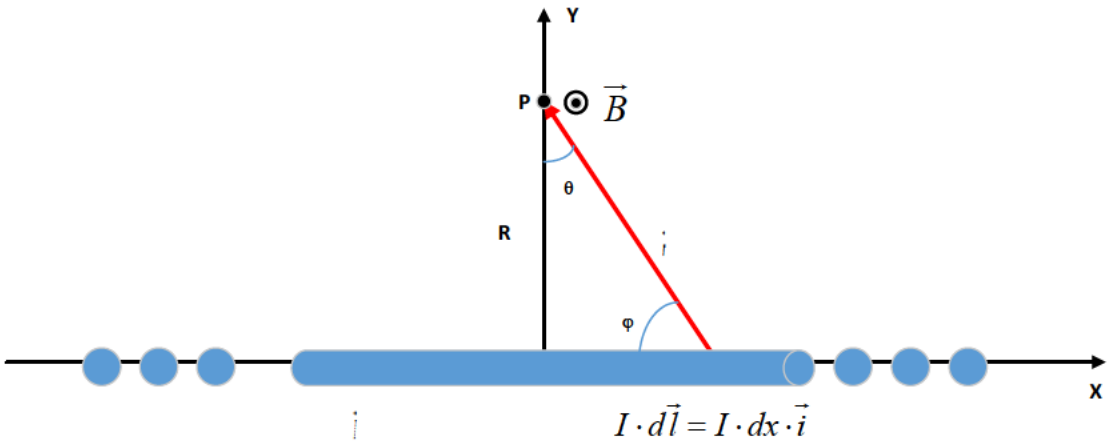

Figure 2-8: Magnetic field generated by an electric current flowing through a straight wire of infinite length.

Where,

dx, is an infinitesimal element of the straight wire of infinite length, (m).

φ and θ, are angles relating the vector geometry of the straight conductor with the measurement point, see Fig. (2-8).

R, is the minimum perpendicular distance from the straight to the point of calculation of the magnetic field P, (m).

Using integral calculus, the contribution to the magnetic field in the point P for all infinitesimal elements of the straight wire of infinite length is expressed as (2-4).

$$B = \frac{\mu_0}{4\pi}\frac{2 \cdot I}{R} \tag{2-4}$$

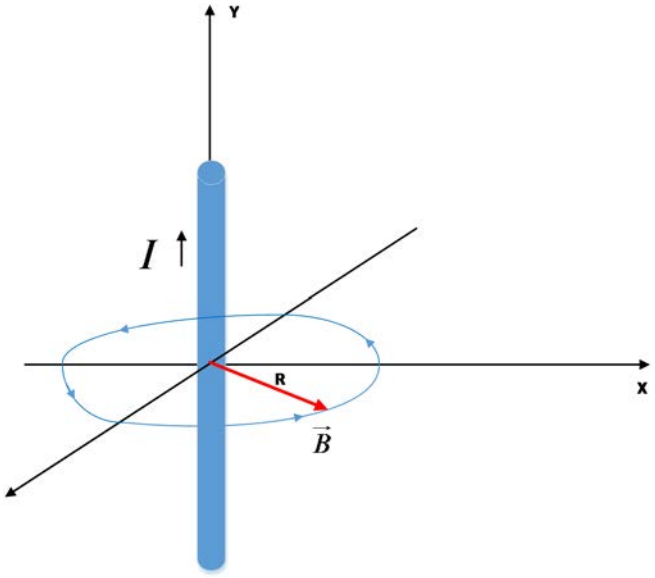

Figure 2-9: Representation of the direction of generated magnetic field.

With some simplifying hypothesis, from (2-4) and Fig. (2-9) the expression for the calculation of magnetic field generated by electrical cables can be obtained [2-12].

2.2.3 Magnetic Field Generated by Underground Cables

Subsequently to the literature, in the present work the following assumptions are considered to calculate the magnetic field *B* at a point *P*, due to currents I_1, I_2,..,*In* flowing in *n*-cables [2-12].

- The earth does not have effect on the magnetic field generated by cables, ($\mu_r = 1$).
- The total magnetic field at a point is equal to the linear superposition of the magnetic field generated by the currents flowing in each individual conductor.
- The effect on the magnetic field of induced currents flowing in metallic sheath is negligible. It means that currents flowing in metallic sheaths are null. This condition is fulfilled in the cross-bonding or single point metallic sheath earthing connection.
- Each cable is considered to be infinitely long and straight.
- The direction of the currents through the conductors is out of the page.

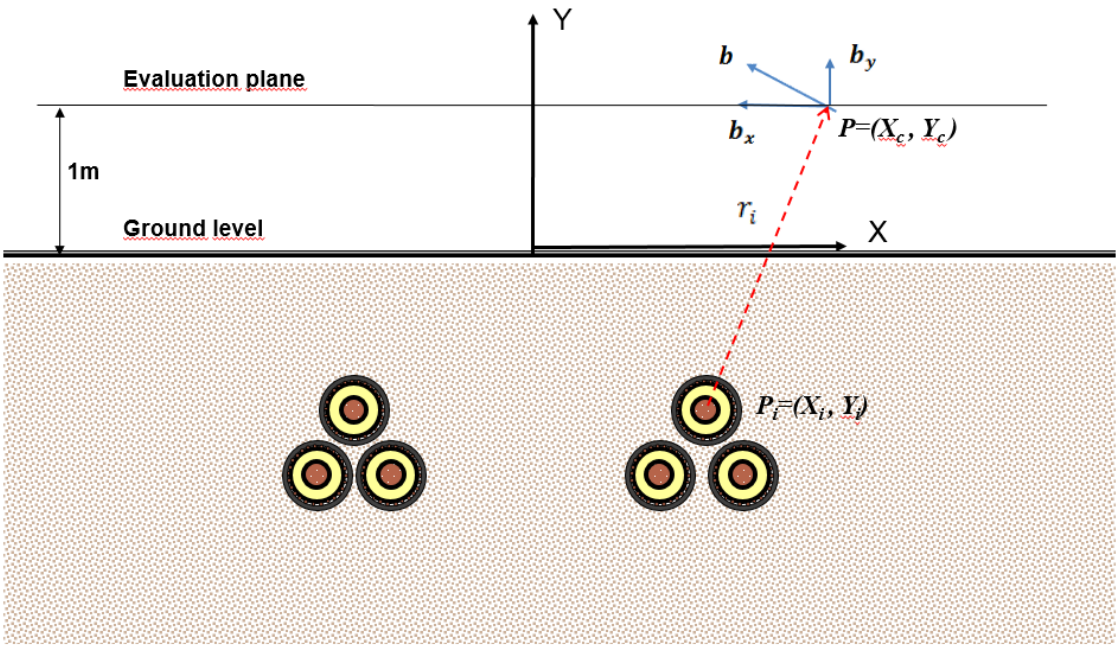

Figure 2-10: Two buried cable bundles for magnetic field calculation.

The magnetic field generated for current I_i flowing in the conductor placed in $P_i=(X_i,Y_i)$ and measured in the point $P=(X_c,Y_c)$ can be calculated as, [2-12]:

$$\vec{B} = \frac{\mu_0 \cdot I_i}{2 \cdot \pi \cdot r_i} \vec{a}_i \tag{2-5}$$

Where,

$\vec{a}_i$, is the unit vector tangent to the circular path around the cable with current I_i at the point P.

r_i, is the distance from the conductor to the point P.

Besides, in power systems with sine-wave currents, I_i can be represented through its phasor $\mathfrak{I}_i$. Thus, magnetic field is also decomposed along horizontal and vertical axes in two phasor components, as follow [2-12]:

$$\mathfrak{B}_x = \frac{\mu_0 \cdot \mathfrak{I}_i}{2 \cdot \pi \cdot r_i^2} (Y_i - Y_c) \tag{2-6}$$

$$\mathfrak{B}_y = \frac{\mu_0 \cdot \Im_i}{2 \cdot \pi \cdot r_i^2}(X_i - X_c) \tag{2-7}$$

The total magnetic field generated by the *n* currents flowing in *n* cables at point *P* is calculated by (2-8) and its magnitude by (2-9). This generalization is obtained adding the magnetic field generated by the *n* cables in both equations [2-12].

$$\vec{B} = \left(\sum_{i=1}^{n} \mathrm{B}_{xi} \right) \overrightarrow{a_x} + \left(\sum_{i=1}^{n} \mathrm{B}_{yi} \right) \overrightarrow{a_y} \tag{2-8}$$

$$\left| \vec{B} \right| = \sqrt{\left(\sum_{i=1}^{n} \left| \mathrm{B}_{xi} \right| \right)^2 + \left(\sum_{i=1}^{n} \left| \mathrm{B}_{yi} \right| \right)^2} \tag{2-9}$$

Formulas for the calculation of magnetic fields in power lines conductors for general cases, without the simplifying assumptions described previously, are obtained in [2-13]. In [2-14], the characteristics of the magnetic field under ac and dc transmission lines are also analyzed.

2.3 Magnetic Field Exposure Limits

In the society, the concern about potential environmental and health negative effects produced by the technological advances we enjoy nowadays is increasing. In this context, magnetic fields are view with apprehension. Besides, electric utility workers can have a higher exposure to magnetic field, affecting their labor safety; some studies have been developed analyzing this problem [2-15], [2-16].

Following section focus on recent legislation limiting the exposure of human people to electromagnetic fields, in order to protect the population from possible negative effects.

2.3.1 Standards

The International Commission on Non-Ionizing Radiation Protection (ICNIRP) is an independent organization with the objective of the protection of people and the environment against adverse effects of non-ionizing radiation [2-17]. In order to accomplish this aim, ICNIRP provide scientific advice on the health and environmental effects of non-ionizing radiation. Scientists and experts from different disciplines, such

as physics, medicine, chemistry, engineering and biology, and different countries work together in collaboration with ICNIRP to assess the risk of non-ionizing radiation and to provide exposure guidance. To prevent negative health effects because of low frequency magnetic and electric fields, ICNIRP recommends reducing the exposure. The "Guidelines for Limiting Exposure to Time-Varying Electric and Magnetic Fields (1 Hz to 100 kHz)" establishes limits to magnetic field exposure at power system frequency, 50 or 60 Hz [2-18]. These guidelines have been used to set exposure limits in numerous countries. Related with exposure to magnetic fields, it can be highlighted the following:

Basis for Exposure Limitation

The Guidelines have been developed from the review of published scientific literature. Only proven solidly effects have been considered, as a basis for the restrictions to the exposure to electromagnetic fields. Biological effects of exposure to electromagnetic fields have been revised by the International Agency for Research on Cancer (IARC), ICNIRP, the World Health Organization (WHO) and national expert groups [2-18].

Basics Restrictions and Reference Levels

The limits to exposure to electric, magnetic and electromagnetic fields variables in time are obtained from basic restrictions, using mathematical modeling. The obtained limits seek prevent from adverse health effects. The electromagnetic field exposure restrictions have been calculated for two groups: occupational and general public.

The general public is referred to the entire population and the occupational exposure is related to these individuals performing regular job activities in electric facilities. Tables 2-1 and 2-2 summarize the reference levels for occupational and general public exposure, setting the limits for electric and magnetic fields to be fulfill.

Table 2-1: Reference levels for occupational exposure to time-varying electric and magnetic fields (Unperturbed rms values) [2-10].

Frequency range	E-field Strength $E(kVm^{-1})$	Magnetic field strength $H(Am^{-1})$	Magnetic Field B(T)
1 Hz-8 Hz	20	$1.63 \times 10^5/f^2$	$0.2/f^2$
8 Hz-25 Hz	20	$2 \times 10^4/f$	$2.5 \times 10^{-2}/f$
25 Hz – 300 Hz	$5 \times 10^2/f$	8×10^2	1×10^{-3}
300 Hz – 3 kHz	$5 \times 10^2/f$	$2.4 \times 10^5/f$	$0.3/f$
3 kHz – 10 MHz	1.7×10^{-1}	80	1×10^{-4}

Table 2-2: Reference levels for general public exposure to time-varying electric and magnetic fields (Unperturbed rms values) [2-10].

Frequency range	E-field Strength $E(kVm^{-1})$	Magnetic field strength $H(Am^{-1})$	Magnetic Field B(T)
1 Hz-8 Hz	5	$3.2 \times 10^4/f^2$	$4 \times 10^{-2}/f^2$
8 Hz-25 Hz	5	$4 \times 10^3/f$	$5 \times 10^{-3}/f$
25 Hz – 50 Hz	5	1.6×10^2	2×10^{-4}
50 Hz – 400 Hz	$2.5 \times 10^2/f$	1.6×10^2	2×10^{-4}
400 Hz – 3 kHz	$2.5 \times 10^2/f$	$6.4 \times 10^4/f$	$8 \times 10^{-2}/f$
3 kHz – 10 MHz	8.3×10^{-2}	21	2.7×10^{-5}

2.3.2 Legislation

As previously expressed, legislation around the world sets magnetic field limitations as based in the “Guidelines for Limiting Exposure to Time-Varying Electric and Magnetic Fields (1 Hz to 100 kHz)” in its previous version [2-19].

At European level, the applicable legislation is the "*Council Recommendation of 12 July 1999 on the Limitation of Exposure of the General Public to Electromagnetic Fields (0 Hz to 300 GHz)*". This legislation recommends limits for 50Hz magnetic fields: 100μT for the general public and 500 μT for occupational exposure [2-20]. Most

European countries follows this recommendation; however, some countries have established more restrictive limits. For general public, in Poland the limit is 75 μT, in Slovenia and in Flanders (the northern region of Belgium) the maximum value is 10 μT, and in Italy 3 or 10 μT, depending on new facilities or existing ones. Some other European countries outside European Union have specified also stronger limits. In Russia, the limit is 10 μT and in Switzerland is the very small value of 1 μT [2-21], [2-22].

In some states of the USA, limits are lower than those specified in ICNIRP guidelines. In Florida, the limit is 15 μT for 230 kV and 20 μT for 500 kV power lines. In New York, the limit is 20 μT [2-23].

For occupational exposure, the European Union set a recommendation of 500 μT (5 times larger than the limit for general public). However, Luxembourg settled a restriction of 100 μT and Poland of 251 μT. In Russia, the limit value for occupational public is also 100 μT [2-21], [2-24].

In Spain, applicable legislation is the *Real Decreto 1066/2001 of 28 September*, by which the regulation that establishes conditions for protection of the radioelectric public domain, restrictions on emissions of radio and measures of health protection from radio broadcasts is approved. This legislation is focused on the limitation of the general public exposure to electromagnetic fields produced for radio emissions [2-25]. This legislation complies the proposals expressed in the resolutions of Spanish Congress of Deputies and Senate, compelling the Government to develop a regulation related to the general public exposure to general radio emissions from mobile phone antennas. This legislation is not a specific legislation to limit magnetic fields generated by power system facilities, at 50 or 60 Hz. Nevertheless, it set the general public limit for 50 Hz magnetic field at 100 μT.

Besides, some regional Governments published their own legislation. Four of them, Castilla and León, Balearic islands, La Rioja and Madrid, have the same limits than the previous national legislation. In Cataluña, Navarra and Castilla-La Mancha, the limits have been reduced 50%, to 50 μT [2-26].

2.4 Literature Review of Proposed Methods for Limiting Magnetic Field of Power Lines

The limitation of magnetic field generated by power lines is a subject with growing interest. Several methods have been proposed, in the profuse published literature about the matter. These methods can be classified in three large different methodologies or approaches: Conductor allocation management, magnetic field compensation and shielding by metallic materials [2-27], [2-28]. Following, the main features of these methodologies are exposed.

2.4.1 Conductor Allocation Management

These methods are used to compensate magnetic fields generated by several parallel conductors. The reduction of magnetic field is obtained by allocating in appropriate positions the conductors, attaining magnetic field compensations. Magnetic field depends on the geometrical arrangement of the conductors, the distances between conductors, the measure point and the phase and module components of the currents. Next figures show the cross sectional view of magnetic field generated by the currents of a three-phase balanced power system [2-27]. In Figure 2-11, magnetic field generated by a flat and a delta configuration are shown. It can be observed that delta contour curves are closer to conductors and magnetic field decay faster.

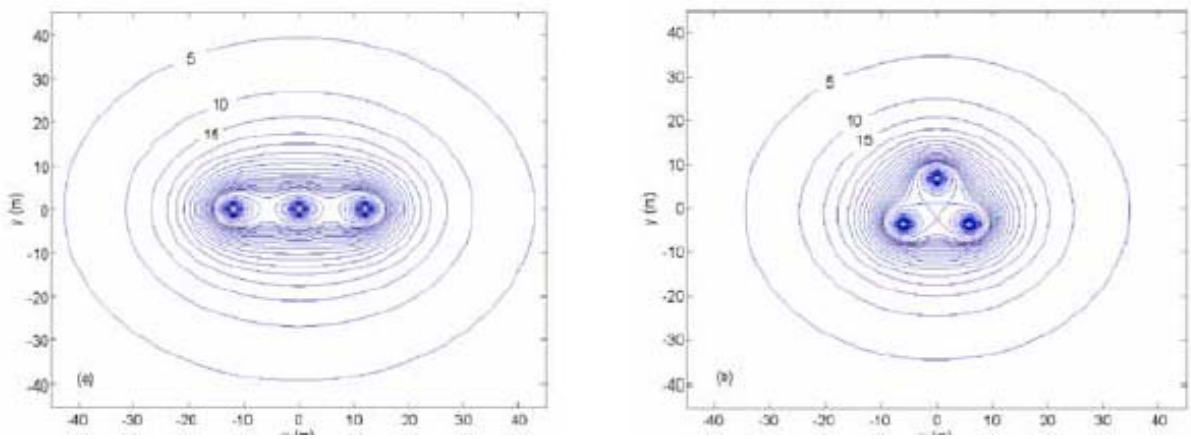

Figure 2-11: Curves of magnetic field generated by flat and delta configurations with a 12m phase-to-phase distance and currents of 2,000 A [2-27].

Higher magnetic field reductions can be obtained decreasing the distances between the phases. Fig. 2-12 shows the previous configurations, with the distances between phases reduced 50%. A important reduction on the magnetic field can be observed.

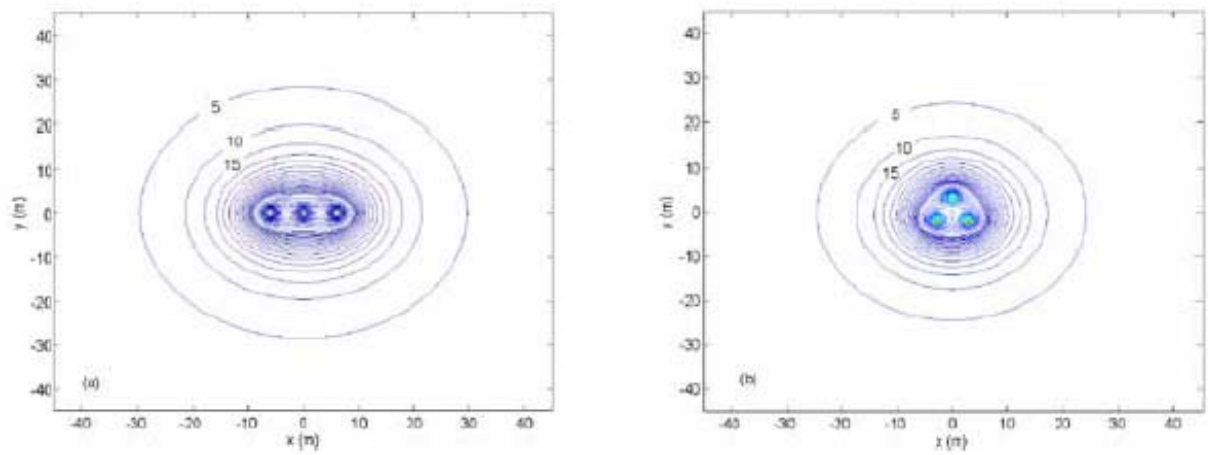

Figure 2-12: Curves of magnetic field generated by flat and delta configurations with a 6m phase-to-phase distance and currents of 2,000 A. [2-27].

Higher distances between conductors imply higher values of magnetic field. So, for the limitation of magnetic field in a specific area, the geometrical distances between conductors and also the separation with the measure points should be considered [2-27].

Besides, a compensation of the magnetic field can be achieved by the properly placement of conductors with different phases, obtaining low magnetic field configurations [2-27]. In Fig. 2-13, magnetic field generated for two different phase configurations are shown. It can be observed that the interchange of conductors positions can provide a lower magnetic field configuration.

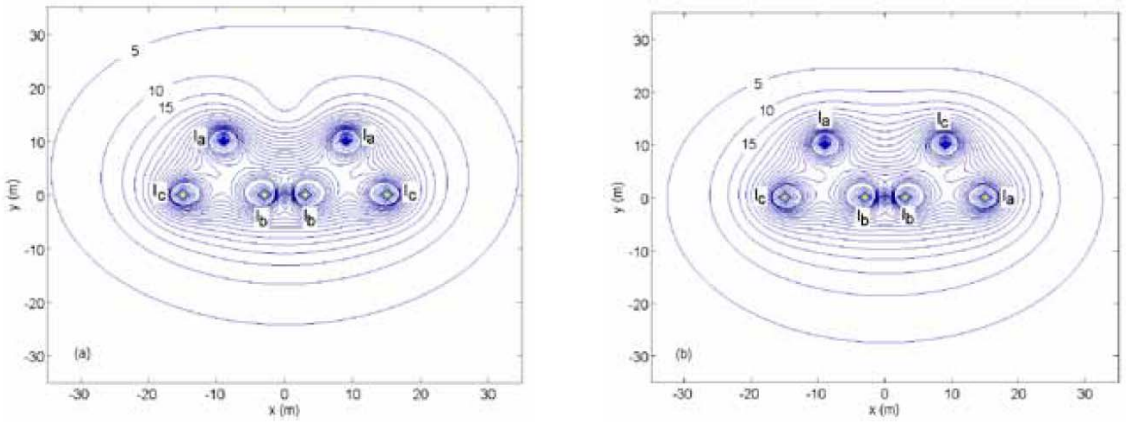

Figure 2-13: Curves of magnetic field contour curves (in μT) in two delta configuration (phase currents of 2000A and phase-to-phase clearances of 12m [2-27].

Several methods for magnetic field mitigation, based in the principle of optimal arrangement of conductors, can be found in literature [2-12], [2-27] - [2-34]. The new methods for minimization of construction costs and magnetic field proposed in this work can be framed into this methodology.

2.4.2 Magnetic Field Compensation

This method consists on the generation of an external source of magnetic field, compensating the magnetic field created by the powerline. These compensation techniques can be either active or passive [2-27], [2-28].

In the passive compensation method, the alternative magnetic field created by the power line induces a current in an external loop, appropriately placed. The magnetic field generated by the current in the external loop generates an opposing magnetic field, compensating the original magnetic field. In this method, the additional Joule losses appearing in the passive loop can be significant. As an example, in Figure 2-15 an instant of the interaction between a passive compensation loop and a powerline is represented [2-27].

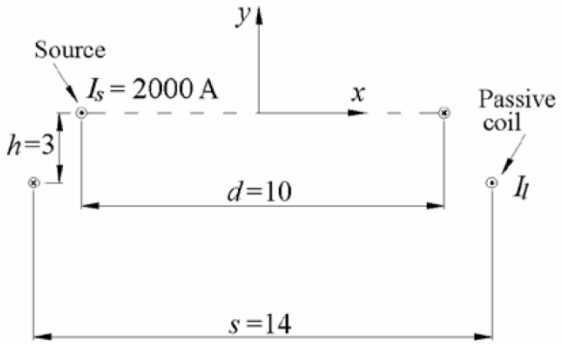

Figure 2-14: Magnetic field source constituted by two long conductors and a compensating single-turn loop, composed by long conductors shortcircuited at both ends (units in m) [2-27].

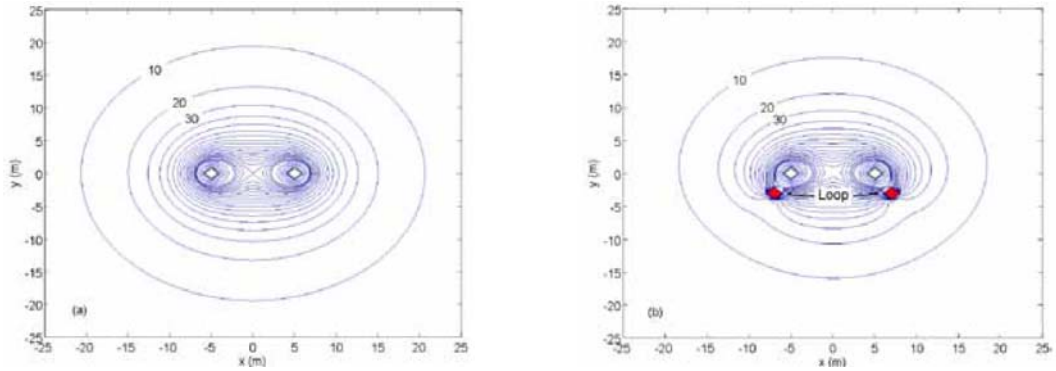

Figure 2-15: Magnetic field contour curves (in μT) created by the source and final field after placement of the passive loop [2-27].

In order to increase the magnetic field compensation in selected areas, an active external current source can be used, injecting appropriate values of currents in the external loop. This active method requires an external current source and a control system, resulting in a more complex system [2-27].

Methods for magnetic field mitigation based in magnetic field compensation are widely covered in technical literature [2-28], [2-35] - [2-41].

2.4.3 Shielding by Metallic Materials

Other possible technique for the reduction of magnetic field in specified regions is using metallic materials, forming shields and changing the magnetic field distribution. Shielding metallic materials separate the magnetic field from a specific region, changing the magnetic field lines and reducing the magnetic field in the selected area [2-27], [2-28], [2-42].

Two physical phenomena are involved in the magnetic field shielding method, the eddy currents created in the metallic material with high conductivity and the ferromagnetic behavior of high-permeability materials.

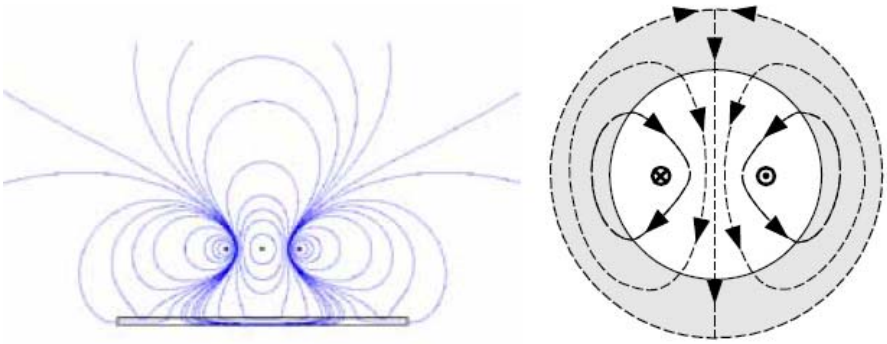

Figure 2-16: Displacement of magnetic field by an open shield (three phase field) and close shield field with internal source (single-phase field) [2-27].

Increase in the losses, impacts in ampacity, material and installation costs, limitations for the maintenance and possible corrosion in the metallic shield could be negative aspects to consider in these magnetic field reduction methods [2-27].

2.5 References

[2-1] PHISICS for Scientists and Engineers, Third Edition. Paul A. Tipler. Editorial Reverté.

[2-2] ABB High Voltage Cables, available online: http://new.abb.com/cables , last visit, June 2016.

[2-3] R. Grandino, M. Portillo, J. Planas, "Undergrounding the first 400kV transmission line in Spain using 2500mm2 XLPE cables in a ventilated tunnel: The Madrid Barajas Airport project", Jicable 2003.

[2-4] F.G Ibarra Romo, C. F. Fuentes Estrada, J. T. Arriaga Flores, M. Mammeri, "Modernization Manzanillo I. The Mexican largest transmission network of 400kV with XLPE cable systems: Design and Construction", B1-106, CIGRE 2012.

[2-5] Roberto Benato, Claudio Di Mario, Hermmann Koch, "High Capability Applications of Long Gas-Insulated Lines in Structures", IEEE Transactions on Power Delivery, Vol. 22, pp. 619 – 626, Jan-2007.

[2-6] REAL DECRETO 223/2008, de 15 de febrero, por el que se aprueban el Reglamento sobre condiciones técnicas y garantías de seguridad en líneas eléctricas de alta tensión y sus instrucciones técnicas complementarias ITC-LAT 01 a 09.

[2-7] Prysmian cables and systems. High voltaje systems, 31st of Oct., 2012. Avaliable in: http://www.prysmiangroup.com/en/business_markets/markets/hv-and-submarine/downloads/Brochures/

[2-8] Curso Especialista en proyecto y construcción de infraestructuras eléctricas de Alta tensión de la Universidad Pontificia Comillas de Madrid. Módulo: líneas de transporte de energía eléctrica. Tema: tecnología de líneas de cables aislados.

[2-9] Normas UNE 21144-1-1:1997 Cables eléctricos. Cálculo de la intensidad admisible. Parte 1: Ecuaciones de intensidad admisible (factor de carga 100%) y cálculo de pérdidas. Sección 1: Generalidades

[2-10] W. Moutassem and G. J. Anders. Configuration Optimization of Underground Cables for Best Ampacity. IEEE Transactions on Power Delivery, vol. 25, no. 4, October (2010).

[2-11] R. de Lieto Vollaro, L. Fontana and A. Vallati. Thermal analysis of underground electrical power cables buried in non-homogeneous soils. Applied Thermal Engineering, vol. 31, issue 5, 2011, pp. 772–778, April 2011.

[2-12] G. G. Lai, C. Yang, H. Huang, and C. Su, Senior Member, IEEE "Optimal Connection of Power Transmission Lines with Underground Power Cables to Minimize Magnetic Flux Density Using Genetic Algorithms." IEEE Transaction on Power Delivery, Vol. 23, Nº 3, July 2008.

[2-13] IEEE Magnetic Fields Task Force Report , Magnetic Fields from Electric Power Lines Theory and Comparison to Measurements, IEEE Trans. on Power Delivery, 3(4) (1988) 2127-2136.

[2-14] H. M. Ismail, Characteristics of the Magnetic Field under Hybrid ac/dc High Voltage Transmission Lines, Electric Power Systems Research, 79 (2009) 1–7.

[2-15] Bracken, T. Dan, "Assessing compliance with power-frequency magnetic-field guidelines", Health Physics, September 2002, Volume 83, Issue 3, pp 409-416.

[2-16] A.S. Farag, M.M. Dawoud, T.C. Cheng, Jason S. Cheng, "Occupational exposure assessment for power frequency electromagnetic fields", Electric Power Systems Research, Volume 48, Issue 3, 1 January 1999, Pages 151-175.

[2-17] International Commission on Non-Ionizing Radiation Protection website http://www.icnirp.org

[2-18] "International Commission on Non-Ionizing Radiation Protection, Guidelines for Limiting Exposure to Time Varying Electric and Magnetic Fields (Up To 100 kHz)", ICNIRP Guidelines, 2010.

[2-19] ICNIRP Guidelines: Guidelines for Limiting Exposure to Time Varing Electric, Magnetic, and Electro Magnetic Fields (Up To 300 Ghz) – International Commission on Non-Ionizing Radiation Protection. 17 November 1997.

[2-20] European Commission, Council Recommendation of 12 July 1999 on the Limitation of Exposure of the General Public to Electromagnetic Fields (0 Hz to 300 GHz), The Council of The European Union, 1999.

[2-21] Rianne Stam (Laboratory for Radiation Research, National Institute for Public Health and the Environment, the Netherlands), Comparison of International Policies on Electromagnetic Fields (Power Frequency and Radiofrequency Fields), May 2011.

[2-22] European Commission, Report on the implementation of the Council Recommendation on the limitation of exposure of the general public to electromagnetic fields (0 Hz – 300 GHz) (1999/519/EC) in the EU Member States, Commission staff working paper, 2008.

[2-23] "Limits in the USA", EMFS, available online: http://www.emfs.info/, last visit, Jan. 2016.

[2-24] European Commission, Directive 2004/40/EC, The Council of The European Union, 2004.

[2-25] REAL DECRETO 1066/2001, de 28 de Septiembre, por el que se aprueba el Reglamento que establece condiciones de protección de dominio público radioeléctrico, restricciones a las emisiones radioeléctricas y medidas de protección sanitaria frente a emisiones radioeléctricas.

[2-26] Informe del ministerio de Sanidad y Consumo sobre la aplicación del Real Decreto 1066/2001, de 28 de Septiembre, por el que se aprueba el Reglamento que establece condiciones de protección de dominio público radioeléctrico, restricciones a las emisiones radioeléctricas y medidas de protección sanitaria frente a emisiones radioeléctricas.

[2-27] CIGRE Working Group C4.204. Mitigation Techniques of Power Frequency Magnetic Fields Originated from Electric Power Systems, Feb. 2009.

[2-28] Ippolito, M. G., Puccio, A., Ala, G., Ganci, S., "Attenuation of low frequency magnetic fields produced by HV underground power cables", *Power Engineering Conference (UPEC), 2015 50th International Universities,* pp. 1-5, 2015.

[2-29] V.S. Rashkes y R. Lordan. "MAGNETIC FIELD REDUCTION METHODS: EFFIFIENCY AND COST." IEEE Transactions on Power Delivery, Vol. 13, Nº2, April 1998.

[2-30] G. G. Karady, C. V. Nunez and R. Raghavan, "The Feasibility of Magnetic Field Reduction by Phase Relationship Optimization in Cable Systems", IEEE Transactions on Power Delivery, Vol. 13, No. 2, April 1998.

[2-31] E. I. Mimos, D. K. Tsanakas and A. E. Tzinevrakis, "Optimum phase configurations for the minimization of the magnetic fields of underground cables", Electrical Engineering, vol. 91, no. 6, pp. 327-335, 2010.

[2-32] G. G. Lai, C. Yang and C. Su, "Estimation and management of magnetic flux density produced by underground cables in multiple-circuit feeders", European Transactions on Electrical Power, vol. 20, (2010), pp. 545–558, 2010.

[2-33] M. S. H. Al Salameh and M. A. S. Hassouna. Arranging Overhead Power Transmission Line Conductors using Swarm Intelligence Technique to Minimize

Electromagnetic Fields. Progress in Electromagnetics Research B, vol. 26, (2010), pp. 213-236, 2010.

[2-34] C. F. Yang, G. G. Lai, C. T. Su and H. M. Huang, "Mitigation of magnetic field using three-phase four-wire twisted cables", Int. Trans. Electr. Energ. Syst. Vol. 23, pp 13–23, 2013.

[2-35] J. C. Pino López, P. Cruz-Romero, L. Serrano-Iribarnegaray, and J. Martínez-Román, "Magnetic field shielding optimization in underground power cable duct banks", Electric Power Systems Research, vol. 114, pp. 21-7, Sep. 2014.

[2-36] Canova, A., Bavastro, D., Freschi, F., Giaccone, L., Repetto, M. "Magnetic shielding solutions for the junction zone of high voltage underground power lines," *Electric Power Systems Research*, Vol. 89, pp. 109–115, 2012.

[3-37] A. Canova and L. Giaccone. A Novel Technology for Magnetic-Field Mitigation: High Magnetic Coupling Passive Loop. IEEE Transactions on Power Delivery, vol. 26, no. 3, July (2011).

[2-38] A. Canova, F. Freschi, L. Giaccone and A. Guerrisi. The High Magnetic Coupling Passive Loop: A Steady-State and Transient Analysis of the Thermal Behavior. Applied Thermal Engineering, 37, (2012), pp. 154–164., May 2012.

[2-39] A.R. Memari, W. Janischewskyj, "Mitigation of Magnetic Field Near Power Lines", IEEE Transactions on Power Delivery, Vol. 11, Nº. 3, July 1996.

[2-40] Kenichi Yamazaki, Tadashi Kawamoto, and Hideo Fujinami, "Requirements for Power Line Magnetic Field Mitigation Using a Passive Loop Conductor", IEEE TRANSACTIONS ON POWER DELIVERY, VOL. 15, NO. 2, APRIL 2000.

[2-41] Pedro Cruz, Carlos Izquierdo, and Manuel Burgos, "Optimum Passive Shields for Mitigation of Power Lines Magnetic Field", IEEE Transactions on Power Delivery, vol. 18, Nº. 4, October 2003

[2-42] Karim Wassef, Vasundara V. Varadan, and Vijay K. Varadan, Magnetic Field Shielding Concepts for Power Transmission Lines, IEEE Transactions on Magnetics, vol. 34, Nº. 3, May 1998.

Chapter 3. Optimal Geometric Configurations for Mitigation of Magnetic Fields of Underground Power Lines

3.1 Abstract

In this chapter, a nonlinear optimization problem for calculating the optimal configuration of underground power lines is proposed. In the analysis, considerations of geometry, economy and maximum magnetic field are taken into account. The cable bundles are allowed to be placed freely in the available space to achieve the most economical configuration. Real test cases are used to evaluate the methodology. Based on the results, it is observed that the rotation of the cables is important to improve interaction and decrease the magnetic field in desired locations. These rotations can be obtained simply through the appropriate manipulation of the cables during the construction phase. Negligible magnetic fields can be obtained in the measurement plane when the optimal geometrical configuration is used. Sensitively analyses are performed in the solution, for evaluating the effect of differences in angles and modules of the currents in the cables. The content of this article has been partially published in the *IEEE PowerTech Conference, Eindoven, 2015*.

3.2 Introduction

Underground transmission lines have several advantages, including reduced visual impact, shorter required distances to other objects and increased security for users. However, an underground transmission line produces electromagnetic fields, as does any other transmission line. Therefore, restrictions must be enforced to reduce the potential risk of human exposure to these electromagnetic fields. From 1998, the International Commission on Non-Ionizing Radiation Protection (ICNRP) issued specific recommended limits on population exposure to magnetic fields. In 2010, ICNRP settled recommended maximum value of magnetic fields for general public exposure to 200 μT, for a frequency of 50Hz [3-1]. However, in other countries [3-2] and regions [3-3], values lower than this maximum are enforced to decrease the exposure of citizens to magnetic fields.

In [3-4], more than 140 papers are reviewed and discussed to summarize the possible techniques for mitigating extremely low-frequency magnetic fields in transmission lines, focalizing in overhead power lines. Also, how to calculate the optimal configuration of underground cables for the reduction of the magnetic fields has attracted the interest of the scientific community. In [3-5], a method is proposed for reducing the magnetic fields in a multi-circuit underground cable system that is carrying unbalanced loads by optimizing the phase relations. In [3-6], underground cables in arrangements of two, three and more than three 3-phase systems are investigated to determine the optimal combinations for reducing the magnetic fields present in the ground. The authors of [3-7] analyze multiple-circuit underground cable feeders with randomly varying loads, with the intent of reducing the magnetic fields produced by the feeders, using genetic algorithms. In [3-8], the authors propose the use of twisted cables to reduce the magnetic fields produced by the cables. In [3-9], an optimization process, also based on a genetic algorithm, is presented for the minimization of the cost (including losses) of ferromagnetic and conductive shields.

In most of the papers cited above, the geometries of the problems are fixed, and the algorithms can choose only among several pre-specified alternatives. Moreover, some of these formulations require advanced solution methods (such as genetic algorithms) to obtain their solutions. The present chapter proposes a nonlinear optimization problem (using all continuous variables), in which the most economical positions for the cables

are calculated by considering the construction costs for installation and the magnetic fields generated by the underground cables. The solution of the optimization problem is reached using conventional commercial solvers. This method is applied to cases of 4 and 6 3-phase cable bundles. The results demonstrate that it is possible to nearly cancel the effect of the magnetic fields in the measurement zone using the appropriate geometrical configuration.

3.3 The Optimization Problem

In the present work, the objective is to determine the optimal coordinates for underground cables arranged in *n* 3-phase cable bundles to achieve the minimum possible construction costs. The major costs associated with the installation of underground transmission lines are the cost of civil construction and the right-of-path cost. Civil construction costs include the cost of digging plus the cost of filling and compacting a trench with a rectangular cross section in which the bundles are laid. Moreover, for security reasons and to prevent the possible collapse of the walls of the trench, it is necessary to shore up the walls during installation, which incurs additional costs. The proposed optimization problem is summarized by equations (3-1)-(3-13).

$$min\ f(x) = c_x \frac{\sum_{i=1}^{n}|x_i|}{n} - c_y y_1 - c_{vol} y_1 \frac{\sum_{i=1}^{n}|x_i|}{n} \tag{3-1}$$

s.t.

$$b_x^{\,k} = \frac{\mu_0}{2\pi}\left(\Im_{1a} \frac{y_{1a}-Y_c}{(X_c-x_{1a})^2+(Y_c-y_{1a})^2} + \Im_{1b} \frac{y_{1b}-Y_c}{(X_c-x_{1b})^2+(Y_c-y_{1b})^2} + \Im_{1c} \cdot \frac{y_{1c}-Y_c}{(X_c-x_{1c})^2+(Y_c-y_{1c})^2} + \dots \right.$$
$$\left. + \Im_{na} \frac{y_{na}-Y_c}{(X_c-x_{na})^2+(Y_c-y_{na})^2} + \Im_{nb} \frac{y_{nb}-Y_c}{(X_c-x_{nb})^2+(Y_c-y_{nb})^2} + \Im_{nc} \cdot \frac{y_{nc}-Y_c}{(X_c-x_{nc})^2+(Y_c-y_{nc})^2} \right) \tag{3-2}$$

$$b_y^{\,k} = \frac{\mu_0}{2\pi}\left(\Im_{1a} \frac{X_c-x_{1a}}{(X_c-x_{1a})^2+(Y_c-y_{1a})^2} + \Im_{1b} \frac{X_c-x_{1b}}{(X_c-x_{1b})^2+(Y_c-y_{1b})^2} + \Im_{1c} \frac{X_c-x_{1c}}{(X_c-x_{1c})^2+(Y_c-y_{1c})^2} + \dots \right.$$
$$\left. + \Im_{na} \frac{X_c-x_{na}}{(X_c-x_{na})^2+(Y_c-y_{na})^2} + \Im_{nb} \frac{X_c-x_{nb}}{(X_c-x_{nb})^2+(Y_c-y_{nb})^2} + \Im_{nc} \frac{X_c-x_{nc}}{(X_c-x_{nc})^2+(Y_c-y_{nc})^2} \right) \tag{3-3}$$

$$\left(b_x^{\,k}\right)^2 + \left(b_y^{\,k}\right)^2 \le B_{max}^2 \tag{3-4}$$

$$\left(x_{ia}-x_{ib}\right)^2+\left(y_{ia}-y_{ib}\right)^2=d^2 \tag{3-5}$$

$$\left(x_{ia}-x_{ic}\right)^2+\left(y_{ia}-y_{ic}\right)^2=d^2 \tag{3-6}$$

$$\left(x_{ib}-x_{ic}\right)^2+\left(y_{ib}-y_{ic}\right)^2=d^2 \tag{3-7}$$

$$\frac{x_{ia}+x_{ib}+x_{ic}}{3}=x_i \tag{3-8}$$

$$\frac{y_{ia}+y_{ib}+y_{ic}}{3}=y_i \tag{3-9}$$

$$\left(x_i-x_j\right)^2+\left(y_i-y_j\right)^2 \geq {d_{Min}}^2 \ , \ i \neq j \tag{3-10}$$

$$y_1 \leq y_i \ , \ i \neq 1 \tag{3-11}$$

$$-X_{Max} \leq x_i \leq X_{Max} \tag{3-12}$$

$$-Y_{Max} \leq y_i \leq -Y_{Min} \tag{3-13}$$

$i, j = 1,\ldots,n$, k= 1, …, k_{Max}

Where,

μ_0 is the permeability of free space, (H m^{-1}).

b is the magnetic field, (μT).

B_{max} is the maximum magnetic field allowed in the evaluation plane, (μT).

b_{xi} and b_{yi} are the modules of phasors of horizontal and vertical components of magnetic field, cable *i*, (μT).

c_i are the costs, (€/m^2) or (€/m^3).

d is the distance between two centers of cables in a bundle, (m).

I_{il} is the phasor of current flowing through the cable in the *i*-bundle of cables, phases $l=\{a, b, c\}$, (A).

X_{Max} is the maximum horizontal distance allowed from the center of a bundle and the horizontal reference, (m).

Y_{Max} and Y_{Min} are the maximum and minimum depth allowed to the center of any 3-phase cable bundles, (m).

The variables are:

b_x^k, horizontal component of the magnetic field in the *k*-point of the evaluation plane, (μT).

b_y^k, vertical component of the magnetic field in the *k*-point of the evaluation plane, (μT).

(x_i, y_i), coordinates of the centre of the *i*-bundle of cables, (m).

(x_{il}, y_{il}), coordinates of the centre of the *l*-cable in the *i*-bundle of cables, corresponding to phase *l*.

The objective function (3-1) contains three terms, considering horizontal costs per unit associated to the occupation of the land (c_x), vertical costs per unit related with digging operations (c_y) and volumetric costs per unit due to movements of terrain (c_{vol}). In the first term, the mean value of the cables distance is calculated and multiplied by the horizontal costs (c_x), to obtain a more compact solution. As the cable bunches may be located on either side of the vertical axis (Fig. 3-1), the module of the x_i values must be used in (3-1).

In the second term of (3-1), the vertical construction costs are calculated for both digging and shoring operations. The depth is defined by the deepest bundle. In the present simulation case, if all cables carry the same current (in module), any of them can be assumed to be the deepest. In Eq. (3-11), bundle 1 is defined as the deepest one. The third term of (3-1) represents the volumetric construction costs associated with digging, filling and compacting the trench. In the present study, the values of the costs per unit used for the simulations are obtained from a general reference for construction costs in Spain: c_x = 10 €/m², c_y= 14.59 €/m² and c_{vol}= 6.5 €/m³. As presented, in (3-1), only construction costs are considered; the costs of the cables themselves are not included.

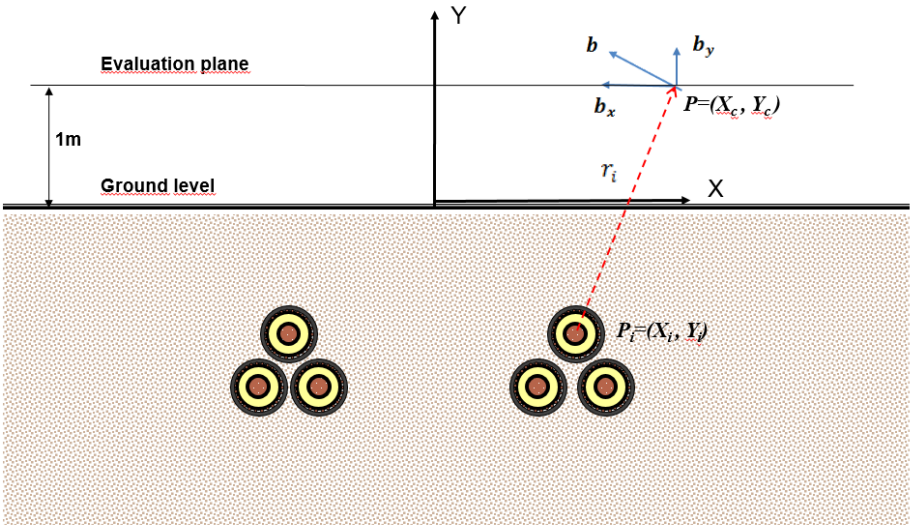

Figure 3-1. Magnetic field generated by a conductor at point P.

Equations (3-2) and (3-3) calculate modules of phasors of the horizontal and vertical components of the magnetic field at each of the k measurement points. These points are located along the line 1 m above the terrain, with separations of 0.2 m between them (see Fig. 3-1). In the present simulations, k_{Max} is equal to 51, representing a measurement line of 10 m, 5 m to either side of the vertical axis. The module of the magnetic field at all measurement points is restricted to a specified maximum value B_{max}^2 by (3-4).

The centers of the cables in each bundle must be located on the vertices of an equilateral triangle, as specified in (3-5)-(3-7). The separation between cables in the same bundle is very important to the design of the circuit. A lower separation allows for more compact solutions with lower construction costs. However, the ampacity of the bundle may be compromised by the inter-heating transfer among the cables in the bundle and the resulting limits on the allowed maximum current. Moreover, the separation between the cables affects the interaction of the magnetic fields, as indicated by (3-2) and (3-3). In the present study, the results of simulations using d = 0.32 m are presented, value dues to the dimensions of the cables.

The centers of the cable bundles are calculated by (3-8) and (3-9). To guarantee that none of the 3-phase cable bundles overlap and to ensure sufficient distance between

circuits (related to the desired ampacity), a minimum distance between circuits is imposed, (3-10). In the present simulations, the results correspond to d_{Min} = 0.8 m. This is a typical value for Spanish underground lines as the here analyzed.

For security reasons, Spanish legislation forbids the installation of wires at depths less than 0.6 m; in addition, burial depths greater than 3 meters are beyond the capacity of the construction equipment and the maximum distance between two circuits is limited to 6 meters because of the nature of urban terrain. In the present cases, 220kV balanced underground power circuits of single core XLPE cables, with a cupper conductor of 2,500 mm² section, are used. The previous geometrical constraints are represented in the optimization problem by inequalities (3-12) and (3-13), related to the centers of the bundles, where X_{Max} = 2.765 m, Y_{Min} = -0.835 m and Y_{Max} = -2.765 m.

3.4 Results

3.4.1 Same Phase Angles and Currents in the Circuits

The maximum value of magnetic exposure recommended by ICNRP (200 μT for general public, [3-1]) is generally easily obtained for most underground transmission lines. However, several European countries and regions are adopting more restrictive values, for increasing the security of the population [3-2], [3-3], [3-10], [3-11]. The goal of this study is to evaluate optimal geometrical configurations for reduced exposure limits of magnetic fields and to analyze this reduction effects in the construction costs. Therefore, the proposed optimization problem is solved 6 times for the following maximum values of the magnetic field allowed in the evaluation plane, in (3-4): B_{max}={10, 6, 3, 2, 1, 0.3}. In the first analysis, four and six 3-cables bundles with balanced currents flowing through them with module of 1,700 A and the same phase angle between circuits, are studied.

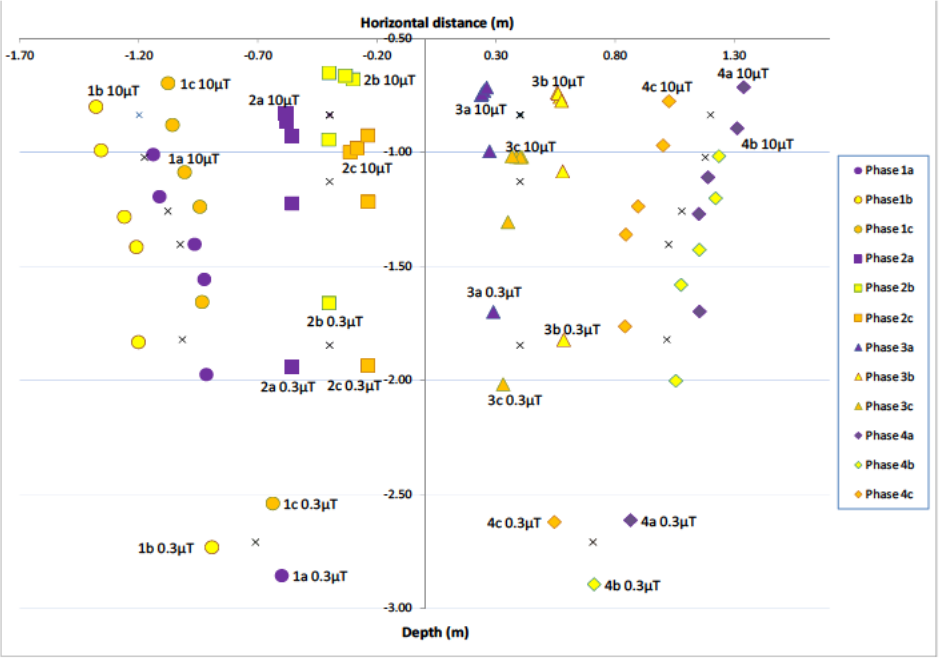

Figure 3-2. Optimal positions of the cables and bundle centers for 4 circuits and B_{max} = {10, 6, 3, 2, 1, 0.3} μT.

In Fig. 3-2, for a maximum magnetic-field value of 10 μT and 4 cable bundles, all bundles are at the same depth, the minimum allowed by legislation. This configuration corresponds to the lowest possible construction cost. However, it must be stressed that the optimal configuration doesn't correspond to a conventional bundle cable position (two lowest cables at the same depth and the third placed above them, Fig. 3-3, but to a rotated position. For maximum magnetic-field values decreasing from 10 to 2 μT, the central bundles remain at nearly the same positions (a small rotation is observed), but the farthest bundles move to greater depths. To reach a maximum magnetic-field value of below 2 μT, the depths of the central bundles must also increase. It must be emphasized that the proposed method allows the magnetic field in the measurement plane to be mitigated to nearly undetectable values, 0.3 μT, simply by changing the positions of the bundles.

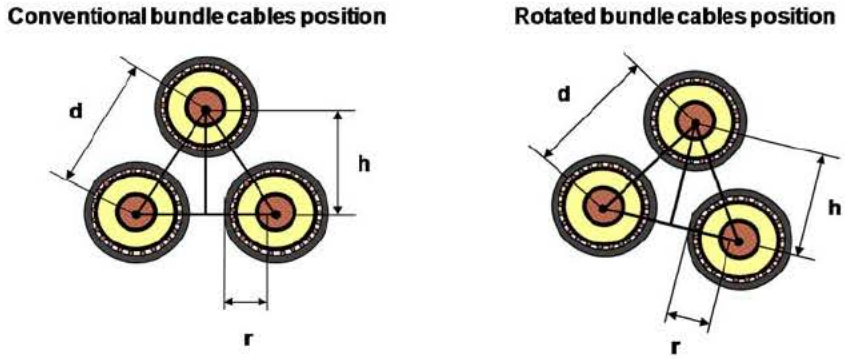

Figure 3-3. Diagram of the geometry of conventional and rotated bundle cables.

From Fig. 3-4, the blue line shows that the reduction in the magnetic field is associated with an increase in the construction costs. In this figure, an additional point is depicted, the construction cost for Bmax = 20 μT, to show the trend of costs for larger values of Bmax. It must be highlighted that almost negligible magnetic fields can be obtained in the measure plane, with the adequate geometrical configuration.

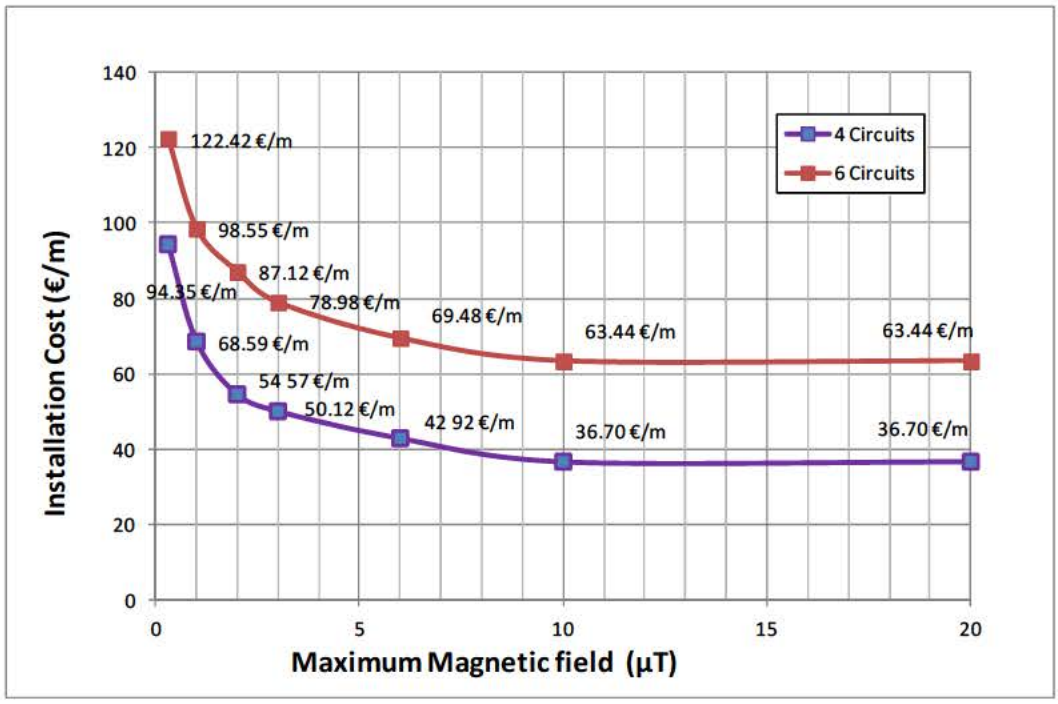

Figure 3-4. Installation costs for Bmax = {10, 6, 3, 2, 1, 0.3}

The rotation of the bundles has a strong influence on the magnetic field generated by the cables, as it can be seen in Fig. 3-5. In this figure, the optimal positions of the bundles (as obtained from the solution of the proposed optimization problem, B_{max} = 0.3 μT) and the most near conventional positions are depicted.

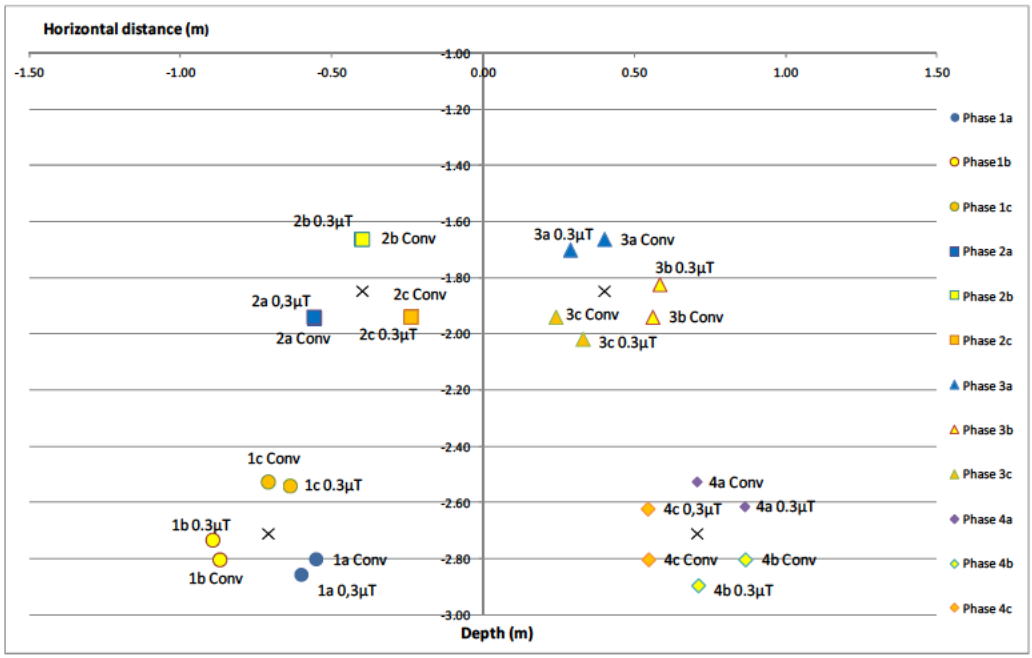

Figure 3-5. Positions of cables and bundle centres with conventional and optimally rotated arrangements, Bmax = 0.3 μT and 4 cable bundles.

The maximum magnetic field generated by the conventional configuration of Fig. 3-5 is approximately 13.79 μT, 4,597% larger than the maximum value obtained for the optimally rotated bundles.

For 6 bundles of 3 cables each one, the optimization problem has been solved 6 times again, for the same maximum values of magnetic field allowed in the evaluation plane Bmax = {10, 6, 3, 2, 1, 0.3} μT. In Fig. 3-6, the positions of the centers of the cable bundles for the 6 circuits are shown. Due to the complexity of the figure, the cables are not represented.

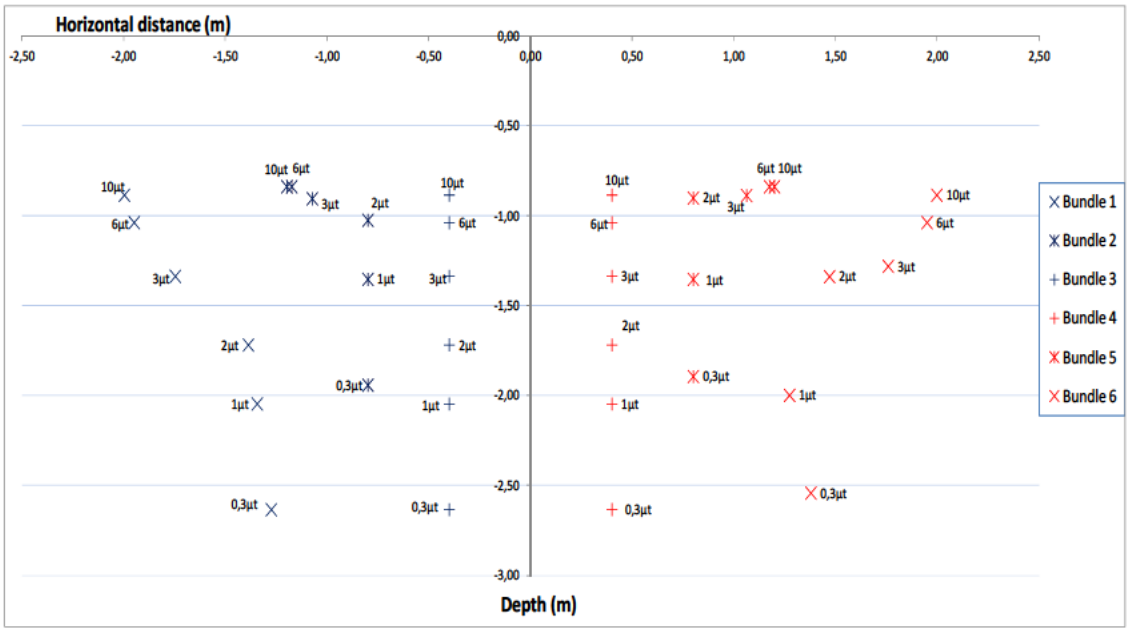

Figure 3-6. Optimal positions of the bundle centres for 6 circuits, B_{max} = {10, 6, 3, 2, 1, 0.3} μT.

With 6 circuits, the optimal solution for B_{max} = 10 μT allocate the bundles at the most superficial positions with low-price construction costs, as in the previous case of 4 cable bundles (Fig. 3-2). For more restricted values of B_{max} (between 10 and 3 μT) 2 of the bundles remains at superficial positions (the 2 and 5 in Fig. 3-6), whereas the other 4 displace to deeper points. For required B_{max} lower than 3 μT, also the most superficial bundles have to move to deeper positions. It must be highlighted that, with the adequate positions, the magnetic field can also be restricted to negligible values (lower than 0.3 μT) in the measure plane, however the system of 6 3-phase circuits with 1,700 A flowing in each cable. For B_{max} = 0.3 μT, the optimal solution for 6 circuits (Fig. 3-6) requires approximately the same deep of excavation (2.6 m) than the optimal solution for 4 circuits (Fig. 3-2). However, the width of the excavation is larger, due to the increased number of circuits and the minimum required separation between them.

The red line of Fig. 3-4 shows the construction costs for the different limits in the maximum magnetic field for 6 cable bundles. The minimum construction cost (63.44€/m) is 172.86% larger than the minimum construction cost for 4 circuits (36.70 €/m). This increment of costs is due to the larger number of circuits and the required distance between circuits, for limiting the inter-heating. For reduced values of magnetic field in the measure plane, the costs increases. Maintaining a maximum of 0.3 μT with 6

circuits (122.43 €/m) is almost twice more expensive (192.98%) than for a maximum of 10 μT. It must be stressed that, with the considered costs, maintaining an almost negligible magnetic field (0.3 μT) with 6 circuits is only 30.33% more expensive than with 4 circuits. However, increasing from 4 to 6 the number of circuits results in 50% of enlarged capacity. Therefore, the more profitable solution (larger number of circuits in the same excavation) can be used without compromising the healthy constraints.

3.4.2 Different Phase and Module Currents in the Circuits

Different phases or modules in the currents of the circuits result in different interactions of the magnetic fields, and therefore in differences in the optimal positions and costs. In the practice, the currents are more or less dissimilar in the circuits. A sensitivity study is here performed, for the case of four circuits.

For evaluating the phase difference influence, a first study considers balanced currents with modules of 1,700 A and phase angles (-45°, -15°, 15° and 45°) in (I_{1a}, I_{2a}, I_{3a} and I_{4a}), respectively. In other study, balanced currents with same phase angles and different modules are represented (two circuits with 1,700 A and two with 850 A).

As in previous cases, optimal positions of cables and installation costs for maximum magnetic field generated of 10, 6, 3, 2, 1 and 0.3 μT have been calculated. Fig. 3-7 compares installation costs for both previous studies: the blue line for circuits with equal currents and different phase angles and the red line for different modules. For comparison, the green line reproduces the same balanced case in all four circuits of Fig. 3-4.

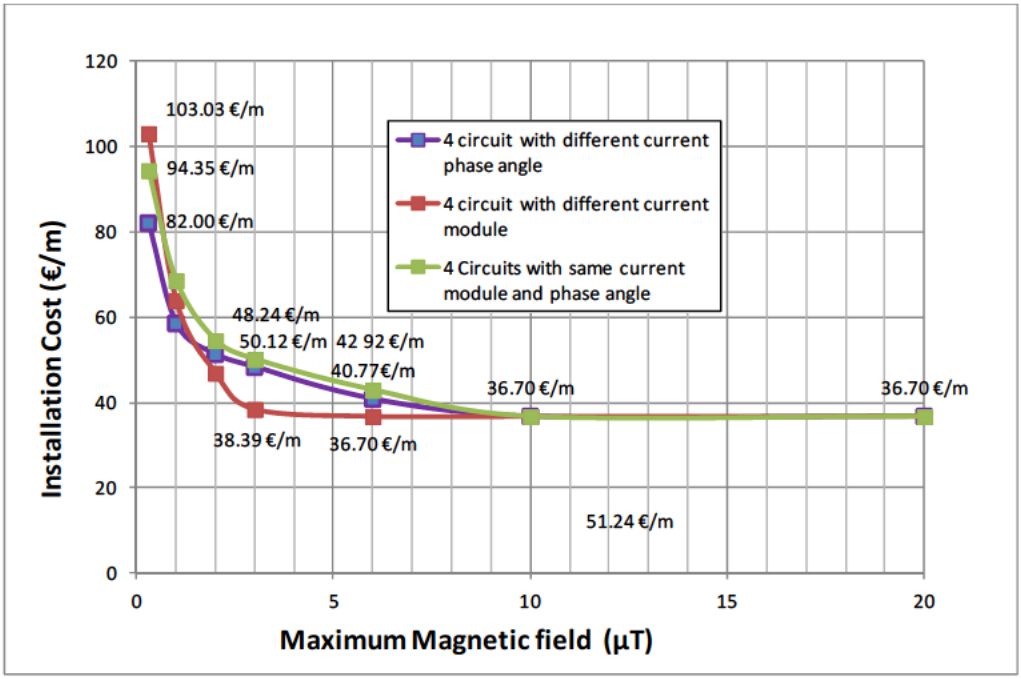

Figure 3-7. Installation costs for B_{max} = {10, 6, 3, 2, 1, 0.3} µT with different current phase angles and modules in circuits.

From the curves, in the studied cases the installation costs are not largely modified for module or phase differences in the currents. In fact, for more than 10 µT, the installation costs are the same for all the cases. It can be highlighted that the differences in the currents modules (in this case, a reduction in two of the bundles) result in the highest installation costs for 0.3 µT and the fastest cost reduction.

The evolution of costs and positions of cables, when only one of the circuits changes the phase angle and module of the current, is also studied. On two additional studies, I_{1a} changes the phase angle from -20° to 20° or the module of current from 80% to 100% of the rated current 1,700 A. Figs. 3-8 and 3-9 show the optimal positions for all the cables in both cases, respectively. In these studies, a maximum magnetic field of 2 µT is considered, the other three circuits have angle 0º and rated current 1,700 A, I_{1b} and I_{1c} are always dephased ±120º with I_{1a} and $|I_{1a}|=|I_{1b}|=|I_{1c}|$.

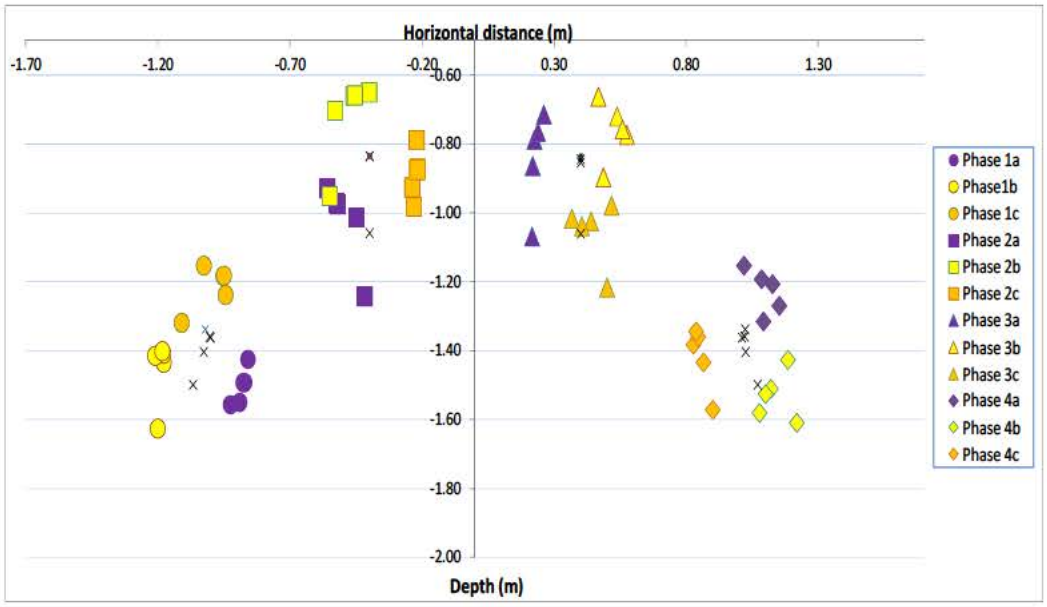

Figure 3-8. Position of cables with current phase angle of one circuit varying from -20° to 20°.

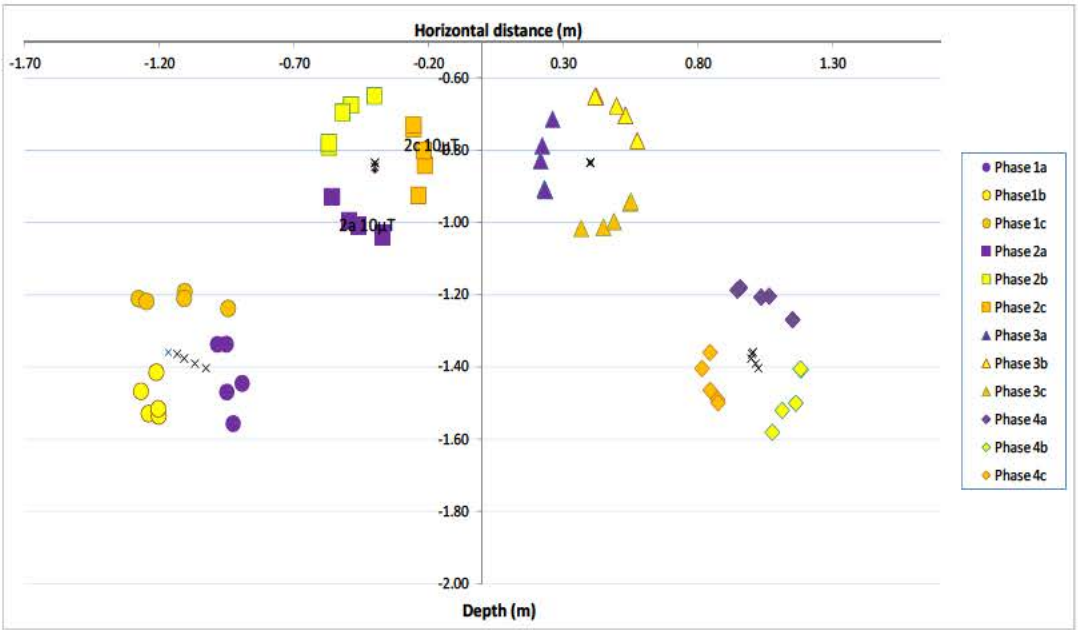

Figure 3-9. Position of cables with module current of one circuit varying from 80% to 100%, of rated current 1,700A.

From Figs 3-8 and 3-9, the optimal positions of all cables are modified when angles or modules of currents flowing in one of them are changed. On the studied cases, the variation of phase angle in one circuit produces more construction changes than the modifications in the module of the current.

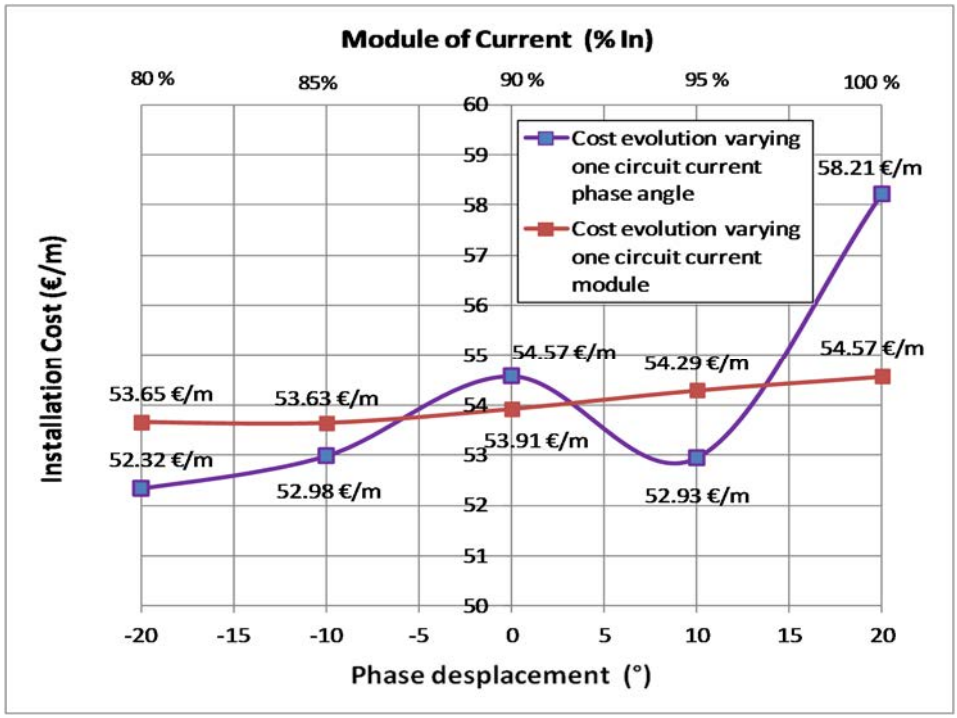

Figure 3-10. Installation costs with different module and phase angle in one circuit.

In Fig. 3-10, the costs in the optimal solutions for the variations studied in Figs. 3-8 and 3-9 are depicted. Changes in the value of the module of currents in one bundle (red curve of Fig. 3-10) results in small variations in the construction cost. As expected, less currents result on smaller costs. The angles of the currents modify up to 11% the construction costs (blue curve in Fig. 3-10), for the same amount of current.

Finally, phase angle and module of I_{1a} are varied, keeping the optimal positions calculated for balanced currents (Fig. 3-2) in all the cables. As previously, the optimal solution for B_{max} = 2 μT is considered. Fig. 3-11 shows the magnetic field when phase angle of I_{1a} varies from -20° to 20° (I_{1b} and I_{1c} are always dephased ±120º with I_{1a}, respectively).

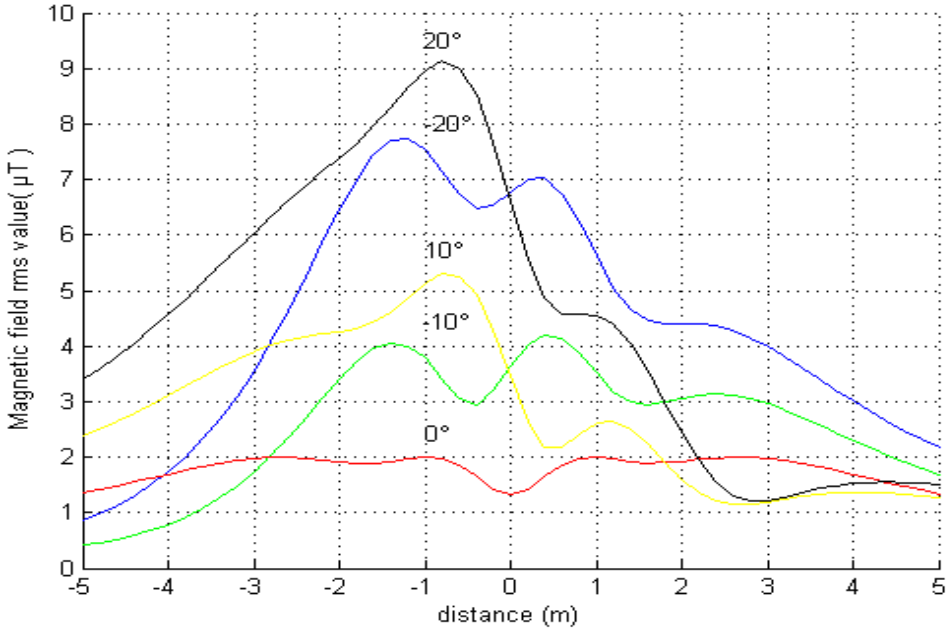

Figure 3-11. Maximum magnetic field when current module in one circuit changes, keeping the optimal positions of cables of Fig. 3.2.

From Fig. 3-11, the maximum magnetic field profiles in the evaluation plane dues to the optimal position of cables for balanced and equals modules and phases of the currents (red line) is symmetrical and restricted to 2 µT. When maintaining the same geometrical positions in all the cables, phase differences in I1 produce a peak of the maximum magnetic field in the measure plane. From the curves, the magnetic field increases mainly in function of the module in the value of the angle. However, positive angle deviations result in larger magnetic fields than negative ones.

Similarly, Fig. 3-12 depicts the profiles of maximum magnetic field, when varying the current modules of I1a, I1b and I1c from 80 to 100% of rated current 1,700 A, if all the cables maintain the optimal position of Fig. 2 with Bmax = 2 µT and $|I_{1a}|=|I_{1b}|=|I_{1c}|$ in all the simulations.

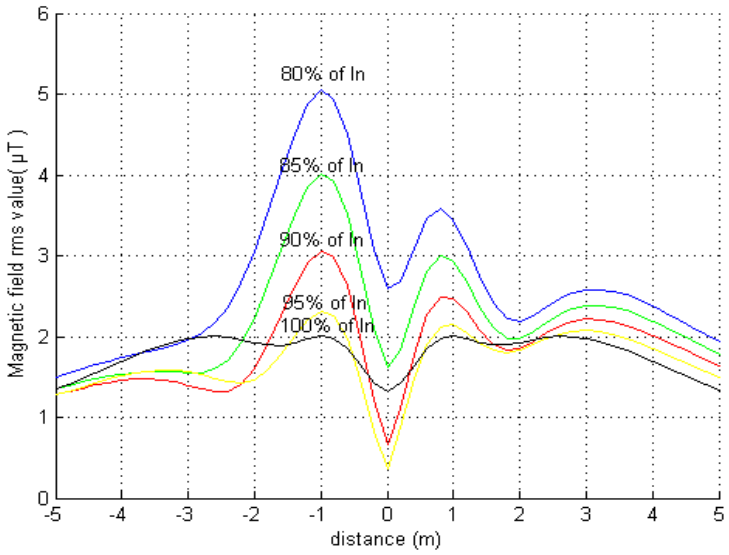

Figure 3-12. Maximum magnetic field when current module in one circuit changes, keeping the optimal positions of cables of Fig. 3-2.

In Fig. 3-11, reductions in the module of I_1, maintaining positions and other currents unchanged, result in larger values of maximum magnetic field in the measure plane. A reduction of 20% in I_{1a} increases 250% the maximum magnetic field, when the positions of the cables are retained. For this, possible differences in both angles and modules of the currents in the cables during the operation must be carefully considered in the design of the project, because they can produce large peaks of magnetic fields in some points of the evaluation plane.

3.5 Conclusion

In the present chapter, a new formulation for calculating the optimal positions of underground cables is proposed. The algorithm considers geometrical constraints and maximum allowed magnetic fields for reducing the construction costs in the installation of the bundles. Results with: a) 4 and 6 underground circuits, b) different maximum constraints on the magnetic field, c) phase differences between the phase lines and d) module differences between the circuits are presented.

The results show that the costs are heavily depending on the maximum allowed magnetic field. Differences in the phases or modules of the currents don't changes significantly the costs of installation. However, these differences can produce large increases on the magnetic field, if they are not considered in the design stage.

3.6 References

[3-1] "International Commission on Non-Ionizing Radiation Protection, Guidelines for Limiting Exposure to Time Varing Electric and Magnetic Fields (Up To 100 kHz)", ICNIRP Guidelines, 2010.

[3-2] Rianne Stam (Laboratory for Radiation Research, National Institute for Public Health and the Environment, the Netherlands), Comparison of International Policies on Electromagnetic Fields (Power Frequency and Radiofrequency Fields), May 2011.

[3-3] Spanish Presidency, Report of the Spanish Ministry of Health on the implementation of the RD 1066/2001, of September 28, 2005. Available online (in Spanish) at http://www.msc.es/ciudadanos/saludAmbLaboral/docs/informeCemRD1066agosto05.pdf

[3-4] CIGRE Working Group C4.204. Mitigation Techniques of Power Frequency Magnetic Fields Originated from Electric Power Systems, Feb. 2009.

[3-5] G. G. Karady, C. V. Nunez and R. Raghavan, "The Feasibility of Magnetic Field Reduction by Phase Relationship Optimization in Cable Systems", IEEE Transactions on Power Delivery, Vol. 13, No. 2, April 1998.

[3-6] E. I. Mimos, D. K. Tsanakas and A. E. Tzinevrakis, "Optimum phase configurations for the minimization of the magnetic fields of underground cables", Electrical Engineering, vol. 91, no. 6, pp. 327-335, 2010.

[3-7] G. G. Lai, C. Yang and C. Su, "Estimation and management of magnetic flux density produced by underground cables in multiple-circuit feeders", European Transactions on Electrical Power, vol. 20, (2010), pp. 545–558, 2010.

[3-8] C. F. Yang, G. G. Lai, C. T. Su and H. M. Huang, "Mitigation of magnetic field using three-phase four-wire twisted cables", Int. Trans. Electr. Energ. Syst. Vol. 23, pp 13–23, 2013.

[3-9] J. C. Pino López, P. Cruz-Romero, L. Serrano-Iribarnegaray, and J. Martínez-Román, "Magnetic field shielding optimization in underground power cable duct banks", Electric Power Systems Research, vol. 114, pp. 21-7, Sep. 2014.

[3-10] European Commission, Council Recommendation of 12 July 1999 on the Limitation of Exposure of the General Public to Electromagnetic Fields (0 Hz to 300 GHz), The Council of The European Union, 1999.

[3-11] European Commission, Report on the implementation of the Council Recommendation on the limitation of exposure of the general public to electromagnetic fields (0 Hz – 300 GHz) (1999/519/EC) in the EU Member States, Commission staff working paper, 2008.

Chapter 4. Statistical Calculation of Optimal Positions for Underground Cable Bundles for Reducing Maximum Magnetic Fields and Costs

4.1 Abstract

Underground cables are intensively used, especially for transporting energy in urban areas. The optimal installation of these cables must consider geometry, magnetic fields and arrangement costs. This chapter proposes and analyses different statistical calculations of these optimal locations. The application of the methods to real data demonstrates the effectiveness of the statistical approaches in terms of costs and magnetic fields. The content of this article has been submitted for its publication in a relevant technical journal.

4.2 Introduction

Underground cables currently transport a huge amount of electrical energy in urban environments. Additionally, underground cables are increasingly used in transmission lines when particular landing characteristics motivate their utilization instead of using overhead power lines. As with any other electrical line, underground cables produce magnetic fields, which must be restricted in the interest of the population. The limits on maximum magnetic fields vary between countries and regions for the industrial frequency of 50/60 Hz. In 2010, the International Commission on Non-Ionizing Radiation Protection (ICNRP) recommended a maximum value of magnetic fields for general public exposure of 200 μT [4-1].This large limit is different in certain countries. In the USA, a federal normative has not been introduced yet; however, some states, such as Florida (15 μT for up to 230 kV and 20 μT for higher voltages) and New York (20 μT), have introduced magnetic field limits [4-2]. In Europe, a maximum magnetic field of 100 μT is recommended, [4-3]. Although most European countries follow this recommendation, some countries have settled on stronger restrictions: in Belgium, the maximum value is 10 μT (Flanders region); in Italy, it is 3 or 10 μT (for new or existing installations); in Poland, it is 75 μT; and in Slovenia, it is 10 μT. Russia specified a maximum value of 10 μT, and Switzerland settled on a very small value of 1 μT [4-4], [4-5].

In [4-6], more than 140 papers are reviewed and discussed, therein summarizing possible techniques for mitigating extremely-low-frequency magnetic fields in transmission lines, focusing on overhead power lines. Calculation methods for obtaining the optimal configuration of underground transmission lines are also present in the literature. The reduction in magnetic fields produced by underground cables is an increasingly popular research field with interesting practical applications. A multi-circuit underground cable system with unbalanced loads is analysed in [4-7]. The proposed algorithm finds the optimal configuration of an arrangement, therein selecting between specified locations of the cables. The reduction in magnetic field in a measurement plane 1 m above ground is searched in [4-8] for arrangements of 2, 3 and 4 three-phase systems. The optimal phase disposition of the currents is calculated, therein shifting the currents between fixed available positions. In [4-9], the possibility of twisting the cables is studied, which reduces the magnetic fields in the ground. In [4-

10], [4-11] and [4-12], different shielding solutions are proposed for fixed-position underground cables.

In previous references, cable positions were fixed. In some of the studies, currents are allocated to pre-specified cable positions to search for the optimal phase configuration that reduces the magnetic field in a measurement plane. For shifting between positions, integer variables are generally used in the formulations, thus increasing the difficulty of the problem (in [4-13], a genetic algorithm is utilized to solve the optimization problem). In [4-14], a new formulation with all continuous variables is proposed in an attempt to calculate the optimal position of the underground cables. The algorithm obtains optimal positions and phase dispositions of the cables, therein searching for the minimization of construction costs. In this and previous studies, optimal dispositions of cable arrangements are calculated for specific values of currents. However, the currents in the cables change according to the load variations. In [4-15], multiple-circuit underground cable feeders with randomly varying loads are studied. The load current in all feeder circuits is considered as normally distributed. The optimal phase arrangement of the currents in a set of selected positions is calculated using a genetic algorithm. The authors conclude that the statistical approach results in better arrangements than when considering only a single value of current.

In the present work, two new algorithms, using a statistical approach, for calculating the optimal geometry and phase disposition of underground cables are proposed and compared. The optimization considers construction costs, geometry of the terrain and variations in the currents over time. Real data from a system of four three-phase single-core cables are used. The results show that the proposed statistical approach provides less expensive configurations and results in smaller magnetic fields.

4.3 The Optimization Problems

In the present work, the objective is to determine the optimal coordinates for underground cables arranged in 3-phase cable bundles to achieve minimum possible construction costs and magnetic fields generated by time-varying currents flowing through n circuits. In the study, changes in the currents over time are considered to allocate the cables to the centres of optimal positions. The optimization formulation is

proposed for a general number of circuits. In the following, the two optimization problems solved in this work are described.

4.3.1 Minimization of Costs and Magnetic Field Generated by N-Cable Bundles with Specified Currents

The objective of the first optimization problem is to calculate the optimal coordinates of a set of underground cables arranged in *n* 3-phase cable bundles such that the minimum construction cost is attained. The calculation is performed for a specified maximum magnetic field in a measurement plane created by previously known currents. Two types of solutions can be obtained: a) the case where cables at the position resulting in the minimum construction cost (as allowed by geometrical constraints) generate less than the maximum allowed magnetic field in the measurement plane and b) the case where the cables must be allocated to a more costly position to fulfil the magnetic field constraints. In the first case, the optimization problem seeks to calculate the optimal arrangement that reduces the maximum value of the maximum magnetic field in the measurement plane. In case b), the optimization problem obtains the minimum cost positions for the specified magnetic field conditions. The proposed optimization problem has the advantage that it can be used for any limit of maximum magnetic field, easily integrating the two different goals.

For specified currents in the cables and a maximum magnetic field allowed in the measurement plane, the proposed optimization problem can be summarized using equations (4-1)-(4-14).

$$min\, f\left(x,y,\Delta B_{max}\right) = c_x \frac{\sum_{i=1}^{n}|x_i|}{n} - c_y y_1 - c_{vol} y_1 \frac{\sum_{i=1}^{n}|x_i|}{n} - Kp\ \Delta B_{max} \tag{4-1}$$

s.t.

$$b_x^k = \frac{\mu_0}{2\pi}\left|\left(\tilde{\Im}_{1a}\frac{y_a - Y_c}{(X_c - x_a)^2 + (Y_c - y_{1a})^2} + \tilde{\Im}_{1b}\frac{y_b - Y_c}{(X_c - x_b)^2 + (Y_c - y_b)^2} + \tilde{\Im}_{1c}\cdot\frac{y_{1c} - Y_c}{(X_c - x_{1c})^2 + (Y_c - y_{1c})^2} + \ldots\right.\right.$$
$$\left.\left. + \tilde{\Im}_{na}\frac{y_{na} - Y_c}{(X_c - x_{na})^2 + (Y_c - y_{na})^2} + \tilde{\Im}_{nb}\frac{y_{nb} - Y_c}{(X_c - x_{nb})^2 + (Y_c - y_{nb})^2} + \tilde{\Im}_{nc}\cdot\frac{y_{nc} - Y_c}{(X_c - x_{nc})^2 + (Y_c - y_{nc})^2}\right)\right| \tag{4-2}$$

$$b_y^k = \frac{\mu_0}{2\pi}\left|\left(\underset{\sim}{\mathfrak{I}}_{1a}\frac{X_c - x_{1a}}{(X_c - x_{1a})^2 + (Y_c - y_{1a})^2} + \underset{\sim}{\mathfrak{I}}_{1b}\frac{X_c - x_{1b}}{(X_c - x_{1b})^2 + (Y_c - y_{1b})^2} + \underset{\sim}{\mathfrak{I}}_{1c}\frac{X_c - x_{1c}}{(X_c - x_{1c})^2 + (Y_c - y_{1c})^2} + \ldots \right.\right.$$
$$\left.\left. + \underset{\sim}{\mathfrak{I}}_{na}\frac{X_c - x_{na}}{(X_c - x_{na})^2 + (Y_c - y_{na})^2} + \underset{\sim}{\mathfrak{I}}_{nb}\frac{X_c - x_{nb}}{(X_c - x_{nb})^2 + (Y_c - y_{nb})^2} + \underset{\sim}{\mathfrak{I}}_{nc}\frac{X_c - x_{nc}}{(X_c - x_{nc})^2 + (Y_c - y_{nc})^2}\right)\right| \quad (4\text{-}3)$$

$$\left(b_x^k\right)^2 + \left(b_y^k\right)^2 \le B_{max}^2 - \Delta B_{\max}^2 \quad (4\text{-}4)$$

$$\left(x_{ia} - x_{ib}\right)^2 + \left(y_{ia} - y_{ib}\right)^2 = d^2 \quad (4\text{-}5)$$

$$\left(x_{ia} - x_{ic}\right)^2 + \left(y_{ia} - y_{ic}\right)^2 = d^2 \quad (4\text{-}6)$$

$$\left(x_{ib} - x_{ic}\right)^2 + \left(y_{ib} - y_{ic}\right)^2 = d^2 \quad (4\text{-}7)$$

$$\frac{x_{ia} + x_{ib} + x_{ic}}{3} = x_i \quad (4\text{-}8)$$

$$\frac{y_{ia} + y_{ib} + y_{ic}}{3} = y_i \quad (4\text{-}9)$$

$$\Delta B_{\max} > 0 \quad (4\text{-}10)$$

$$\left(x_i - x_j\right)^2 + \left(y_i - y_j\right)^2 \ge {d_{Min}}^2, \; i \ne j \quad (4\text{-}11)$$

$$y_1 \le y_i \quad (4\text{-}12)$$

$$-X_{Max} \le x_i \le X_{Max} \quad (4\text{-}13)$$

$$-Y_{Max} \le y_i \le -Y_{Min} \quad (4\text{-}14)$$

$$i, j = 1, \ldots, n, \; k = 1, \ldots, k_{Max}$$

Where,

b_x^k and b_y^k are the modules of phasors of the horizontal and vertical components of the magnetic field at point *k* of the evaluation plane, in μT.

(x_i,y_i) are the coordinates of the centre of the bundle of cables *i*, in μT.

(x_{il},y_{il}) are the coordinates of the centre of cable *l* in the bundle of cables *i*, in m.

ΔB_{Max} is the complementary variable measuring the difference between the maximum magnetic field allowed B_{Max} and the real maximum magnetic field observed in the evaluation plane.

The constraints are:

μ_0 is the permeability of free space, in H m^{-1}.

$\dot{\mathfrak{I}}_{il}$ is the phasor of currents flowing through the bundle of cables *i,* phases $l=\{a, b, c\}$, in A.

b is the magnetic field, in μT.

b_{xi} and b_{yi} are horizontal and vertical projections, respectively, of the magnetic field phasors generated by cable i, in μT.

B_{Max} is the maximum magnetic field allowed in the evaluation plane, in m.

d is the distance between two centres of cables in a bundle, in m.

X_{Max} is the maximum horizontal distance allowed from the centre of a bundle and the horizontal reference, in m.

Y_{Max} and Y_{Min} are the maximum and minimum depth, respectively, allowed to the centre of any 3-phase cable bundle, in m.

The main costs associated with the installation of underground transmission lines are related to the civil construction and the right-of-path costs. Civil construction costs include expenses for digging plus filling and compacting the rectangular trench in which bundles are laid. Moreover, for security reasons and to prevent the possible collapse of the walls of the trench, it is necessary to shore up the walls during installation, which incurs additional costs. The right-of-path costs are associated with the occupation of the space.

Objective function (4-1) contains four terms. The firsts three terms consider the following: horizontal costs per unit associated with the occupation of the land (c_x), vertical costs per unit related to digging operations (c_y) and volumetric costs per unit due to movements of terrain (c_{vol}). Because the depth (y_i) is a negative variable, the second and third term are negative expressions. The first three terms of (4-1), therefore, attempt to reduce civil construction and right-of-path costs. When the magnetic fields allowed in the measurement plane are relatively large, cables can adopt the minimum cost positions allowed by construction restrictions. In this case, the fourth term of (4-1) attempts to minimize the maximum magnetic field in the measurement plane, thereby increasing the complementary variable ΔB_{Max}. The penalty coefficient Kp is a small value and is lower than the costs in the first three terms of (4-1).

In (4-2) and (4-3), the modules of the phasors of the horizontal and vertical components of the magnetic field at each of the k measurement points in the measurement plane are calculated. These points, which are separated by 0.2 m, are located along a line 1 m above the terrain (see Fig. 4-1.a). In the present simulations, k_{Max} is equal to 51, thus representing a measurement line of 10 m, 5 m to either side of the vertical axis. The square module of the magnetic field at all measurement points is restricted to the square of a specified maximum value, as in (4-4).

The centres of the cables in each bundle must be located on the vertices of an equilateral triangle, as specified in (4-5)-(4-7). In the present formulation, bundles can be rotated from conventional bundle cable positions (the two lowest cables at the same depth and the third placed above them, as in Fig. 4-1.b). Rotation of the bundles enables higher compensation and hence lower magnetic fields, [4-14], and this is obtained at negligible construction costs. Moreover, an approximation to near the conventional position can be used (Fig. 4-1.c) if rotated positions (Fig. 4-1.b) are not implemented in the installation of bundles.

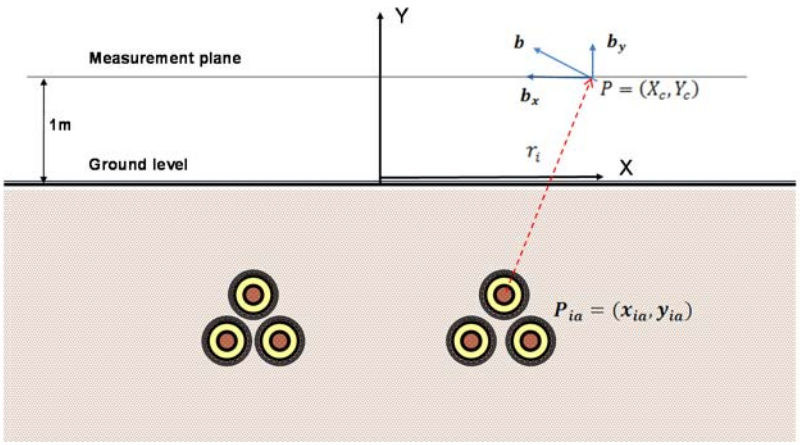

a. Magnetic field generated by a conductor at point k

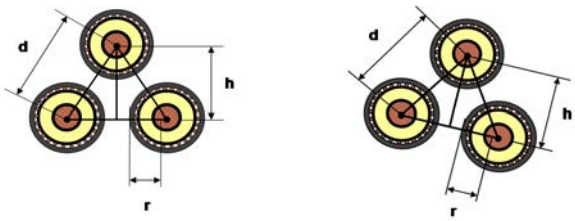

b. Conventional bundle cable *c. Rotated bundle cable.*

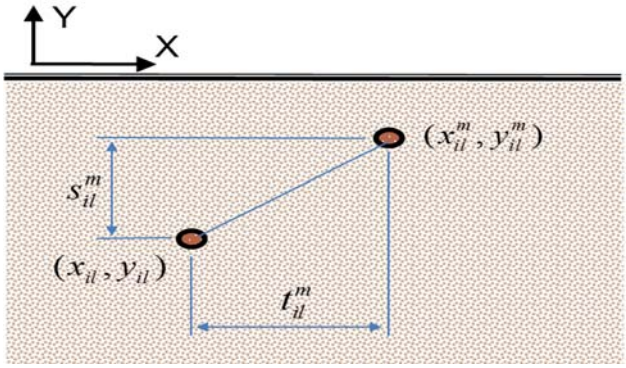

d. Coordinates of the position of a cable for a mean arrangement and a sample

Figure 4-1: Geometrical diagrams.

The separation between cables in the same bundle is very important in the design of the circuit. A lower separation allows more compact solutions with lower construction costs. However, the ampacity of the bundle may be compromised by the inter-heating transfer among the cables in the bundle and the resulting limits on the allowed maximum current. Additionally, separation between the cables affects the interaction of the magnetic fields, as indicated by [4-6] and [4-7]. In the present study, the results of simulations using d = 0.32 m are presented; this value is based on the dimensions of the cables and in practical uses in Spain.

The coordinates of centres of the bundles i are calculated in (4-8)-(4-9). To guarantee that none of the 3-phase cable bundles overlap and to ensure sufficient distance between circuits (related to the desired ampacity), a minimum distance between circuits is imposed, as in (4-11). In the present simulations, the results correspond to d_{Min} = 0.8 m.

The depth of the trench (y_1) is defined by the deepest bundle. In (4-12), bundle i=1 is defined as the deepest bundle. For security reasons, Spanish legislation forbids the installation of wires at depths of less than 0.6 m. In addition, burial depths greater than 3 metres are beyond the capacity of usual construction equipment, and the maximum distance between two circuits is limited to 6 metres because of the nature of urban terrain, as in (4-13)-(4-14).

4.3.2 Calculation of Mean Coordinates For N Cable Bundles in M Scenarios

The current in the cables varies during a day and depends on both the variations in the load and the dispatch of the grid. Magnetic fields interact with each other, thereby increasing or decreasing the values in the measurement plane. Therefore, the calculation of the optimal positions of the cable bundles must consider the possible variations in the currents. To calculate the optimal design based on a realistic situation, a simulation of alternative scenarios based on the distributions of current intensity is proposed, as presented in [4-15]. In the present study, real hourly data from 3 years of recording in underground installations are used to perform the statistical analyses. In contrast to [4-15], the distributions of the recorded currents were found to be non-normal. Furthermore, the empirical distributions show evidence of bimodality, mainly due to the presence of daily and weekly cycles. Trying to fit the data to some known distribution seems then a complex task. The proposed statistical approach is thus based on simulating the scenarios by resampling from the historical data. To this end, M samples, with replacement, of hourly current recordings conform to the scenarios of the study. For each of the scenarios, the optimization problem in (4-1)-(4-14) is solved, resulting in M optimal positions for the cable bundles.

The mean coordinates of the optimal arrangement of n 3-phase cable bundles can be calculated by obtaining the mean coordinates of the cables in the M scenarios satisfying geometrical constraints imposed on the bundles and cables. A second optimization problem is required here and is defined as follows:

$$min\, h(x) = \sum_{m=1}^{M}\sum_{i=1}^{n}\left(\left(s_{ia}^{m}\right)^2 + \left(s_{ib}^{m}\right)^2 + \left(s_{ic}^{m}\right)^2 + \left(t_{ia}^{m}\right)^2 + \left(t_{ib}^{m}\right)^2 + \left(t_{ic}^{m}\right)^2\right) \tag{4-15}$$

s.t.

Eqs. (5)-(9) and (11).

$$x_{il} - s_{il}^{m} = x_{il}^{m} \tag{4-16}$$

$$y_{il} - t_{il}^{m} = y_{il}^{m} \tag{4-17}$$

Eqs. (13)-(14)

$i = 1,\ldots,n$, $l = a,b,c$, $m = 1,\ldots,M$.

4.4 Case Study

In this section, a case based in real data is analysed. The problem is the optimal connection of four 220-kV underground power circuits of single-core XLPE cables, which use copper conductor with a 2,500 mm² cross-section. The cables are bundled in a trefoil configuration and directly buried. These circuits share a common path in the proximity of one substation where they are all are connected. Two of the circuits end at different substations (Circuits 1 and 2). The other two circuits go to another substation, following partially divergent paths (Circuits 3 and 4). Here, the initial path with the four circuits in the same path is studied. The instantaneous values of active and reactive powers flowing through the four circuits have been recorded every hour for three years, generating a total of 24×365×3=26,280 registers. Based in these values, proportional the active and reactive currents, $I = (I_d + j\ I_q)$, represented in Figs. 4-2.a and 4-2.b, are calculated.

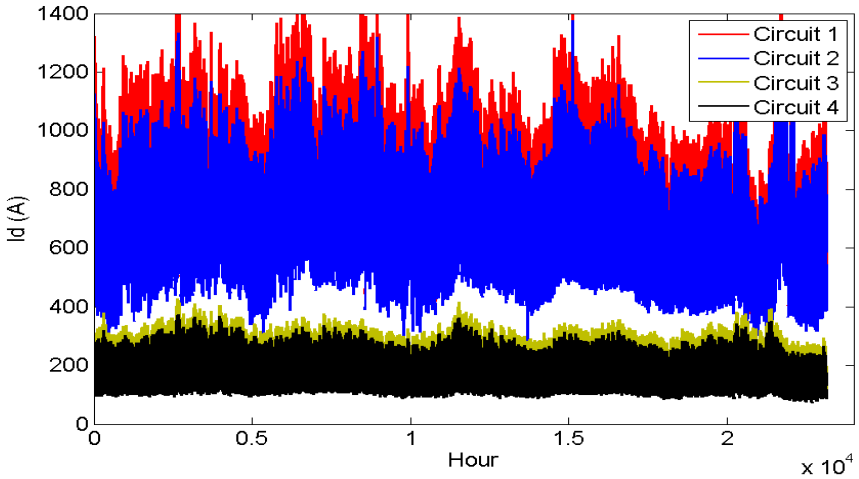

a. I_d (A).

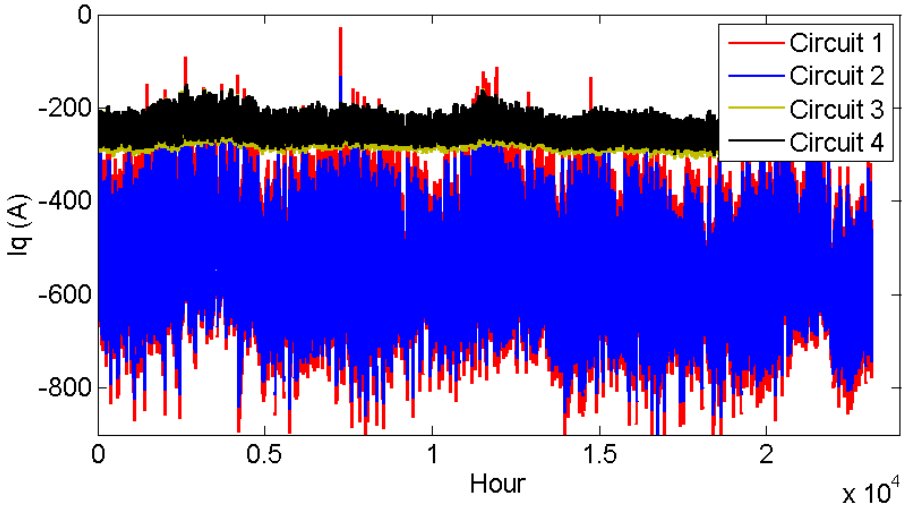

b. I_q (A).

Figure 4-2. Active currents of the four circuits.

Demand, generation and even topology in power systems change continuously but usually follow certain seasonal patterns depending on the hour of the day, the day of the week and the season. Therefore, currents flowing through circuits vary over time but follow relatively similar patterns. Figs. 4-3.a and 4-3.b provide a sample of four weeks of data for active and reactive currents I_d and I_q.

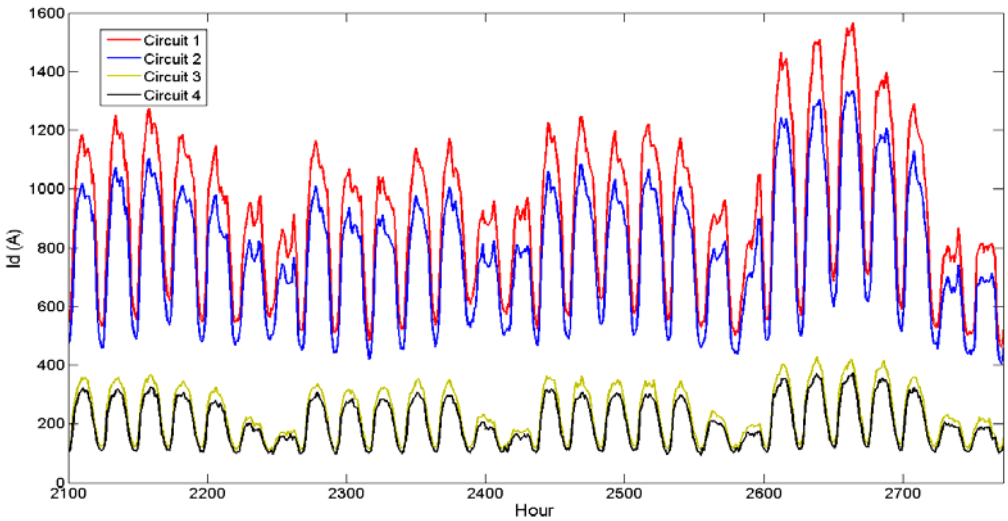

a. Id (A), four first weeks.

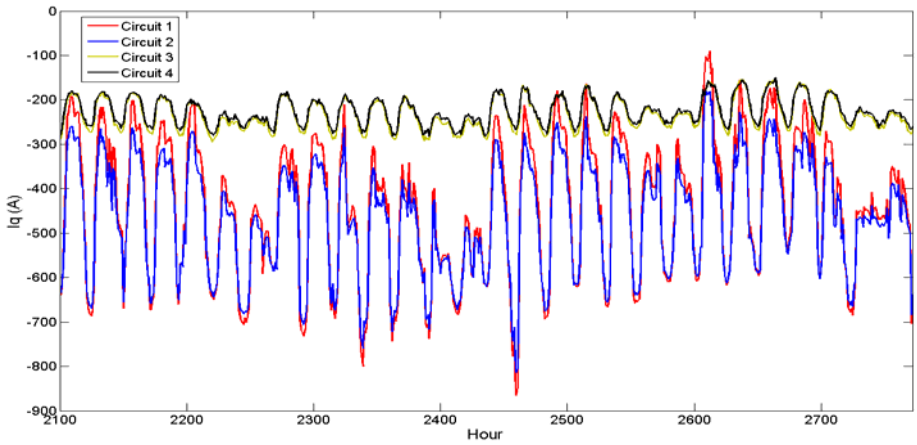

b. Iq(A), four first weeks.

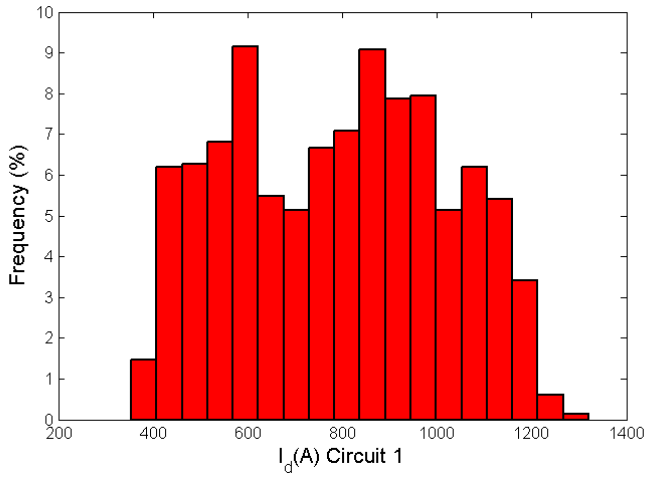

c. Histogram of Iq (A) in Circuit 1.

Figure 4-3. Sample of current contributing active power.

In Figs. 4-3.a and 4-3.b, a stochastic seasonal evolution of currents over the course of a day and between days in a week can be observed. The currents in Circuits 3 and 4 follow very similar profiles, whereas somewhat larger differences can be observed between Circuits 1 and 2. These figures also reveal an important fact: the statistical properties of the time series of currents are stable across time, i.e., there are not increasing or decreasing trends, and the seasonal (stochastic) patterns are maintained over time. Thus, it can be concluded that the unconditional distributions of the currents are stable. Hence, resampling from these distributions can provide a representative sample of the system. Then, the simulation of the behaviour of the whole configuration is performed by resampling from the unconditional distribution of the vector of currents. By doing so, it is possible to not only reproduce the univariate distribution of each

current, which is not normal, but also preserve the interdependence between the currents. As an example, Fig. 4-3.c shows the histogram of I_q in Circuit 1. The histogram shows that the distribution is not normal; the distribution presents a multimodality that is due to its cyclic behaviour. The distributions of the remaining variables exhibit similar patterns.

To perform the statistical simulations, a random sample of size M = 150 time instants, from the available span of time, is selected. For each time instant, the corresponding vector of currents shown in Figs. 2.a and 2.b is obtained. The optimization problem (4-1)-(4-14) is solved for each of these 150 scenarios. In these simulations, the utilized values of the costs per unit are obtained from a general reference for construction costs in Andalusia, a southern region in Spain: c_x = 10 €/m², c_y= 14.59 €/m² and c_{vol} = 6.5 €/m³ [4-16]. In (4-1), only construction costs are considered; the costs of the cables themselves are not included. The penalty factor in the fourth term of (4-5) is (Kp=0.05·c_{vol}), therein prioritizing the cost reduction objective and, after that, the reduction in maximum magnetic fields (only if the minimum cost position is reached). For the geometrical constraints (4-13) and (4-14), which are related to the centres of the bundles, the values of X_{Max}=2.765 m, Y_{Min}=-0.835 m and Y_{Max}=-2.765 m are used.

4.5 Results

The proposed methodology is implemented and compared with more traditional solutions: the conventional position of bundles without rotation and a unique deterministic calculation with the maximum values of the currents. In total, six optimal configurations are compared. They are labelled as follows:

- *Med*: This configuration is based on the proposed statistical method. From historical data, M = 150 scenarios of instantaneous currents are randomly sorted. In each scenario, the optimization problem given in (4-1)-(4-14) is solved. Then, the mean arrangement of cables is calculated following the procedure described in Section II.B.

- *MedStandard*: The Med configuration can utilize the benefits of rotated positions (as shown in Fig. 4-1.c). From this rotated configuration, MedStandard, the closest conventional bundle cable positions without rotation (as in Fig. 4-1.b) to the Med arrangement, is obtained.
- *Max*: This configuration is also based on the proposed statistical method. From the M=150 solutions corresponding to the simulated scenarios specified for the Med configuration calculation, Max is the configuration of the optimal position with the maximum cost. This configuration can be viewed as the worst-case combination of currents.
- *MaxStandard*: This configuration represents the closest conventional bundle cable positions (as in Fig. 4-1.b), obtained from the Max configuration.
- *Opt*: Opt is the deterministic calculation of the optimal configuration, therein solving the optimization problem (4-1)-(4-14) once for the maximum thermal current (1700 A) and power factor 0.8i in all cables. This configuration is similar to the situations studied in most of the literature [4-7]-[4-14].
- *OptStandard*: The closest conventional (without rotation, as in Fig. 4-1.b) bundle cable positions of Opt.

Different limits are specified for the maximum magnetic field across the world. To observe restrictive limits can be very difficult in many situations. The optimization method proposed in this work attempts to calculate the optimal positions of the underground cables under these restrictive conditions. Three cases are presented:

- *Bmax = 10 μT*. For values larger than 10 μT for the maximum magnetic field in the measurement plane, the minimum cost position can be reached for almost all the currents considered in the Med, Max and Opt configurations. Therefore, when solving optimization problem (4-1)-(4-14) for Bmax = 10 μT, the main objective is to search the optimal positions of cables generating the lowest maximum magnetic field at the minimum cost positions while meeting the geometrical constraints.

- *Bmax = 3 μT*. In general, this value of the maximum magnetic field requires configurations with costs that are larger than the minimum.
- *Bmax = 1 μT*. Most constringent condition studied here.

The three cases are presented below. Later, a cost comparison between configurations is performed.

4.5.1 B_{max} = 10 μT

With B_{max} = 10 μT, all configurations share the same centres of the cable bundles. Therefore, they have the same construction costs, i.e., 36.70 €/m, the minimum allowed by the geometrical constraints. Circuits 1 and 2 are allocated to the two central positions, and Circuits 3 and 4 (with smaller currents) are allocated to external points. However, the positions of the cables of the phases in each configuration are different, as depicted in Fig. 4-5.a. In all 150 sorted scenarios, the minimum cost position is obtained. Therefore, the *Max* and *MaxStandard* configurations are not applicable and are not represented in this case.

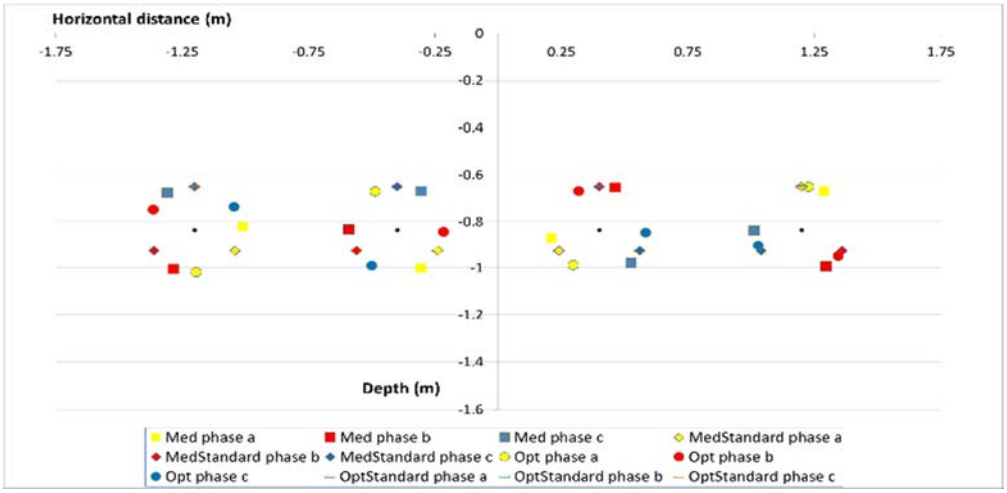

a. Positions of cables for six configurations.

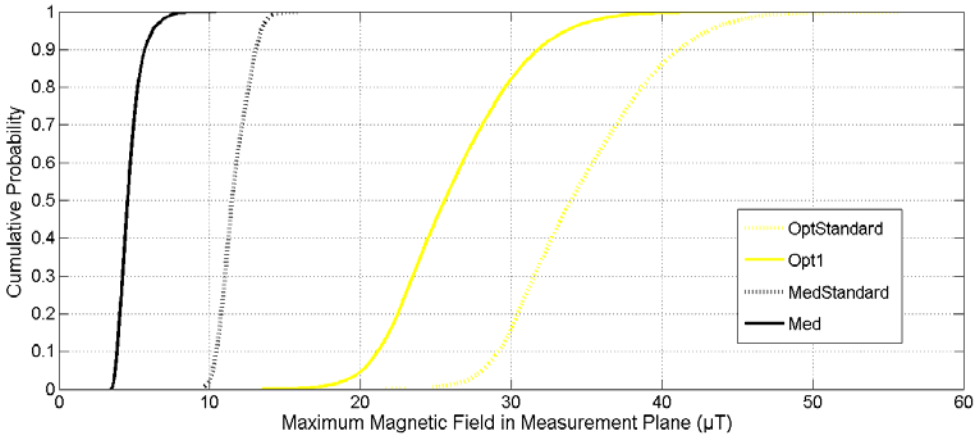

b. Empirical cdf of maximum magnetic field for four configurations.

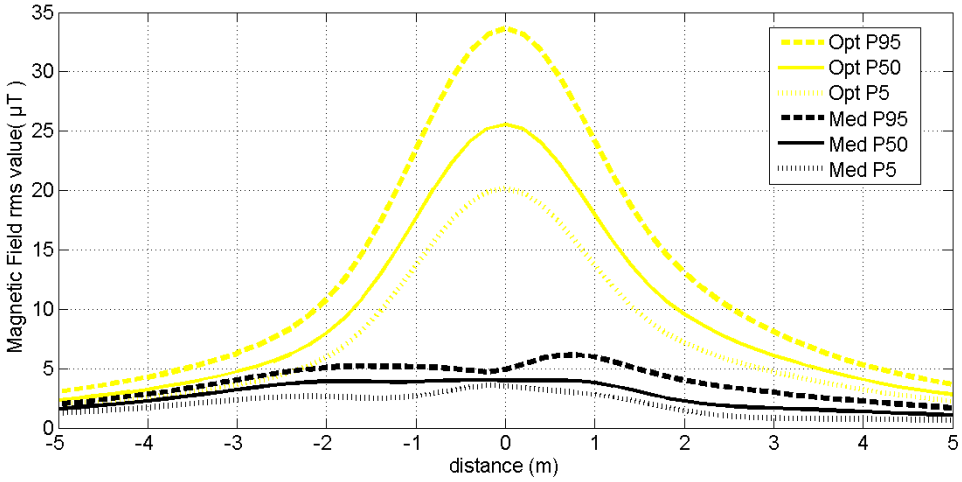

c. Percentiles of the Maximum Magnetic Field under the Opt and Med Configurations.

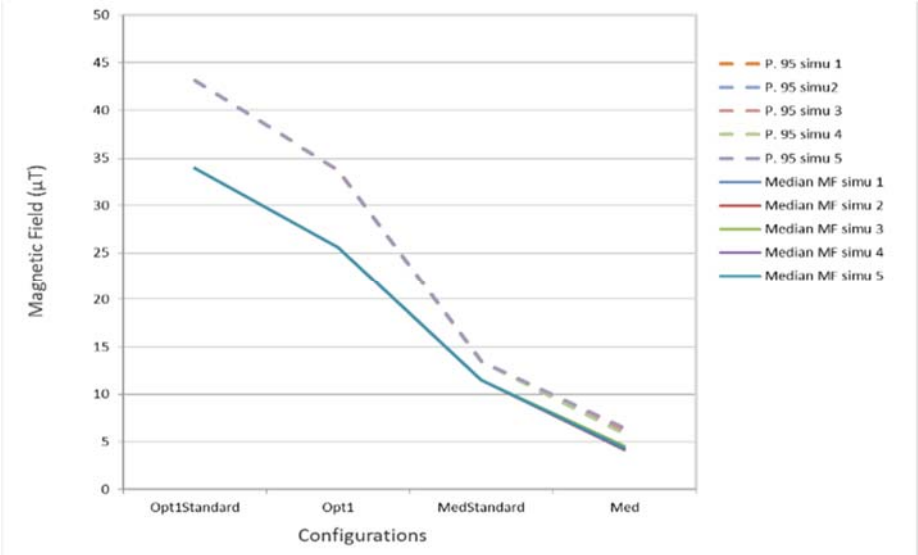

d. Comparison of P. 95 and Median Magnetic Field in five simulations.

Figure 4-4: Results for Bmax = 10 μT.

All the hourly recorded values of Figs. 4-2.a and 4-2.b are applied to the *Med*, *MedStandard*, *Opt* and *OptStandard* configurations of Fig. 4-4.a. In Fig. 4-4.b, the respective empirical cumulative distribution functions (cdfs) are depicted, therein providing statistical values of the probability of maximum magnetic field generated in the measurement plane. *Med* provides the best configuration, with maximum magnetic fields lower than 10.41 μT for all combinations of currents presented in the historical data. The advantages of the rotated positions are also observed in the figure; the *Med* and *Opt* configurations produce smaller magnetic fields than do the *MedStandard* and *OptStandard* configurations, respectively, for all the historical data.

In Table 4-1, the median and 5th and 95th percentiles of all the hourly recorded values for the four configurations are presented. The median values of the *MedStandard*, *Opt* and *OptStandard* configurations are 152%, 461% and 645%, respectively, larger than the *Med* configuration mean. Additionally, the magnetic field produced by the *Med* configuration is lower than 6.2 μT 95% of the time. As observed in Fig. 4-4.b and Table 4-1, the *Med* and *MedStandard* configurations have nearly vertical distributions, with a small dispersion in the values. The almost flat distribution of the magnetic fields under the *Med* configuration can also be observed in Fig. 4-4.c, where some percentile levels of magnetic fields generated in all three years of hourly recorded values in the measurement plane are shown.

Table 4-1. Bmax = 10 μT, Some values of the cdfs.

CONFIGURATION	MAGNETIC FIELD VALUE (μT)		
	5th Percentile	Median	95th Percentile
OptStandard	28.08	33.96	43.03
Opt	20.12	25.56	33.69
MedStandard	10.20	11.48	13.42
Med	3.75	4.56	6.20

To analyse the influence of the sample size in the *Med* and *MedStandard* calculations, five different sets of 150 values are used to calculate these configurations. In Fig. 4-4.d, the median and 95th percentile of the maximum magnetic field for the configurations in the five sets are depicted. As observed, the differences are negligible.

4.5.2 B_{max} = 3 μT

With B_{max} = 3 μT, the six previously described configurations are calculated. In general, the centres of the cable bundles are positioned deeper than the minimum cost position in all simulations. Fig. 4-5 shows the empirical cdf of the maximum magnetic field in the six configurations. In Table 4-2, the median, the 5th and 95th percentiles and the cost of the six configurations are presented. The installation cost of the *Med* configuration is 39.4 €/m, 7.36% more expensive than the minimum cost. The average positions calculated in the *Med* configuration work very well with the historical data, resulting in a median value of 3.42 μT for the three recorded years. The magnetic field is larger than 5.32 μT only 5% of the time at certain positions of the measurement plane. The most expensive configuration, *Max,* presents 5.56% and 23.3% lower median and 95th percentile values at an increased cost of 25.23% over the *Med* construction cost.

In this case, the deterministic calculation performed using the *Opt* configuration is clearly the most ineffective method. The *Opt* configuration is obtained by solving the optimization problem (1)-(14) once, with B_{max} = 3 μT and the maximum thermal currents (1700 A) in all the cables. When applying the historical data to this configuration, the median value is 14.67 μT, namely, 328.95% larger than that in the *Med* configuration and 354.18% larger than that in the *Max* configuration. Moreover, the cost of the *Opt* configuration is 35.56% and 8.07% larger than the cost of these configurations, respectively.

To analyse the influence of the sample size under the *Med* and *Max* configurations, another five different sets of 150 values are used. Again, under different positions of the bundles, the median and maximum magnetic field generated by the *Med* configuration are negligible.

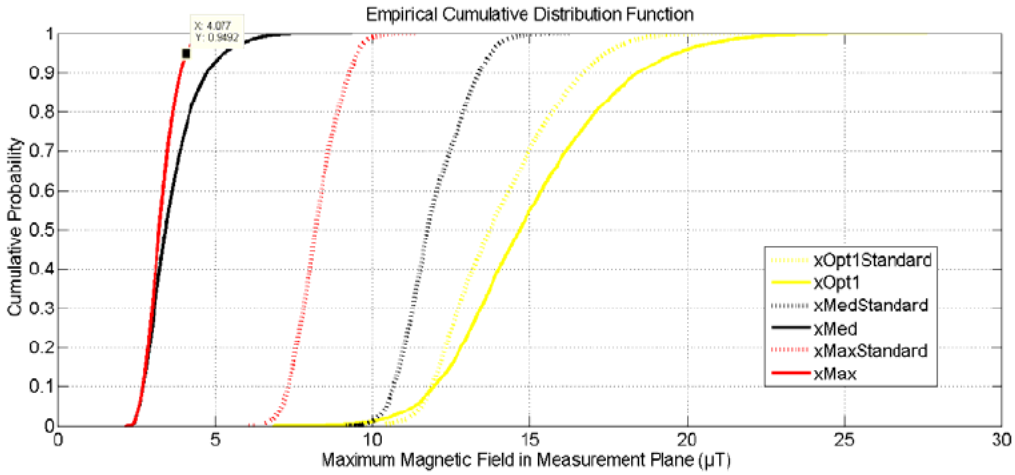

Figure 4-5. Bmax = 3 μT, Empirical cdf of Maximum Magnetic Field for Six Configurations.

Table 4-2. Bmax = 3 μT, Some values of the cdfs.

CONFIGURATION	MAGNETIC FIELD VALUE (μT)			COST (€/m)
	5th Percentile	Median	95th Percentile	
OptStandard	11.54	13.73	17.44	53.41
Opt	11.30	14.67	19.69	53.41
MedStandard	10.42	11.75	13.76	39.40
Med	2.57	3.42	5.32	39.40
MaxStandard	7.10	8.18	9.52	49.42
Max	2.57	3.23	4.08	49.42

4.5.3 B_{max} = 1 μT

The calculation of the low cost positions of cables for very low magnetic fields and time-varying currents is a very difficult task. In the present study, the six configurations are calculated for B_{max} = 1 μT. However, due to the extremely difficult target, the number of scenarios used to calculate the *Med* and *Max* configurations can severely impact the results. In a first analysis, five different samples of 150 values of currents are used. In Fig. 4-6.a, the median and 95th percentile of the maximum magnetic field under the *Med* configuration are shown, with appreciable differences being found between samples. Therefore, the sample size for the *Med* and *Max* calculations is increased to M = 750. Using M = 750, the differences between different sets of data are negligible.

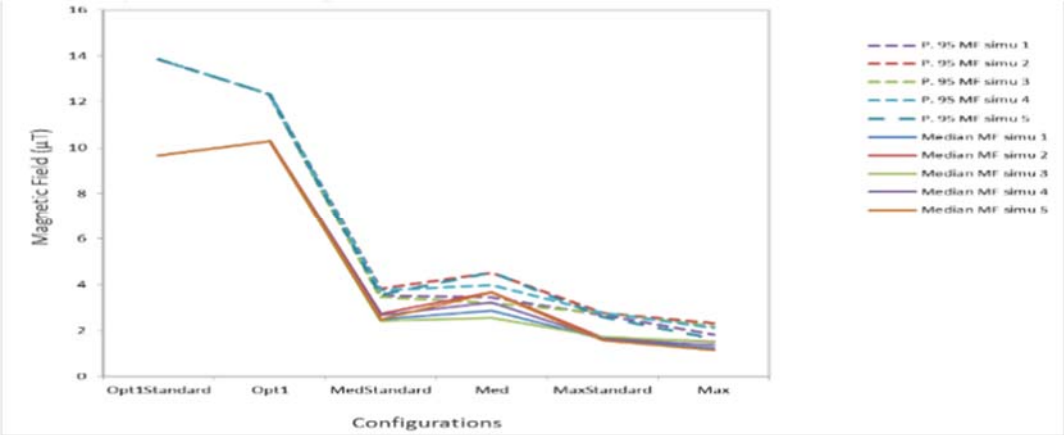

a. Comparison of P. 95 and Median Magnetic Field in five simulations, M =150

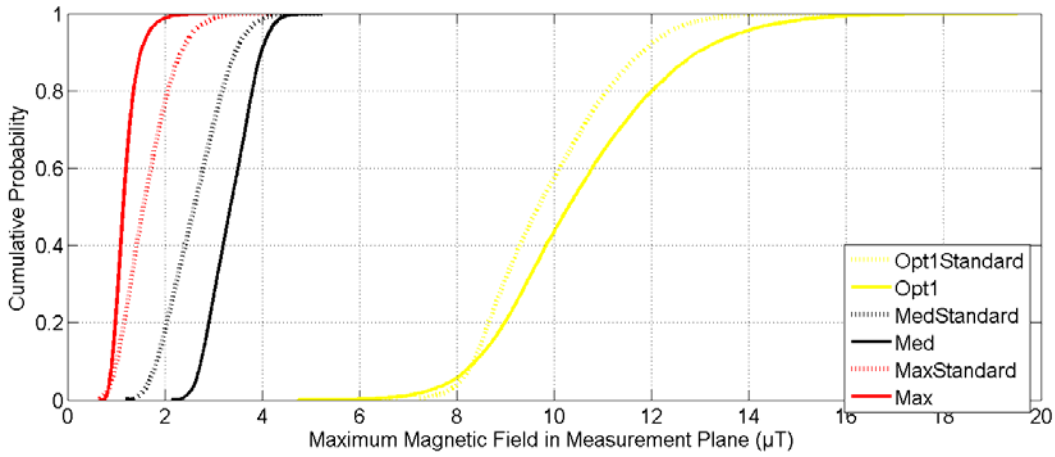

b. Empirical cdf of Magnetic Field for Six Configurations.

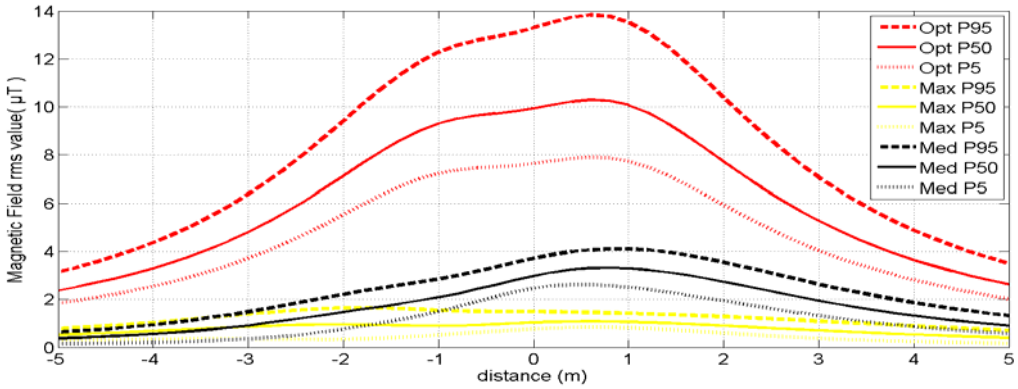

c. Percentiles of Magnetic Field in Measurement Plane.

Figure 4-6. Bmax = 1 μT.

In Fig. 4-6.b and Table 4-3, the empirical cdf, the median and the 5th and 95th percentiles for the six configurations are presented. *Med*, *Max* and their respective

conventional *MedStandard* and *MaxStandard* configurations present better distribution functions than do *Opt* and *OptStandard*. The *Med* configuration has a median value of 2.60 μT when applied across all historical data. This value is larger than the objective (1 μT) due to the variations in the modules and angles of the currents in the recorded data. In Fig. 4-6.c, the distribution of median values and 5th and 95th percentiles in the measurement plane are presented. Larger magnetic fields can be observed on the right side of the curves due to asymmetries between the real currents in the circuits.

From Table 4-3, the *Opt* configuration has a median value of 10.29 μT, the largest value of the six configurations. On the other hand, the *Max* configuration median (1.15 μT) is closer to the proposed objective (1 μT), with a cost 29.33% higher than that of the *Med* configuration. For extremely reduced objectives concerning magnetic fields, adopting more expensive configurations (even calculating with $Bmax < 1$ μT) than average may be convenient despite increasing installation costs.

Table 4-3. Bmax = 1 μT, Some values of the cdfs.

CONFIGURATION	MAGNETIC FIELD VALUE (μT)			COST (€/m)
	5th Percentile	Median	95th Percentile	
OptStandard	8.07	9.67	12.34	68.63
Opt	7.90	10.29	13.83	68.63
MedStandard	1.68	2.60	3.71	61.76
Med	2.63	3.35	4.13	61.76
MaxStandard	0.91	1.56	2.57	79.88
Max	0.87	1.15	1.66	79.88

4.5.4 Cost Comparisons

In Fig. 4-7, the median and 95% percentile of the maximum magnetic field under the *Max*, *Med* and *Opt* configurations are presented as a function of the installation price. To obtain maximum magnetic fields larger than $B_{max} = 5$ μT, the *Med* configuration requires lower installation costs according to the curve of mean values of the magnetic fields. However, for stronger magnetic field constraints ($B_{max} < 5$ μT), the *Max* configuration seems to be preferable.

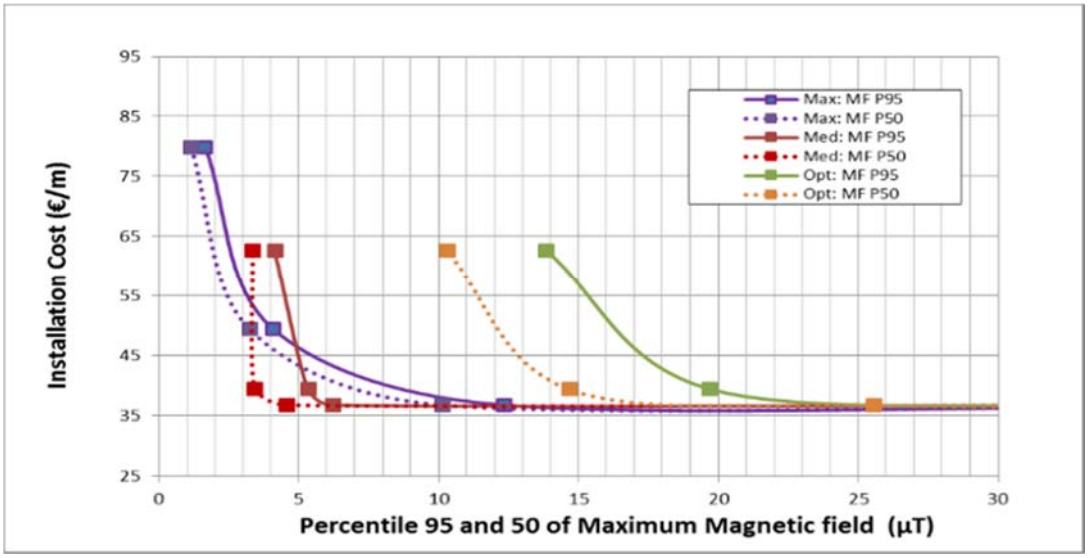

Figure 4-7: Mean and 95th Percentile curves vs. installation cost.

4.6 Conclusions

This work proposes and compares methods for optimizing the allocation of n bundles of cables with time-varying currents through them, therein considering maximum magnetic field, geometrical constraints and installation cost. A real-world case with four cable bundles and three years of historical data is analysed. Two statistical configurations, namely, the worst-case combination of currents and the mean calculation, are compared with the usual deterministic calculation method. Additionally, benefits due to the rotated positions of cables are determined.

In the case study, the proposed statistical approach is found to be far more convenient than the traditional deterministic method. The deterministic method can be up to 36% more costly and can produce magnetic fields that are 350% larger than those of the statistical methods. The rotation of bundles provides greater reductions in the magnetic fields.

4.7 References

[4-1] "International Commission on Non-Ionizing Radiation Protection, Guidelines for Limiting Exposure to Time Varying Electric and Magnetic Fields (Up To 100 kHz)", *ICNIRP Guidelines*, 2010.

[4-2] "Limits in the USA", *EMFS*, available online: http://www.emfs.info/, last visit, Jan. 2016.

[4-3] European Commission, *Council Recommendation of 12 July 1999 on the Limitation of Exposure of the General Public to Electromagnetic Fields (0 Hz to 300 GHz)*, The Council of The European Union, 1999.

[4-4] Rianne Stam (Laboratory for Radiation Research, National Institute for Public Health and the Environment, the Netherlands), *Comparison of International Policies on Electromagnetic Fields (Power Frequency and Radiofrequency Fields)*, May 2011.

[4-5] European Commission, *Report on the implementation of the Council Recommendation on the limitation of exposure of the general public to electromagnetic fields (0 Hz – 300 GHz) (1999/519/EC) in the EU Member States*, Commission staff working paper, 2008.

[4-6] CIGRE Working Group C4.204. *Mitigation Techniques of Power Frequency Magnetic Fields Originated from Electric Power Systems*, Feb. 2009.

[4-7] Karady, G. G. , Nunez, C. V., Raghavan, R. , "The Feasibility of Magnetic Field Reduction by Phase Relationship Optimization in Cable Systems", *IEEE Transactions on Power Delivery*, Vol. 13, No. 2, April 1998.

[4-8] Mimos, E. I., Tsanakas, D. K., Tzinevrakis, A. E., "Optimum phase configurations for the minimization of the magnetic fields of underground cables", *Electrical Engineering*, vol. 91, no. 6, pp. 327-335, 2010.

[4-9] Yang, C. F., Lai, G. G., Su, C. T., Huang, H. M., "Mitigation of magnetic field using three-phase four-wire twisted cables", *Int. Trans. Electr. Energ. Syst*. Vol. 23, pp 13–23, 2013.

[4-10] Canova, A., Bavastro, D., Freschi, F., Giaccone, L., Repetto, M. "Magnetic shielding solutions for the junction zone of high voltage underground power lines," *Electric Power Systems Research*, Vol. 89, pp. 109–115, 2012.

[4-11] Pino-López, J.C. del, Cruz-Romero, P., Serrano-Iribarnegaray, L., Martínez-Román, J., "Magnetic field shielding optimization in underground power cable duct banks," *Electric Power Systems Research*, vol. 114, pp. 21–27, 2014.

[4-12] Ippolito, M. G., Puccio, A., Ala, G., Ganci, S., "Attenuation of low frequency magnetic fields produced by HV underground power cables", *Power Engineering Conference (UPEC), 2015 50th International Universities,* pp. 1-5, 2015.

[4-13] Lai, G. G., Yang, C. F., Huang, H. M., Su, C. T., "Optimal Connection of Power Transmission Lines With Underground Power Cables to Minimize Magnetic Flux Density Using Genetic Algorithms", *IEEE Trans. on Power Delivery*, vol. 23, no. 3, July 2008.

[4-14] Hernandez Jimenez, V. J., Castronuovo, E. D., "Optimal geometric configurations for mitigation of magnetic fields of underground power lines", *PowerTech, 2015 IEEE Eindhoven,* pp. 1-6, 2015.

[4-15] Lai, G. G., Yang, C., Su, C., "Estimation and management of magnetic flux density produced by underground cables in multiple-circuit feeders", *European Transactions on Electrical Power*, vol. 20, (2010), pp. 545–558, 2010.

[4-16] *Table of prices of the construction in Andalusia* (Base de Costes de la Construcción de Andalucía (BCCA) 2013. Banco de Precios), 2013 (in Spanish). Available online http://www.juntadeandalucia.es.

Chapter 5. Statistical Calculation of Galleries to Reduce Magnetic Fields and Costs.

5.1 Abstract

The allocation of electric power transmission lines in galleries is a common practice in several applications, such as underground lines in urban areas, connections of cables to substations, mining and railway systems. The construction of galleries requires difficult and costly work. Moreover, limitations of external and internal magnetic fields generated by the currents in the cables of the gallery are needed. The present chapter proposes and analyzes different statistical methods for calculating the optimal dispositions of cables and gallery dimensions to reduce the magnetic fields and costs for time-varying currents in the cables. The implementation of these methods for a four-circuit real-world case is used to assess their effectiveness.

The main contents on this chapter have been sent for publication in a relevant technical journal.

5.2 Introduction

Power cables are widely used to transmit energy in multiple applications. Usually, power plants, mining and railway facilities contain installations of power cables. Moreover, high-voltage underground power lines are common in urban areas, where the use of land or environmental reasons makes it preferable to use underground cables instead of overhead lines. As with all electrical installations, underground cables produce magnetic fields, which can be higher than those in the case of overhead lines due to the reduced distance between cables and persons. For the sake of public health, the magnetic fields that are generated must be restricted. Generally, two types of limits are specified: those for the general public and those for occupational professionals.

For the general public, the International Commission on Non-Ionizing Radiation Protection (ICNRP) has recommended a maximum magnetic field value of 200 μT [5-1]. This relatively large limit has been reduced significantly by several national and regional legislations. Some states of the USA have set lower values for magnetic field limits, such as those in Florida (15 μT for up to 230 kV and 20 μT at higher voltages) and New York (20 μT) [5-2]. The UE has set a recommendation of 100 μT. However, in some European countries, stronger limits have been imposed [5-3]. In Italy, the maximum limits are 3 and 10 μT for new and existing facilities, respectively; in Slovenia, 10 μT; in Flanders, the northern region of Belgium, and in Russia, a maximum limit of 10 μT was set, and Switzerland established the strongest limit of 1 μT [5-4]-[5-5]. For occupational professionals, larger limits are tolerated. ICNRP specified a limit of 1000 μT. The UE set a recommendation of 500 μT (5 times larger than the limit for the general public) [5-6]. This limit is respected in most of the European countries. However, Luxembourg specified a limit of 100 μT, and Poland specified 251 μT. In Russia, the maximum magnetic field for occupational professionals is 100 μT [5-4]. In addition, some studies have focused on the problem of the exposure of workers to magnetic fields. In [5-7], exposures of overhead lineworkers and cable splicers during various works near energized conductors are assessed. In [5-8], occupational exposure to electric magnetic fields is studied. In [5-9], magnetic field measurements in indoor power distribution substations are shown and analyzed.

There is increasing interest in minimizing the magnetic fields generated by cables. In

[5-10], possible techniques for the reduction of magnetic fields in transmission lines are summarized based on the review and discussion of more than 140 papers. Several calculation methods for determining the optimal configurations of underground cables to reduce magnetic fields are present in the literature. In [5-11], an algorithm to obtain the optimal arrangement of an unbalanced loaded multi-circuit underground cable system, from specified locations of cables, is shown. The authors of [5-12] research the reduction of magnetic fields for arrangements of 2, 3 and 4 three-phase systems in a measurement plane 1 meter above ground. The optimal phase arrangement is obtained by interchanging the currents between determined available positions. In [5-13], a genetic algorithm is used to obtain the optimal configuration, also from fixed selected positions. In [5-14], [5-15] and [5-16], several shielding solutions are presented, assuming that the dispositions of underground cables are known. In [5-17], a cost variable is introduced to calculate the optimal position of cables. In this algorithm, all of the variables used are continuous and the optimal geometry of cables and the phase arrangement of currents are calculated in one unique step. Then, the algorithm obtains the optimal arrangement of cables to minimize the construction cost and limit the maximum magnetic field for the general public.

The study of magnetic fields generated for cables in galleries is less often addressed in the literature. However, installations of cables in galleries are very useful in many cases. In [5-18], the authors describe the first 400-kV underground transmission line project, where cables are located in a gallery. In [5-19], the design and construction of the largest 400-kV Mexican transmission network in a gallery are presented. The authors of [5-20] present applications of Gas Insulated Lines (GIL) in tunnels for common corridors and between neighboring countries sharing other infrastructures. The magnetic field generated by a real case of GIL is also shown in the study. Many other applications of large- and medium-size power transmission in galleries can be cited in mining, interconnection and transportation applications. In [5-21], the technology and various feasibility studies of the still-emerging technology of High Temperature Superconductive cables are presented for the transmission of huge quantities of electrical power, and a triaxial cable, with the three electrical phases concentrically assembled around a common central core, is proposed. This design provides total magnetic field compensation and almost zero electro-magnetic emissions for balanced

currents.

In general, optimal cable arrangements are calculated assuming fixed currents. However, in real applications, the electrical currents in cables are usually not constant but are time-varying. Consequently, this stochastic nature of the currents of the cables should be considered to attain an optimal design. In [5-22], multiple-circuit underground cable feeders allocated in a gallery with randomly changing loads are analyzed. A normal distribution is considered for the load current on all feeder circuits. The optimal disposition of cable bundles and phases from fixed selected positions is obtained using a genetic algorithm. The authors conclude that this statistical approach provides better arrangements, generating lower magnetic field values than when considering only a deterministic value of the current.

In the present chapter, new algorithms are proposed and analyzed to obtain optimal dispositions of cables and dimensions of galleries, minimizing construction costs and magnetic fields for both the general and occupational public. Time-changing currents are considered, resulting in a so-called statistical approach. Real data from a system of four three-phase single-core cables are used in the study. The results show that the proposed statistical approach provides cheaper solutions with lower generated magnetic fields than the conventional methods do.

5.3 The Optimization Problems

In the present work, the cables are arranged in four 3-phase trefoil cable bundles, selected for gallery installations. The calculation considers: construction cost, magnetic field limits, geometrical constraints and time-varying currents flowing through the 4 circuits. The gallery has a rectangular section, with two circuits allocated in each side wall of the gallery. Two magnetic field limits are considered:

- In a horizontal plane, one meter above the ground, to limit the exposure of the general public to magnetic fields.
- Inside the gallery, providing a corridor for maintenance work by occupational professionals.

In the present case, 4 cable bundles are allocated in the gallery. Its generalization to some other number of circuits or some other geometry in the gallery can be easily achieved. Subsequently, the three alternative optimization problems used in this work are described.

5.3.1 Calculation of the Optimal Geometry for Four-Cables Bundles in a Gallery, for Specified Currents

In the first optimization problem, the optimal coordinates for the cable bundles and the geometry of the gallery are calculated, minimizing construction costs and ensuring magnetic field constraints for both general and occupational exposures. The proposed optimization problem represents the minimization of the gallery construction and cable installation costs in a single formulation. For the given specified currents in the cables and specified magnetic field limits in the two measurement areas, the proposed optimization problem is summarized in equations (5-1)-(5-17).

$$\begin{aligned} &\min f\left(x,y,t_1,t_2\right)=2\left(c_{VarGal}+c_x\right)\left(x_{lateral}+d_{wall}\right)+c_y\left(h_{gal}-y_{sup\,gal}\right)\\ &+2c_{vol}\left(x_{lateral}+d_{wall}\right)\left(h_{gal}-y_{sup\,gal}\right)-c_p\left(t_1+t_2\right) \end{aligned} \tag{5-1}$$

s.t.

$$b_x^i=\frac{\mu_0}{2\pi}\left|\begin{array}{l}\left(\Im_{1a}\frac{y_{1a}-Y_c^i}{\left(X_c^i-x_{1a}\right)^2+\left(Y_c^i-y_{1a}\right)^2}+\Im_{1b}\frac{y_{1b}-Y_c^i}{\left(X_c^i-x_{1b}\right)^2+\left(Y_c^i-y_{1b}\right)^2}+\Im_{1c}\cdot\frac{y_{1c}-Y_c^i}{\left(X_c^i-x_{1c}\right)^2+\left(Y_c^i-y_{1c}\right)^2}+\ldots\right.\\ \left.+\Im_{4a}\frac{y_{4a}-Y_c^i}{\left(X_c^i-x_{4a}\right)^2+\left(Y_c^i-y_{4a}\right)^2}+\Im_{4b}\frac{y_{4b}-Y_c^i}{\left(X_c^i-x_{4b}\right)^2+\left(Y_c^i-y_{4b}\right)^2}+\Im_{4c}\cdot\frac{y_{4c}-Y_c^i}{\left(X_c^i-x_{4c}\right)^2+\left(Y_c^i-y_{4c}\right)^2}\right)\end{array}\right| \tag{5-2}$$

$$b_y^i=\frac{\mu_0}{2\pi}\left|\begin{array}{l}\left(\Im_{1a}\frac{X_c^i-x_{1a}}{\left(X_c^i-x_{1a}\right)^2+\left(Y_c^i-y_{1a}\right)^2}+\Im_{1b}\frac{X_c^i-x_{1b}}{\left(X_c^i-x_{1b}\right)^2+\left(Y_c^i-y_{1b}\right)^2}+\Im_{1c}\frac{X_c^i-x_{1c}}{\left(X_c^i-x_{1c}\right)^2+\left(Y_c^i-y_{1c}\right)^2}+\ldots\right.\\ \left.+\Im_{4a}\frac{X_c^i-x_{4a}}{\left(X_c^i-x_{4a}\right)^2+\left(Y_c^i-y_{4a}\right)^2}+\Im_{4b}\frac{X_c^i-x_{4b}}{\left(X_c^i-x_{4b}\right)^2+\left(Y_c^i-y_{4b}\right)^2}+\Im_{4c}\frac{X_c^i-x_{4c}}{\left(X_c^i-x_{4c}\right)^2+\left(Y_c^i-y_{4c}\right)^2}\right)\end{array}\right| \tag{5-3}$$

$$\left(b_x^{\,j}\right)^2+\left(b_y^{\,j}\right)^2\le B_{\max gen}^2 \tag{5-4}$$

$$\left(b_x^{\,l}\right)^2+\left(b_y^{\,l}\right)^2\le B_{\max \exp}^2 \tag{5-5}$$

$$\left(x_{m,a}-x_{m,b}\right)^2+\left(y_{m,a}-y_{m,b}\right)^2=d^2 \tag{5-6}$$

$$\left(x_{m,a}-x_{m,c}\right)^2+\left(y_{m,a}-y_{m,c}\right)^2=d^2 \quad (5\text{-}7)$$

$$\left(x_{m,b}-x_{m,c}\right)^2+\left(y_{m,b}-y_{m,c}\right)^2=d^2 \quad (5\text{-}8)$$

$$\frac{x_{1,3a}+x_{1,3b}+x_{1,3c}}{3}=-x_{lateral} \quad (5\text{-}9)$$

$$\frac{x_{2,4a}+x_{2,4b}+x_{2,4c}}{3}=x_{lateral} \quad (5\text{-}10)$$

$$\frac{y_{1,2a}+y_{1,2b}+y_{1,2c}}{3}=y_{\sup gal}-t_1 \quad (5\text{-}11)$$

$$\frac{y_{3,4a}+y_{3,4b}+y_{3,4c}}{3}=t_2+y_{\sup gal}-h_{gal} \quad (5\text{-}12)$$

$$h_{gal}-\left(t_1+t_2\right)\geq d_{\min} \quad (5\text{-}13)$$

$$y_{\sup gal}\leq y_{\sup gal\min} \quad (5\text{-}14)$$

$$y_{\sup gal}-h_{gal}\geq y_{gal\max} \quad (5\text{-}15)$$

$$x_{lateral}\leq l_{\max}-d_{wall} \quad (5\text{-}16)$$

$$y_{\sup gal}-h_{gal}+d_{floor}\leq t_2+y_{\sup gal}-h_{gal}\leq y_{\sup gal}-t_1\leq y_{\sup gal}-d_{ceiling} \quad (5\text{-}17)$$

$i=1,\ldots,\left(k_1+k_2\right)$, $j=1,\ldots,k_1$, $l=1,\ldots,k_2$, $m=1,\ldots 4$

Where,

b_x^i and b_y^i are modules of phasors of horizontal and vertical projections of magnetic field phasors generated by all the cables at the evaluation points of the measurement areas, in μT.

$x_{lateral}$ is the horizontal coordinate of the center of the right bundle of cables, in m.

y_{supgal} is the vertical coordinate of the ceiling of the gallery, in m.

(x_{ml},y_{ml}) are the coordinates of the center of cable l in cable bundle m, in m.

t_1 is the distance from the upper bundles of cables to the gallery ceiling, in m.

t_2 is the distance from the lower bundles of cables to the floor, in m.

The constants are:

μ_0, the permeability of free space, in H m^{-1}.

$\underline{I}_{il}$, the phasor of currents flowing through cable bundle i with phases $l=\{a, b, c\}$, in A.

B_{maxgen}, the maximum magnetic field allowed for the general public external to the gallery evaluation plane, in μT.

B_{maxexp}, the maximum magnetic field allowed for occupational professionals in the area where human transit in the gallery is permitted, in μT.

d, the distance between two cable centers in a bundle, in m.

d_{min}, the minimum distance allowed between two cable bundle centers, in m.

h_{gal}, the height of the gallery, in m.

d_{floor} and $d_{ceiling}$, the minimum distances allowed from the cable bundle centers to the floor and ceiling of the gallery, in m.

d_{wall}, the fixed distance from cable bundle centers to the walls of the gallery, in m.

l_{max}, the maximum horizontal distance allowed from the vertical wall of the gallery to the horizontal reference, in m.

$y_{supgallmin}$, the minimum depth allowed for the ceiling of the gallery for security reasons, in m.

y_{galmax}, the maximum depth allowed for the floor of the gallery for construction and security, in m.

k_1, the number of evaluation points in the external measurement plane.

k_2, the number of evaluation points in the internal area.

The geometry of the gallery is shown in Fig. 5-1. In a first approach, a symmetrical solution is investigated. The cable bundles are allocated at the same horizontal distance from the center of the gallery, at right and left. Additionally, the two upper cables and the two lower ones share the same vertical coordinates. The height of the gallery, h_{gal}, is standard and fixed at 2.5 m. The gallery can more or less buried and more or less wide in function of the magnetic restrictions and costs.

The main fees associated with the installation of underground transmission lines in the gallery are related to the cost of the precast pieces of concrete that constitute the

gallery itself, as well as civil construction and right-of-path costs. These costs can be associated with horizontal, vertical and volumetric terms. The first term of (5-1) considers the costs per unit related to the variable horizontal costs of the gallery (C_{VarGal}) and the occupation of land (c_x). The second and third terms of (1) consider the volumetric (c_{vol}) and vertical (c_y) costs per unit due to digging and shoring operations. The total cost of the gallery is the sum of the three first terms plus the fixed cost, which is related to the fixed cost of manufacturing, the material of the two vertical walls that form the gallery and the cost of the cables, i.e., a fixed cost C_{FixGal}.

To facilitate future maintenance actions, the cable bundles are preferably allocated far from the floor and ceiling. The fourth term of the objective function maximizes these distances, with a small recompense coefficient, c_p, set to 0.5 (€/m), much lower than the costs of the first three terms of (5-1).

To limit the maximum magnetic fields, two measurement areas are considered (see Fig. 5-1). One, for limiting the exposure of the general public, is the horizontal line one meter above the terrain, with $k_1=51$ measurement points, 0.2 m apart, representing a 10-m line. The other is the central area of the gallery, with k_2 = 78 measurement points allocated in the intersections of three rows (the central axis and two others rows detached 0.6 m at left and right) and 26 lines (from floor to ceiling, with separations of 0.1 m between them). In (5-2) and (5-3), the modules of phasors of horizontal and vertical components of the magnetic field at each of the measurement points are calculated.

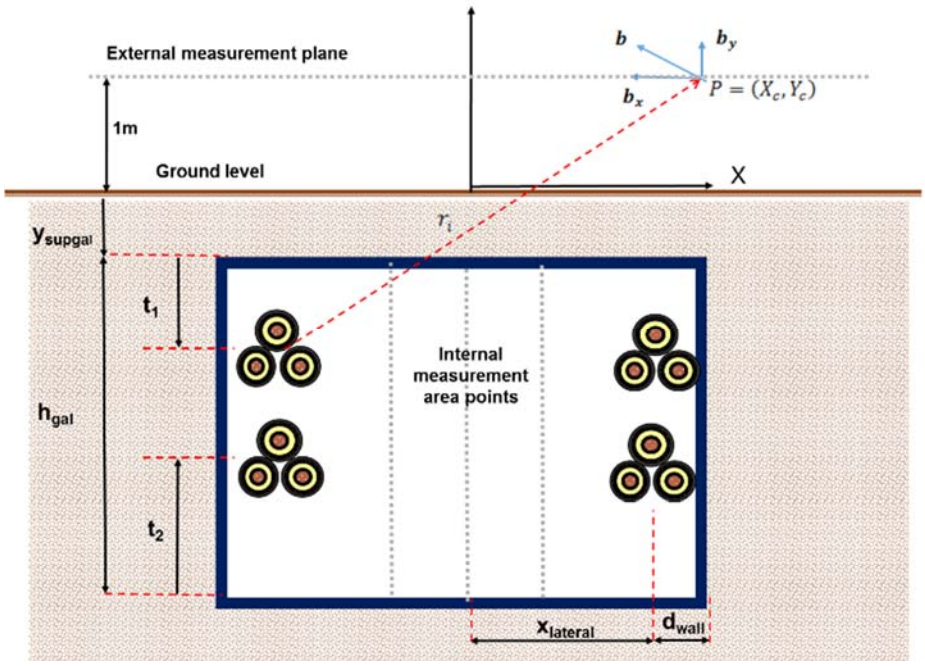

Figure 5-1. Gallery and magnetic field generated by a conductor at point k.

The square module of the magnetic field at the external horizontal plane measurement points is restricted to the square of a specified maximum value B_{maxgen}, considering general public restrictions (5-4). In the internal area, the specified maximum value of restriction is B_{maxexp} for occupational professionals (5-5).

Three cables constitute each bundle of cables, creating the equilateral triangle specified in (5-6)-(5-8). In the algorithm, the optimal rotated position of Fig. 5-2.a is calculated, increasing the magnetic field compensation. In some cases, for construction constraints, the bundles' positions can be approximated to the more conventional bundle cable arrangement (Fig. 5-2.b).

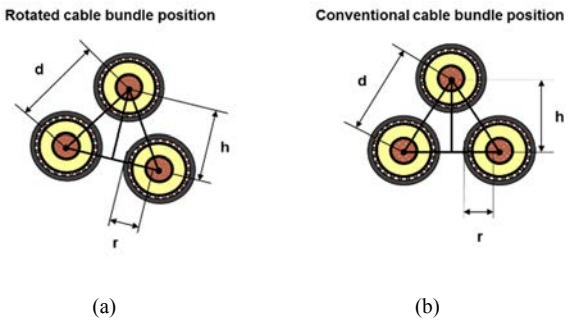

Figure 5-2. Geometrical diagram of conventional and rotated bundle cables.

The position of the centers of cable bundles as a function of the lateral distance to the vertical axis of the gallery ($x_{lateral}$) and the distances to the floor and ceiling of the gallery (t_1 and t_2) are defined by equations (5-9)-(5-12). Two cable bundle centers are in the left wall of the gallery (bundles 1 and 3), and the other two are in the right wall (bundles 2 and 4). At first, for symmetry reasons, both walls have the same distance to the center of the gallery. Moreover, the pairs of cable bundles are constrained to have the same depth (5-9)-(5-12). This symmetry could facilitate further maintenance and the enlargement of the number of circuits in the gallery.

Separation between the cables affects the interaction of the magnetic fields, as in [5-7] and [5-8]. In the present study, the results of simulations using a distance of d = 0.32 m between cables in bundles and a minimum distance of d_{Min} = 0.7 m between bundles, as specified in (5-13), are presented.

For security and construction reasons, the minimum depth allowed for the ceiling of the gallery, $y_{supgalmin}$, is 0.5 m, and the maximum depth for the floor of the gallery, y_{maxgal}, is 5 m (see Eqs. (5-14) and (5-15)). Because of the nature of the urban terrain, the maximum distance between walls of the gallery is limited to 8 m (Eq. (5-16), where l_{max} is 4 m). For maintenance reasons, cable bundles are allocated at a minimum distance from the floor (d_{floor} = 0.2 m) and the ceiling ($d_{ceiling}$ = 0.2 m) of the gallery (see Eq. (5-17)).

Symmetrical solutions can be optimal for balanced circuits. However, in real applications, each circuit transports different power and current. In the present case, historical data of the cables are used, showing different currents in each circuit over time. In this case, asymmetric galleries with different distances from the walls of the gallery to the maintenance path can yield cost benefits. Asymmetric galleries can be calculated, replacing (5-9) and (5-10) with (5-18) and (5-19).

$$\frac{x_{1,3a} + x_{1,3b} + x_{1,3c}}{3} = -x_{lateral1} \tag{5-18}$$

$$\frac{x_{2,4a} + x_{2,4b} + x_{2,4c}}{3} = x_{lateral2} \tag{5-19}$$

where $x_{lateral1}$ is the distance of the two right cable bundles to the center of the maintenance path and $x_{lateral2}$ is the distance of the left cable bundles to the same center.

5.3.2 Calculation of Mean Coordinates for Four Cable Bundles in the Gallery in M Scenarios

Currents in circuits in electrical power systems vary over time depending on changes in demand and generation. The optimal design of the system configuration should then take into account the statistical distribution of the operating values. To this aim, the calculation of the optimal design is based on the actual data gathered from a real case considering three years' of hourly current recordings of four underground circuits with the same path in the proximity of a substation. The proposed statistical approach is based on simulation of random scenarios by resampling from the recorded data. Here, a scenario means a vector of observations corresponding to a unit of time. A set of M random samples, with replacement, compound the scenarios to be analyzed. For each of the M samples, the solution of the optimization problem represented by Eqs. (5-1)-(5-17) results in M optimal dimensions of galleries and positions of cables. The final optimal configuration will be located at some central position of the M optimal configurations. Given the nonlinearity of the problem, these final mean coordinates are obtained in a second optimization problem that takes into account not only the statistical variability of the actual data, as represented by the bootstrapped samples, but also the geometrical restrictions. This optimal configuration is solved as follows:

$$min \quad h(x) = \sum_{m=1}^{M} \sum_{i=1}^{n} \left(\left(s_{ia}^{m}\right)^2 + \left(s_{ib}^{m}\right)^2 + \left(s_{ic}^{m}\right)^2 + \left(t_{ia}^{m}\right)^2 + \left(t_{ib}^{m}\right)^2 + \left(t_{ic}^{m}\right)^2 \right) \tag{5-20}$$

s.t.

Eqs. (5-6)-(5-17).

$$x_{il} - s_{il}^{m} = x_{il}^{m} \tag{5-21}$$

$$y_{il} - t_{il}^{m} = y_{il}^{m} \tag{5-22}$$

$i = 1,..,4,\ l = a,b,c,\ m = 1,\ldots,M$.

Where the variables:

(x_{il},y_{il}) are the mean coordinates of cable l in cable bundle i of the optimal mean arrangement.

s_{il}^m, t_{il}^m are the horizontal and vertical differences from (x_{il},y_{il}) to each of the (x_{il}^m, y_{il}^m) coordinates of the centers of cable l in cable bundle i for the m samples of currents.

In the present optimization problem, (x_{il}^m, y_{il}^m) are fixed values, previously calculated using the optimization problem of (5-1)-(5-17) for each of the M scenarios.

The objective function (5-20) represents the addition of the square differences between the coordinates of the centers of cable l in cable bundle i of sample m to the coordinates of the centers of the cables of the optimal mean arrangement s_{il}^m, t_{il}^m. In total, 24 M terms constitute the objective function. In the present formulation, all of the differences are equally penalized. However, solutions prioritizing less costly positions can also be found. Eqs. (6)-(17) express the geometrical restrictions that cables and bundles must respect, and they are also imposed here. Eqs. (5-21) and (5-22) calculate the differences between the mean centers of the cables and each one of the samples.

5.3.3 Multi-Scenarios Optimization

In the Multi-Scenario approach, a set of N_{sc} selected scenarios are chosen such that they correspond to a set of representative situations. The optimal dimensions of the gallery and positions of cables are then calculated, minimizing the costs for all scenarios simultaneously. The purpose of this approach is to constrain the magnetic field for a set of representative events, such as those corresponding to extreme currents or some particular combination of currents that can have a high impact in terms of magnetic fields. The proposed optimization problem is formulated as follows.

$$\begin{aligned} &\min f\left(x,y,t_1,t_2\right) = 2\left(c_{VarGal}+c_x\right)\left(x_{lateral}+d_{wall}\right)+c_y\left(h_{gal}-y_{sup\,gal}\right) \\ &+2c_{vol}\left(x_{lateral}+d_{wall}\right)\left(h_{gal}-y_{sup\,gal}\right)-c_p(t_1+t_2) \end{aligned} \tag{5-23}$$

s.t.

$$b_{xj}^{\ i} = \frac{\mu_0}{2\pi}\left| \begin{array}{l} \left(I_{iqa}\frac{y_{1a}-Y_c^i}{\left(X_c^i-x_{1a}\right)^2+\left(Y_c^i-y_{1a}\right)^2}+I_{iqb}\frac{y_{1b}-Y_c^i}{\left(X_c^i-x_{1b}\right)^2+\left(Y_c^i-y_{1b}\right)^2}+I_{iqc}\cdot\frac{y_{1c}-Y_c^i}{\left(X_c^i-x_{1c}\right)^2+\left(Y_c^i-y_{1c}\right)^2}+\ldots \right. \\ \left. +I_{4qa}\frac{y_{4a}-Y_c^i}{\left(X_c^i-x_{4a}\right)^2+\left(Y_c^i-y_{4a}\right)^2}+I_{4qb}\frac{y_{4b}-Y_c^i}{\left(X_c^i-x_{4b}\right)^2+\left(Y_c^i-y_{4b}\right)^2}+I_{4qc}\cdot\frac{y_{4c}-Y_c^i}{\left(X_c^i-x_{4c}\right)^2+\left(Y_c^i-y_{4c}\right)^2} \right) \end{array} \right| \tag{5-24}$$

$$b_{yq}^{\ i}=\frac{\mu_0}{2\pi}\left|\begin{array}{l}\left(I_{1qa}\frac{X_c^i-x_{1a}}{\left(X_c^i-x_{1a}\right)^2+\left(Y_c^i-y_{1a}\right)^2}+I_{1qb}\frac{X_c^i-x_{1b}}{\left(X_c^i-x_{1b}\right)^2+\left(Y_c^i-y_{1b}\right)^2}+I_{1qc}\frac{X_c^i-x_{1c}}{\left(X_c^i-x_{1c}\right)^2+\left(Y_c^i-y_{1c}\right)^2}+\ldots\right.\\ \left.+I_{4qa}\frac{X_c^i-x_{4a}}{\left(X_c^i-x_{4a}\right)^2+\left(Y_c^i-y_{4a}\right)^2}+I_{4qb}\frac{X_c^i-x_{4b}}{\left(X_c^i-x_{4b}\right)^2+\left(Y_c^i-y_{4b}\right)^2}+I_{4qc}\frac{X_c^i-x_{4c}}{\left(X_c^i-x_{4c}\right)^2+\left(Y_c^i-y_{4c}\right)^2}\right)\end{array}\right| \quad (5\text{-}25)$$

$$\left(b_{xq}^{\ j}\right)^2+\left(b_{yq}^{\ j}\right)^2\le B_{\max gen}^2 \quad (5\text{-}26)$$

$$\left(b_{xq}^{\ l}\right)^2+\left(b_{yq}^{\ l}\right)^2\le B_{\max \exp}^2 \quad (5\text{-}27)$$

Eqs. (6) – (17).

$i=1,\ldots,\left(k_1+k_2\right)$, $j=1, \ldots, k_1$, $l=1, \ldots, k_2$, $q=1,\ldots., N_{sc}$

Objective function (5-23) is the same as that used in the optimization problem of Section II.A. One unique position of the cables and gallery is calculated for the N_{sc} chosen scenarios. In (5-24) – (5-25), for the N_{sc} scenarios of representative currents, the horizontal and vertical components of the magnetic field at each one of the measurement points are calculated. Eqs. (5-26) and (5-27) limit the maximum magnetic field allowed for the general and occupational public in each scenario. The geometrical restrictions on the position of cables, bundles and dimensions of gallery in (5-6)-(5-17) are applicable to this optimization problem as well. As in Section II.A., if the asymmetric configuration is calculated, (5-8)-(5-9) is substituted by (5-18)-(5-19).

In the present work, 6 representative events are considered. Instead of using a single scenario for each event, we form a cluster with the 3 nearest scenarios with the aim of reducing sampling variability and increasing robustness. Therefore, a total of N_{sc} = 18 representative scenarios are selected and represented in the optimization problem as follows:

- From the historical data, the three scenarios with the maximum differences and the three scenarios with the minimum differences of modules between the two circuits with the largest modules of currents (circuits 1 and 2).
- From the historical data, the three scenarios with the maximum differences and the three scenarios with the minimum differences of phase angle.

- From the *M* scenarios solved in Section II.b, the three scenarios with the maximum costs and the three scenarios with the minimum costs.

5.4 Case of Study

In this work, a case of four 220-kV balanced underground power circuits of single-core XLPE cables, with a cupper conductor of 2,500 mm², is studied based in real data. The four circuits are connected to the same substation and share a path in its proximity. Instantaneous values of active and reactive power have been recorded every hour for three years. There are a total of 26.280 valid recordings. Active and reactive currents, I_d and $I_{q,}$, proportional to these recordings have been calculated and are shown in Figs. (5-3) and (5-4).

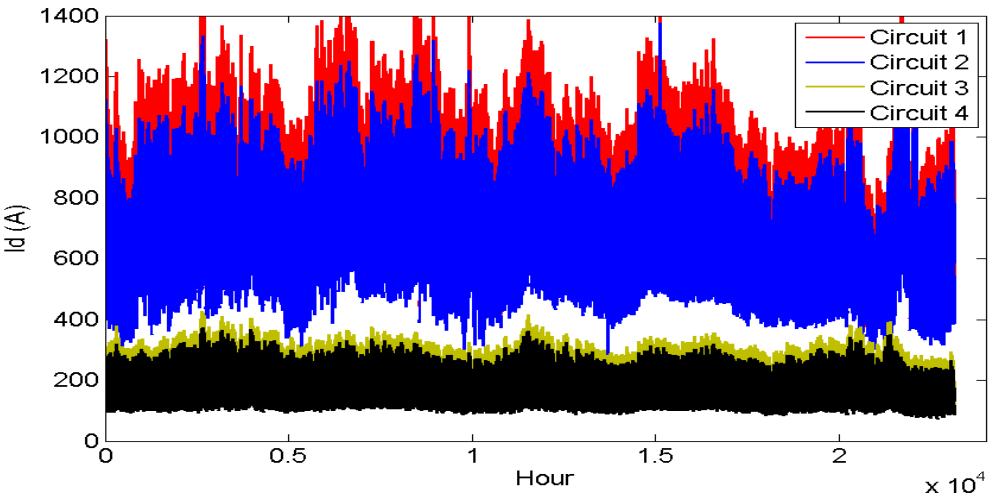

Figure 5-3. Active Currents in the four circuits – I_d (A).

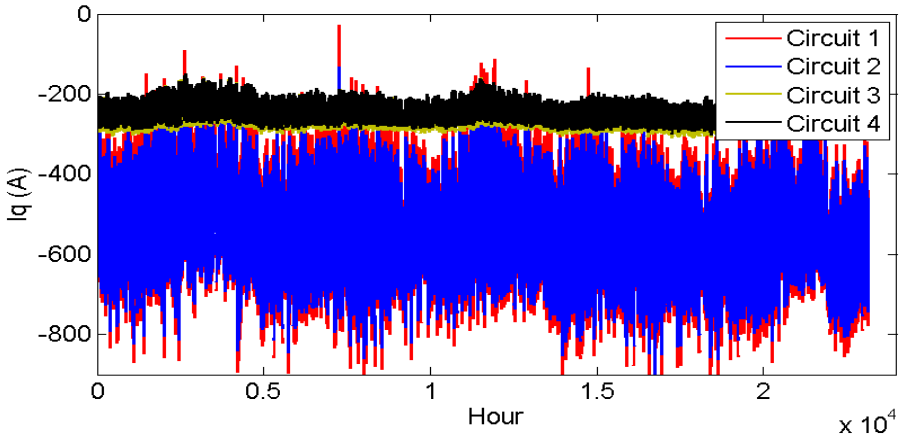

Figure 5-4. Reactive currents in the four circuits – Iq (A).

This figure reveals that the statistical properties of the series of currents are stable over time. There is an absence of patterns of growth or decay, and the daily and weekly seasonal (stochastic) patterns are stable over time. Moreover, the time series are large enough to reflect the actual variability. Consequently, resampling from the unconditional distributions can provide a representative sample of the multivariate distribution of the currents.

To perform the statistical approach, M = 150 random samples of currents in Figs. 4 and 5 are sorted. For each one of these samples, the optimization problem of (5-1)-(5-17) is solved. In these simulations, the costs per unit are obtained from a general reference for construction costs: c_{FixGal}=210 €/m, c_{VarGal}=70 €/m, c_x = 10 €/m², c_y= 14.59 €/m² and c_{vol} = 6.5 €/m³ [5-23]. In (5-1), only construction costs are considered; the costs of the cables themselves are not included. In the fifth term of (5-1), for maintenance reasons, c_p= 0.5.

Regarding the geometrical constraints (5-13)-(5-17), the following values are used: d_{min}=0.7 m, $y_{supgalmin}$= -0.5 m, y_{galmax}= -5 m, l_{max}= 8 m, $d_{ceiling}$= d_{floor}= 0.4448 m, h_{gal}= 2.5 m and d_{wall}= 0.3348 m.

5.5 Results

The proposed methodologies are implemented and compared with a more traditional solution: the conventional position of bundles without rotation and a unique deterministic calculation with the maximum values of the currents. In total, five optimal

configurations are compared. They are labeled as follows:

- *Opt*: deterministic calculation of the optimal configuration, solving the optimization problem of (5-1)-(5-17) once for the maximum thermal current (1700 A) and power factor 0.8 in all cables. This configuration is similar to the situations studied in most of the literature [5-8]-[5-15]. In this configuration, because the same current is flowing in all of the circuits, only a symmetric solution can be obtained.
- *MedSymmetric:* From historical data, M = 150 scenarios of instantaneous currents are randomly sorted. In each scenario, the optimization problem of (5-1)-(5-17) is solved. Then, the mean arrangement of cables is calculated following the procedure of Section II.B.
- *MedAsymmetric:* Similar to the previous method, but allowing asymmetric galleries. Thus, constraints (5-18)-(5-19) are used instead of (5-9)-(5-10).
- *ClusterSymmetric:* Solving the optimization problem of Section II.C based on the 18 representative currents.
- *ClusterAsymmetric:* Similar to the previous method, but allowing asymmetric galleries. Thus, constraints (5-18)-(5-19) replace (5-9)-(5-10).

The calculation of optimal configurations for galleries and cables with heavy magnetic constraints and time-varying currents is a very difficult task. Two cases are here considered:

- *Case A:* $B_{maxgen} = 10\ \mu T$ *and* $B_{maxexp} = 50\ \mu T$.
- *Case B:* $B_{maxgen} = 3\ \mu T$ *and* $B_{maxexp} = 15\ \mu T$.

5.5.1 Case A: $B_{MAXGEN} = 10\ \mu T$ *and* $B_{MAXEXP} = 50\ \mu T$

MedSymmetric, *MedAsymetric, ClusterSymmetric, ClusterAsymmetric* and *Opt*

configurations are calculated using the Case A magnetic field limits. Then, all of the hourly recorded values of Figs. 5-3 and 5-4 are applied to the configurations. The resulting scheme of the gallery, position of cables and some isolines of the magnetic field are depicted in Fig. 5-5.

Due to the compensation of magnetic fields, the best cost results are obtained for dispositions with similar modules of currents (circuits 1 and 2 and circuits 3 and 4) allocated in the same wall of the gallery. As expected, in asymmetric configurations, the larger currents are allocated farther from the maintenance path. Moreover, the rotation of positions (Fig. 5-2.a) provides an extra compensation of magnetic fields. As observed in isolines of Fig. 5-5, the *Opt* and *Cluster* configurations are able to maintain the specified magnetic limits for all historical data. However, the *Med* configurations have some external and internal points that reach the magnetic limits when they are applied to the historical data at these configurations.

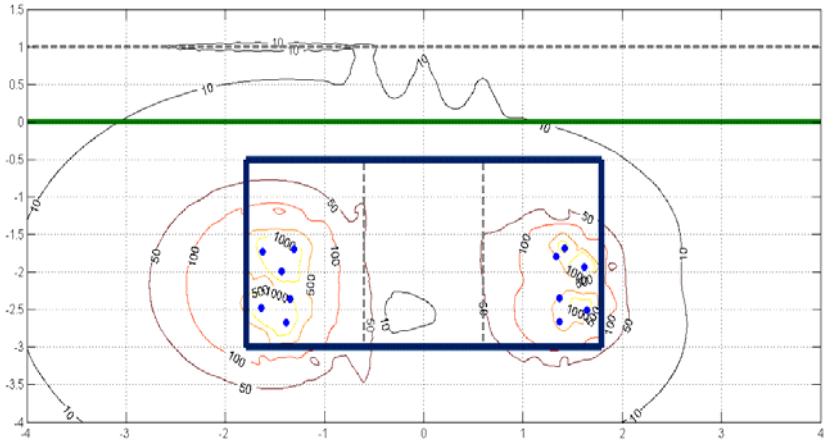

a. MedSymmetric configuration.

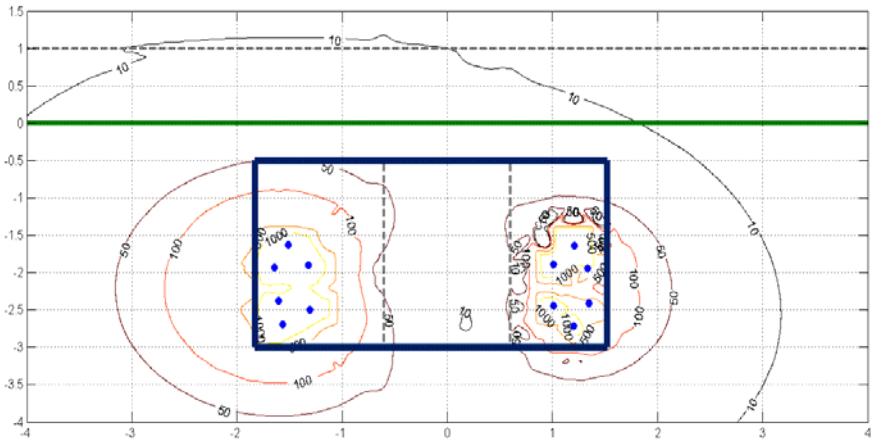

b. MedAsymmetric configuration.

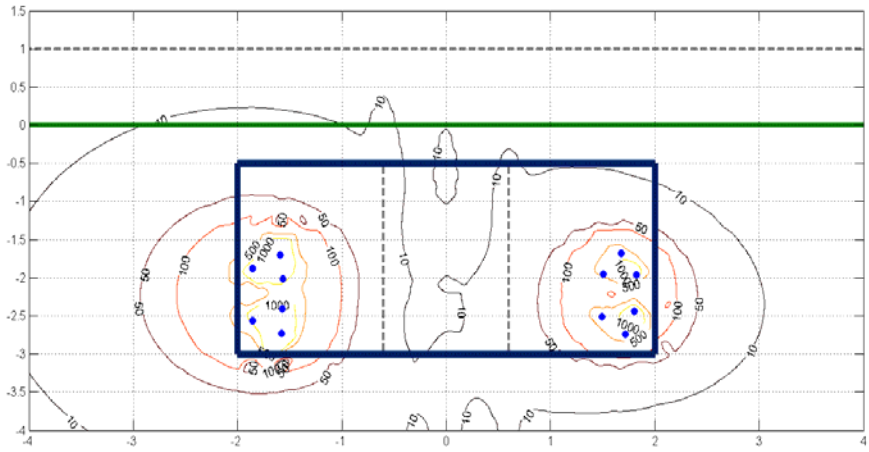

c. ClusterSymmetric configuration.

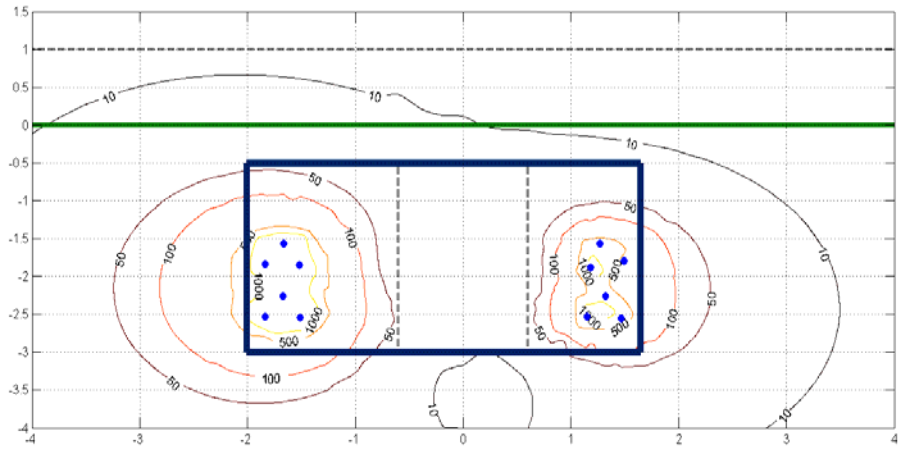

d. ClusterAsymmetric configuration.

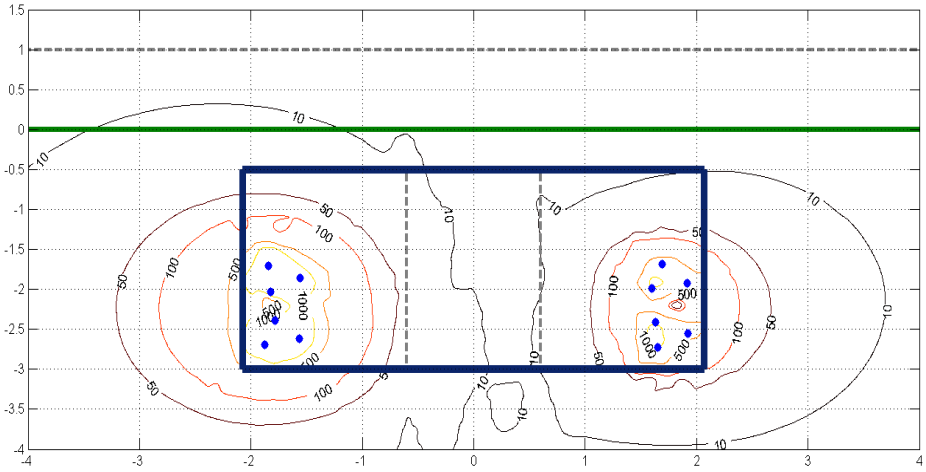

e. Opt configuration.

Figure 5-5. Isolines of the Magnetic Field, Case A.

In Fig. 5-6, a comparison between symmetrical and asymmetrical solutions is shown. *Med* configurations (in blue) result in the lowest width, followed by *Cluster* (in black) and *Opt* configurations (in red). It is remarkable that asymmetric configurations require smaller galleries than symmetric ones.

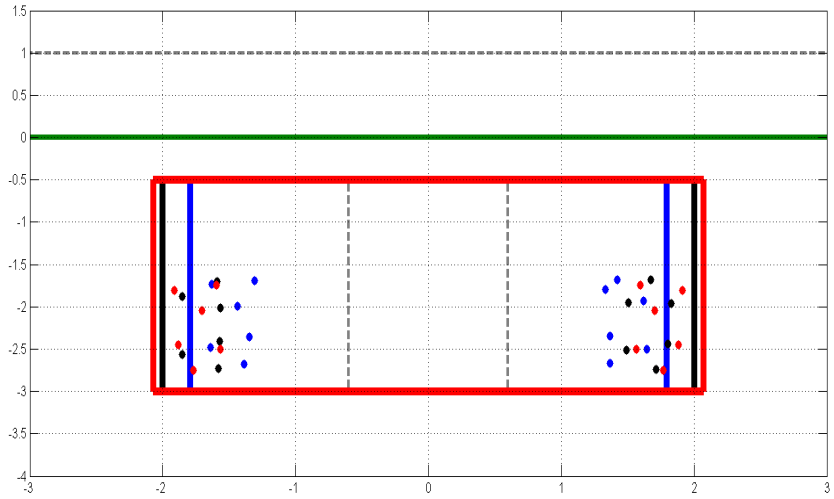

a. Symmetric configurations.

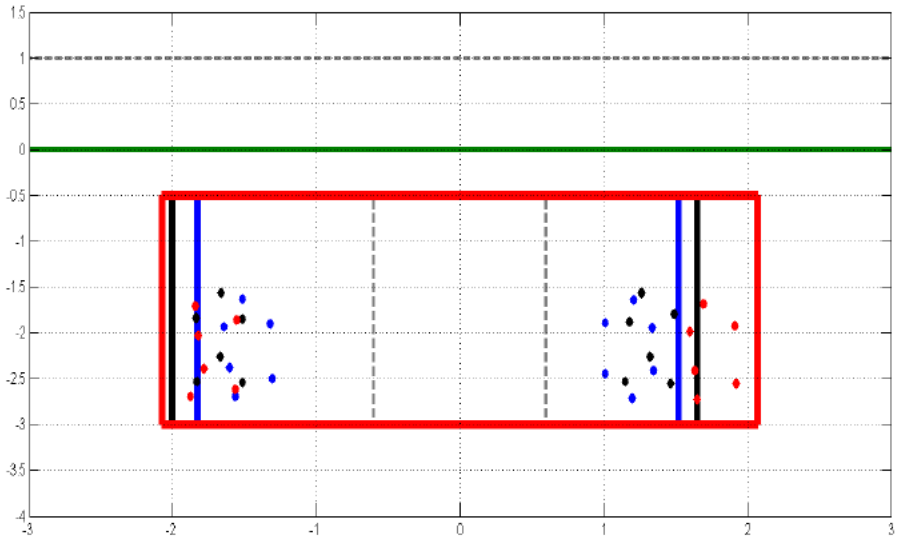

b. Asymmetric configurations.

Figure 5-6. Comparison of dimensions of galleries, Case A.

Considering the values of the magnetic fields generated by the hourly recorded values of currents depicted in Figs. 5-3 and 5-4, Table 5-1 shows the cost and the maximum value of the 95th percentile values of magnetic fields at all of the points that form the external measurement line and the central vertical axis of the maintenance path. It can be seen that the *Med* configurations are cheaper, followed by the *Cluster* and *Opt* configurations. The *Opt* configuration is 12.6% more costly than the *MedAsymmetric* one. In general, asymmetric solutions result in cheaper galleries, thereby reducing the distances of the circuits with lower values of modules of currents to the maintenance path.

Table 5-1. Comparison of cost and values of 95th percentile of magnetic field, Case A.

	Symmetric Configurations			Asymmetric Configurations		
	95th Percentile of Magnetic Field (μT)		Cost (€/m)	95th Percentile of Magnetic Field (μT)		Cost (€/m)
	Exterior	Interior		Exterior	Interior	
Med	11.58	31.54	654.3	12.74	37.6	630.8
Cluster	8.75	18.73	696.3	8.75	19.42	661.3
Opt	6.68	13.81	710	6.68	13.81	710

5.5.2 Case B: B_{maxGEN} = 3 μT and B_{maxEXP} = 15 μT

As previously stated, some countries (such as Italy and Switzerland) require stricter limitations of magnetic fields. Therefore, in Case B, the external constraints are restricted to 3 μT, and the internal constraints have a maximum value of 15 μT. New configurations are calculated in this case, and the historical data of 3 years is applied to these configurations. The galleries are larger and more expensive than in the previous case. As before, circuits with higher modules of currents (Circuits 1 and 2) are placed in the same wall of the gallery, and asymmetric galleries provide smaller and cheaper solutions.

In Figure 5-7, the geometry of galleries is depicted for the five configurations. It must be highlighted that the *Opt* configuration requires a gallery one meter deeper than the *Med* and *Cluster* configurations. Asymmetrical dispositions are narrower than symmetrical ones.

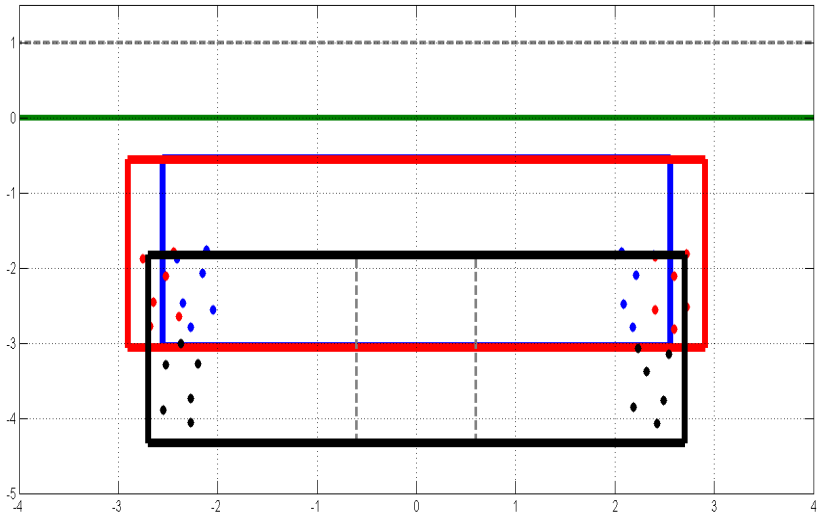

a. Symmetric configurations.

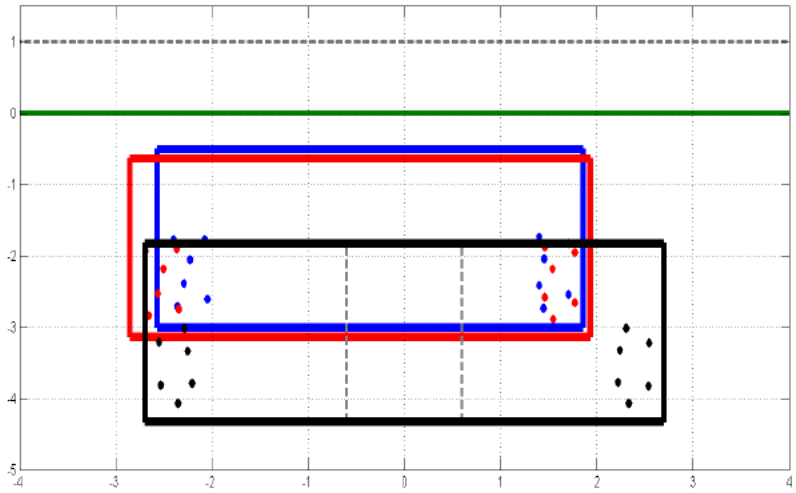

b. Asymmetric configurations.

Figure 5-7. Comparison of dimensions of galleries, Case B.

As before, Table 5-2 shows the cost and the maximum value of the 95th percentiles of the values of magnetic fields at the external measurement line and at the central vertical axis of the maintenance path. *MedAsymmetric* is the cheapest configuration. The *Opt* and *ClusterAsymmetric* configurations are 24.7% and 6% more expensive than *MedAsymmetric*. However, the *Med* configurations fail to maintain the external magnetic field constraint, reaching 3.75 or 3.81 μT for a limit of 3 μT. In this sense, the *Cluster* configurations are 4.6% (symmetrical) and 17.7 % cheaper than the conventional *Opt* configuration while respecting the specified magnetic field limits for all historical data.

Table 5-2. Comparison of cost and values of 95th percentile of magnetic field, Case B.

	Symmetric Configurations			Asymmetric Configurations		
	95th Percentile of Magnetic Field (μT)		Cost (€/m)	95th Percentile of Magnetic Field (μT)		Cost (€/m)
	Exterior	Interior		Exterior	Interior	
Med	3.81	9.7	809.3	3.75	12.0	737.9
Cluster	2.80	9.16	880.1	2.74	9.16	781.7
Opt	2.07	6.02	920.2	2.07	6.02	920.2

5.5.3 Cost Comparisons

In Fig. 5-8, the relationship between the maximum magnetic fields and the costs for the *Opt*, *MedAsymmetric* and *ClusterAsymmetric* configurations is displayed. As observed, the *Opt* configuration is more costly than the other two configurations. Moreover, under the *Opt* configuration, a relatively small reduction of the magnetic fields results in a large increase of the costs. Conversely, the *MedAsymmetric* configuration is the least cost-sensitive to magnetic field reductions, with *ClusterAsymmetric* at intermediate values.

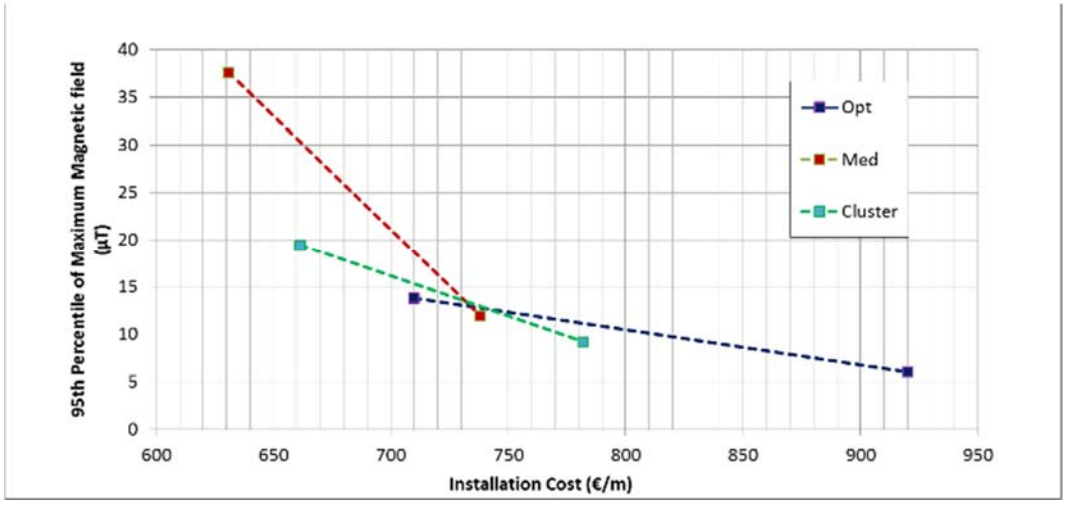

a. Magnetic field in the external plane.

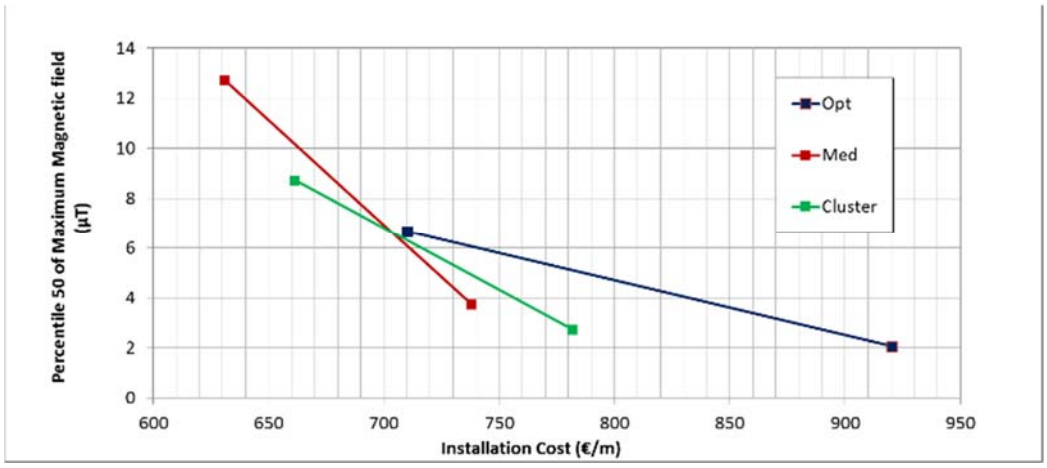

b. Magnetic field in the central internal axis of the maintenance path.

Figure 5-8. 95th Percentile of magnetic field in measurement plane vs. cost

5.6 Conclusions

This work proposes and compares methods for optimizing the allocation of 4 cable bundles and the gallery dimensions for underground lines that are allocated in galleries with stochastically time-varying currents flowing through them, considering maximum magnetic fields, geometrical constraints and installation costs. A real-world case with four cable bundles and three years of historical data is studied. Two statistical configurations, namely, the combination of clusters of currents and the mean calculation, are compared with the usual deterministic calculation method. Additionally, the symmetrical and asymmetrical dispositions of cables are considered in the study.

From the results, the proposed statistical approach is found to be far more convenient than the traditional deterministic method, providing a significant reduction of the construction cost, up to 182.3 €/m and complying with the magnetic field restrictions. The mean arrangement of cables provides cheaper solutions, passing beyond specified magnetic limits in some scenarios of the historical data. Clustering approaches result in interesting reductions of costs, strictly reaching magnetic field constraints.

5.7 References

[5-1] “International Commission on Non-Ionizing Radiation Protection, Guidelines for Limiting Exposure to Time Varing Electric and Magnetic Fields (Up To 100 kHz)”, ICNIRP Guidelines, 2010.

[5-2] "Limits in the USA", EMFS, available online: http://www.emfs.info/, last visit, Jan. 2016.

[5-3] European Commission, Council Recommendation of 12 July 1999 on the Limitation of Exposure of the General Public to Electromagnetic Fields (0 Hz to 300 GHz), The Council of The European Union, 1999.

[5-4] Rianne Stam (Laboratory for Radiation Research, National Institute for Public Health and the Environment, the Netherlands), Comparison of International Policies on Electromagnetic Fields (Power Frequency and Radiofrequency Fields), May 2011.

[5-5] European Commission, Report on the implementation of the Council Recommendation on the limitation of exposure of the general public to electromagnetic fields (0 Hz – 300 GHz) (1999/519/EC) in the EU Member States, Commission staff working paper, 2008.

[5-6] European Commission, Directive 2004/40/EC, The Council of The European Union, 2004.

[5-7] Bracken, T. Dan, "Assessing compliance with power-frequency magnetic-field guidelines", Health Physics, September 2002, Volume 83, Issue 3, pp 409-416.

[5-8] A.S. Farag, M.M. Dawoud, T.C. Cheng, Jason S. Cheng, "Occupational exposure assessment for power frequency electromagnetic fields", Electric Power Systems Research, Volume 48, Issue 3, 1 January 1999, Pages 151-175.

[5-9] A. S. Safigianni, C. G. Tsompanidou, "Measurements of electric and magnetic fields due to the operation of indoor power distribution substations", IEEE Transactions on Power Delivery, Volume 20, Issue 3, July 2005.

[5-10] CIGRE Working Group C4.204. Mitigation Techniques of Power Frequency Magnetic Fields Originated from Electric Power Systems, Feb. 2009.

[5-11] G. G. Karady, C. V. Nunez and R. Raghavan, "The Feasibility of Magnetic Field Reduction by Phase Relationship Optimization in Cable Systems", IEEE Transactions on Power Delivery, Vol. 13, No. 2, April 1998.

[5-12] E. I. Mimos, D. K. Tsanakas and A. E. Tzinevrakis, "Optimum phase configurations for the minimization of the magnetic fields of underground cables", Electrical Engineering, vol. 91, no. 6, pp. 327-335, 2010.

[5-13] G. G. Lai, Chien-Feng Yang, Hunter M. Huang, and Ching-Tzong Su, "Optimal Connection of Power Transmission Lines With Underground Power Cables to Minimize Magnetic Flux Density Using Genetic Algorithms", IEEE Trans. on Power Delivery, vol. 23, no. 3, July 2008.

[5-14] A. Canova, D. Bavastro, F. Freschi, L. Giaccone, M. Repetto, "Magnetic shielding solutions for the junction zone of high voltage underground power lines," Electric Power Systems Research, Vol. 89, pp. 109–115, 2012.

[5-15] J.C. del Pino-López, P. Cruz-Romero, L. Serrano-Iribarnegaray, J. Martínez-Román, “Magnetic field shielding optimization in underground power cable duct banks,” Electric Power Systems Research, vol. 114, pp. 21–27, 2014.

[5-16] M. G. Ippolito, A. Puccio, G. Ala S. Ganci, "Attenuation of low frequency magnetic fields produced by HV underground power cables", Power Engineering Conference (UPEC), 2015 50th International Universities, pp. 1-5, 2015.

[5-17] V. J. Hernandez Jimenez, E. D. Castronuovo, "Optimal geometric configurations for mitigation of magnetic fields of underground power lines", PowerTech, 2015 IEEE Eindhoven, pp. 1-6, 2015.

[5-18] R. Grandino, M. Portillo, J. Planas, “Undergrounding the first 400kV transmission line in Spain using 2500mm2 XLPE cables in a ventilated tunnel: The Madrid Barajas Airport project”, Jicable 2003.

[5-19] F.G Ibarra Romo, C. F. Fuentes Estrada, J. T. Arriaga Flores, M. Mammeri, “Modernization Manzanillo I. The Mexican largest transmission network of 400kV with XLPE cable systems: Design and Construction”, B1-106, CIGRE 2012.

[5-20] Roberto Benato, Claudio Di Mario, Hermmann Koch, “High Capability Applications of Long Gas-Insulated Lines in Structures”, IEEE Transactions on Power Delivery, Vol. 22, pp. 619 – 626, Jan-2007.

[5-21] H. Al-Khalidi, A. Hadbah, A. Kalam, “Performance Analysis of HTS Cables With Variable Load Demand”, Innovative Smart Grid Technologies Asia, 2011 IEEE PES pp. 1 – 8, 2011.

[5-22] G. G. Lai, C. Yang and C. Su, “Estimation and management of magnetic flux density produced by underground cables in multiple-circuit feeders”, European Transactions on Electrical Power, vol. 20, (2010), pp. 545–558, 2010.

[5-23] Table of prices of the construction in Andalusia (Base de Costes de la Construcción de Andalucía (BCCA) 2013. Banco de Precios), 2013 (in Spanish). http://www.juntadeandalucia.es

Chapter 6. Conclusion

In this chapter, conclusions and contributions obtained from the research and development of this thesis are shown. Besides, possible future works to improve this work are presented.

6.1 General Conclusions

Due to strong concerns of the society, the electrical power system need to be developed, managed and operated with very high socio-environmental constraints. The exposure to magnetic field is an important issue, producing deep concern in the population. Thus, legislation and studies have been developed, in order to restrict the magnetic field generated by electrical facilities. Simultaneously, requirements to optimize electrical facilities costs are increasing every day. This work wants to integrate these two goals, in order to optimize costs and magnetic fields produced for underground power cables.

Underground power lines are costly facilities and they can produce high values of magnetic field, affecting the population. Appropriate optimization methods can reduce significantly the construction cost and the generated magnetic field. Even, almost negligible values of magnetic field at moderated construction cost can be achieved, with the adequate configuration.

Three published lines to mitigate magnetic field generated by power lines are presented in literature: conductor allocation management, field compensation and

magnetic shields. Conductor allocation management, the technique used in this work, is able to mitigate magnetic field to very low values, not incurring in extra losses.

In this work, several contributions can be highlighted.

A new nonlinear optimization method with all continuous variables for the calculation of the optimal cables positions of *n* 3-phase trefoil underground circuits, in order to minimize construction cost and to mitigate magnetic field, is proposed. This method has been applied to real data, from four and six 200kV 3-phased circuit underground power lines. Proposed methods allow the free collocation of cables in their optimal position, attaining maximum magnetic field compensation.

When the same current is flowing through all circuits, negligible values of magnetic field can be obtained using the proposed method. The results show that the costs are heavily depending on the maximum allowed magnetic field. Lower magnetic field implies higher costly solutions and the costs increase with the number of cables. Non-conventional rotated bundle configurations provide extra magnetic field compensation and, hence, lower values of magnetic field.

For electrical currents with different values of modules and phase angles through the circuits, geometrical arrangements are achieved with the same reduced values of magnetic field and equivalent cost. The optimal arrangement is heavily depending on the value and phase of the currents. Therefore, it is observed that the optimal arrangements of cables for a set of currents can be non-effective when currents change.

In power systems, currents flowing through underground cables vary along the time. Thus, statistical methods have been proposed in this work for real underground power lines with a set of time changing currents flowing in the circuits, seeking to mitigate the magnetic field and the construction costs. For a real case of four 3-phase circuits, statistical and deterministic optimal solutions have been compared. Proposed statistical methods are much more convenient than traditional deterministic solutions, with cheaper results and magnetic field up to 350% lower than with the traditional method. As previously, the rotation of bundles provides extra magnetic field compensation and lower magnetic fields.

Limits for magnetic field exposure are different for general and occupational population. For electrical workers, accepted limits are higher. Although mitigation of the magnetic field for general population is a largely studied subject in literature, the limitation for occupational population is almost a non-developed matter. In this work, two statistical methods for controlling the magnetic field generated by underground lines allocated in galleries, with time varying currents, for general population and workers, are introduced. As before, these statistical methods are matched with a deterministic method. The statistical approach is far more convenient, providing significant magnetic field and cost reductions.

The two proposed optimization statistical methods are based in mean arrangements of a statistically representative sample of currents and in using clusters of representative currents. Mean arrangements of cables provide cheaper solutions, but they can overpass the magnetic limits in some scenarios of the historical data. Cluster approaches provide good reductions of costs, reaching magnetic field constraints in most of the cases.

6.2 Future Works

This work can be starting point for the development of future studies and researches. In this case, it is suggested:

- Improvement of the optimization model, for considering different patterns of currents in the circuits and particular configurations of cable bundles, like flat or delta configurations.
- Development and application of methods to forecast time varying currents, in the optimization of the arrangement of cables.
- Improvement in the selection of representative clusters of currents, taking into account statistic optimization methods.
- Calculating the effective ampacity of the cables, in function of their positions in the optimization process.
- Proposing optimization methods for the minimization of magnetic field in other electrical facilities, as substations, overhead power lines and others.

- Adapting the optimization problem for other objectives. One of these objectives can be the compensation of reactive power, produced and consumed by the power lines.
- Introducing multi-objective analyses, considering the optimization of several electrical effects at the same time.